Microscopy and Image Analysis

George McNamara,[1] Michael Difilippantonio,[2] Thomas Ried,[3] and Frederick R. Bieber[4]

[1]Biomedical Consultant, Baltimore, Maryland
[2]Division of Cancer Treatment and Diagnosis, National Cancer Institute, National Institutes of Health, Bethesda, Maryland
[3]Section of Cancer Genomics, Genetics Branch, Center for Cancer Research, National Cancer Institute, National Institutes of Health, Bethesda, Maryland
[4]Brigham and Women's Hospital, Boston, Massachusetts

This unit provides an overview of light microscopy, including objectives, light sources, filters, film, and color photography for fluorescence microscopy and fluorescence in situ hybridization (FISH). We believe there are excellent opportunities for cytogeneticists, pathologists, and other biomedical readers, to take advantage of specimen optical clearing techniques and expansion microscopy—we briefly point to these new opportunities. © 2017 by John Wiley & Sons, Inc.

Keywords: light microscopy • digital imaging • fluorescence in situ hybridization • functional genomics

How to cite this article:
McNamara, G., Difilippantonio, M., Ried, T., & Bieber, F. R. (2017). Microscopy and image analysis. *Current Protocols in Human Genetics*, *94*, 4.4.1–4.4.89. doi: 10.1002/cphg.42

INTRODUCTION

This unit provides an overview of light microscopy, including objectives, light sources, filters, and imaging for fluorescence microscopy and fluorescence in situ hybridization (FISH). We encourage thinking outside the usual magnification range of 10× to 100× objective lenses, by ranging from single molecules to whole mice and humans. Traditionally, clinical FISH was chromosome and single or dual gene DNA FISH**.** Single molecule RNA FISH is now a research tool, and has opportunities in the clinic. Genome engineering with clustered regularly interspaced short palindromic repeats (CRISPR)/Cas9, transcription activation-like effector nucleases (TALENs), and zinc finger nucleases requires both on-target validation and off-target safety checks. Computerized image analysis systems currently used in clinical cytogenetics are also discussed, and connected with the larger trend of digital slide scanning in pathology and cytology. We discuss how functional genomics can contribute to cytogenetics and vice versa. Photophysics of fluorescence, and applications of specialized F-techniques, are well reviewed by Ishikawa-Ankerhold, Ankerhold, & Drummen (2012), and Liu, Ahmed, & Wohland (2008). Scanning and transmission electron microscopy as well as confocal microscopy and multi-photon excitation microscopy are not covered in this unit despite their usefulness as invaluable tools for contemporary studies of biological systems; see Diaspro, 2001; Matsumoto, 2002; Minsky, 1988; Paddock, 1999; Pawley, 2005; Shotton, 1993; van der Voort, Valkenburg, van Spronsen, Woldringh, and Brakenhoff, 1987, for further information on confocal and multi-photon microscopies. Since the 2005 version of this unit (*UNIT 4.4*, McNamara, Difilippantonio, & Ried, 2005), Nobel Prizes have been awarded for fluorescent proteins and super-resolution. We have added a table and select references for fluorescent proteins. Super-resolution microscopies are out of the scope of this chapter; we recommend Schermelleh, Heintzmann, & Leonhardt (2010) and Turkowyd, Virant, and Endesfelder (2016) for reviews. We summarize recent advances in light sheet imaging and expansion microscopy, and how these can be useful. We believe there are excellent oppor-

Current Protocols in Human Genetics 4.4.1–4.4.89, July 2017
Published online July 2017 in Wiley Online Library (wileyonlinelibrary.com).
doi: 10.1002/cphg.42

tunities for cytogeneticists, pathologists, and other biomedical readers, to take advantage of specimen optical clearing techniques and expansion microscopy—we briefly point to these new opportunities.

NANO, MICRO, AND MACRO SCALES

Figure 4.4.1 illustrates the nano, micro, and macro scale. The left side is a mouse tissue section, with original dimensions of 40 × 14 mm, acquired on a Meyer Instruments Pathscan Enabler digital slide scanner at the equivalent of a 4× objective lens (Masson trichrome stain, prepared slide from Carolina Biological Supply).

The right side top and second panels are single molecule RNA FISH of GAPDH mRNA of pancreatic cancer cells; top is single plane raw data, the second panel is a Microvolution 100 iteration quantitative deconvolution (*www.microvolution.com*; Biosearch Stellaris FISH oligonucleotides probe set, Quasar 570 dye, detected with a Texas Red filter set on a Leica DMI 6000 microscope with Hamamatsu Flash 4.2 scientific complementary metal-oxide semiconductor [sCMOS] camera, additional details and data at *https://works.bepress.com/gmcnamara/55*). The four bright dots in the left side nucleus are most likely multiple pre-messenger RNA and mRNA molecules from transcriptional bursts at the gene loci (aneuploidy or late S or G2 phase of cell cycle). Fluorescence imaging of single biological molecules on a research fluorescence microscope should now be considered routine. The quantitative deconvolution image processing (second panel) slightly improves spatial resolution (of the raw data), and dramatically increases contrast.

The right middle is a SKY spectral karyotype of a metaphase from a MDA-MB-435 subline (modal chromosome number ~90, this metaphase is ~400), acquired on a Nikon Eclipse fluorescence microscope with 40×/1.3 NA objective lens (width ~250 μm). The image was acquired by Carrie Viars and Steve Goodison (University of California, San Diego) and George McNamara, experiment related to Urquidi et al. (2002).

Finally, the right side fourth and bottom panels are raw and quantitative deconvolution image data of human osteosarcoma cell line SaOS2, double immunofluorescence (RUNX2 red, osteocalcin green) plus Hoechst DNA nuclear counterstain (blue), acquired by Jared Mortus and George McNamara. Three Z-series acquisition time (MetaMorph software, Leica microscope, Flash 4.2 sCMOS camera) and deconvolution time were each ~17 sec (*www.microvolution.com*). Shown is a maximum projection image. See Appendix 4.4.3 (see Supporting Materials) for larger field of view.

HISTORICAL FOUNDATIONS OF MICROSCOPY

Even in medieval times it was understood that curved mirrors and hollow glass spheres filled with water had a magnifying effect. In the early 17th century, men began experimenting with lenses to increase magnification. A compound telescope, with weak convex lens at one end and a concave lens as the eyepiece, was demonstrated by a Dutch spectacle maker to the court at The Hague in September 1608 (Ruestow, 1996). News quickly spread throughout Europe. Galileo made his own compound telescope in 1609, turned it to the planet Jupiter and discovered moons. Galileo soon turned his telescope around and observed flies with it. Credit for the now standard two convex lens microscope goes to the son and father team of Janssen and Janssen. Naturalists Jan Swammerdam (1637 to 1680) and Nehemiah Grew (1641 to 1712), anatomist Regnier Graaf (1641 to 1673), and physiologist Marcello Malpighi (1628 to 1694) made important discoveries using magnifying lenses, especially tiny, strong single lenses (Ruestow, 1996).

Robert Hooke's book, *Micrographia*, published in 1665, contains beautiful drawings based on his microscopic observations. His experimental demonstrations to the Royal Society were interrupted by the 1666 fire of London, after which he and his friend and business partner Christopher Wren had major roles in the surveying and rebuilding of the city (Jardine, 2004). Also in 1666 Sir Isaac Newton found that a prism separates white light into distinct colors, and crucially, brilliantly, discovered the rainbow could be recombined into white light with a second prism (Newton, 1672, 1730). In 1683, the Dutch merchant, Anton van Leeuwenhoek (1632 to 1723), using his own meticulously prepared lenses, published his first of many papers to the Philosophical Transactions of the Royal Society of London (Leewenhoeck, 1683). van Leeuwenhoek's publications of "animalcules," blood cells, sperm and more, were the first multi-decade high throughput microscopy project. In 1773 a Danish microbiologist, Otto Muller (1730 to 1784), used the microscope to

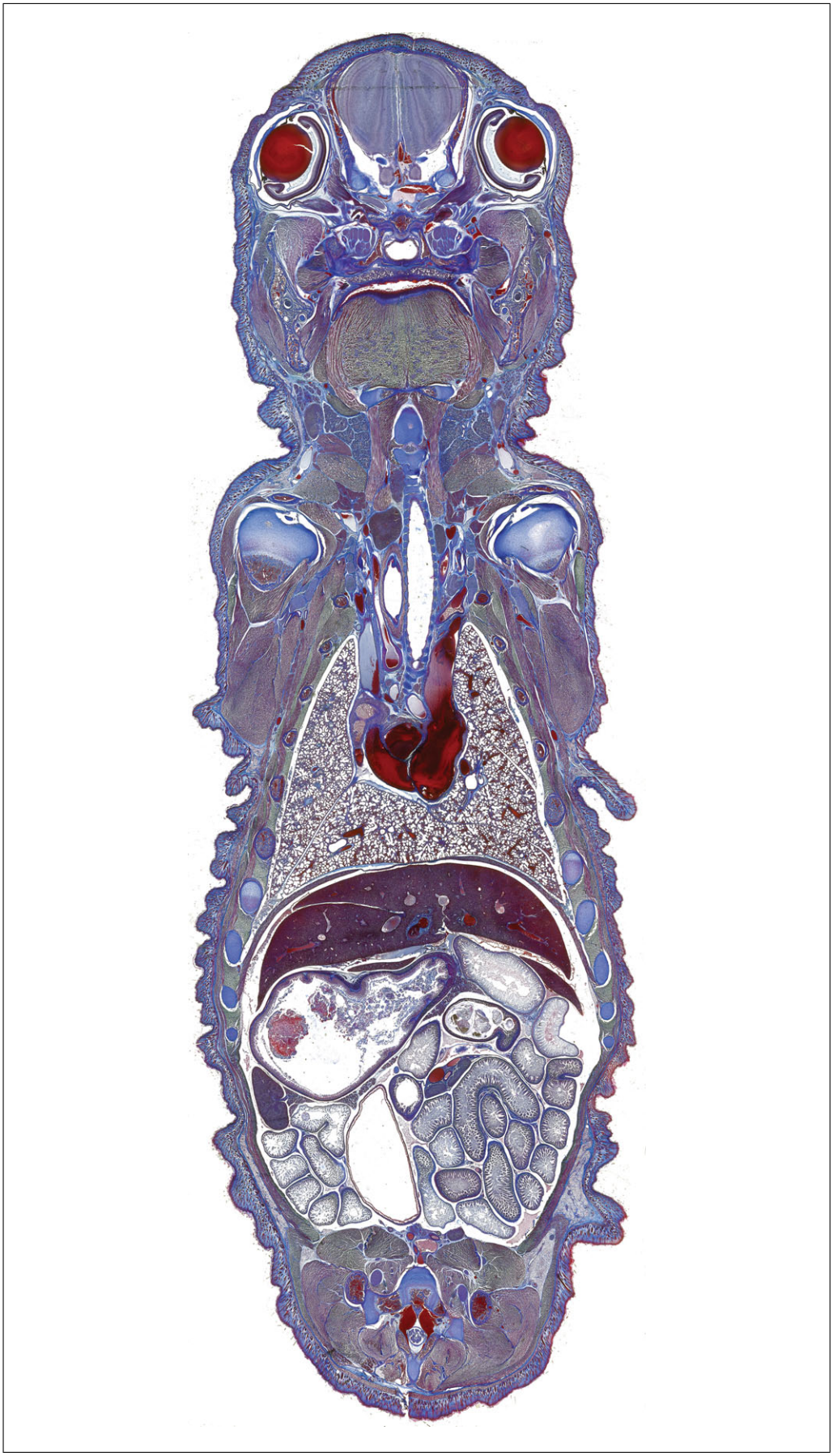

Figure 4.4.1 *(legend appears on next page)*

describe the forms and shapes of various bacteria. In 1833, Robert Brown (1773 to 1858) discovered the consistent presence of nuclei in plant cells. Brown also reported on the microscopic behavior of tiny, non-living clay particles, now called Brownian motion, which Einstein discussed in one of his classic 1905 papers.

In 1856, William Perkin discovered mauve, the first useful synthetic dye. He used his first batch to stain silk. After trial and error he found he could use tannins to color fast stain mauve onto wool and cotton. His successful commercialization revolutionized the textile industry, fashion, and rapidly led to the modern chemical and pharmaceuticals industries (Garfield, 2001; Perkin, 1906). The success of Perkin after dropping out of scholarly chemistry studies has parallels a century later with another successful William: Bill Gates of Microsoft. Mauve was a serendipitous discovery but in 1865 F. August Kekule (1829 to 1896) dreamt his theory of the benzene ring, which together with an understanding of the stoichiometry of molecules and chemical reactions led to chemistry becoming a rational science.

In 1869, Friedrich Meischer isolated nucleic acids. Of the many dyes invented and used in the following decades, we mention that fluorescein was discovered and synthesized in 1871 (see Clark & Kasten, 1983 for a history of staining). In 1879 to 1880 Paul Ehrlich performed a series of studies on the nature of cell and tissue staining by acidic and basic dyes and later went on to found immunology and the idea of magic bullet chemotherapies. Ernst Abbe described the mathematics of diffraction and optimal lens construction in 1876. The firm of Carl Zeiss quickly manufactured high quality oil immersion lenses of Abbe's designs. In 1893, August Köhler, a German zoologist, described the principles of what we now refer to as Köhler illumination (*APPENDIX 3N*, Salmon & Canman, 2003). This was a critical step in generating a uniform field of illumination and providing optimal image resolution. Rudolf Virchow (1821 to 1902) founded modern cell physiology in the midst of these twin revolutions in dye chemistry and microscope optics. Waldeyer coined the term "chromosomes" in 1888 to refer to those colored bodies he saw in dividing cells.

Köhler and Moritz von Rohr made the first ultraviolet microscope, to try to take advantage of shorter wavelengths producing better resolution (summarized in Kohler, 2016). In the course of their studies they made the first fluorescence microscope. In the following decades, the firms of Zeiss and Reichert made the first fluorescence microscopes using transmitted light illumination and simple filters. Among the earliest use of epi-illumination was Singer's (1932) observations on live tissues. While Singer preferred a therapeutic sunshine carbon arc, his use of epi-illumination with a heat absorbing filter, excitation filter, mirror, and emission filter is organized along the lines of a modern fluorescence microscope. In the 1930s and 1940s Strugger and others investigated biological fluorescence staining with acridine orange and other fluorophores. In 1934 Marrack conjugated pathogen-specific antibodies to a dye, however, the weak labeling was hard to see on the bright background of standard transmitted light microscopy. Albert Coons (1912 to 1978) and colleagues (see Coons, 1961; Coons, Creech, & Jones, 1941; Coons, Creech, Jones, & Berliner, 1942) adapted Marrack's dye coupling idea with a fluorescent covalent labeling, introducing the concept of immunofluorescence, which enabled staining with unparalleled molecular specificity. Coons and Kaplan (1950) introduced the use of a fluorescent secondary antibody to detect the antigen specific primary antibody. Secondary antibodies both amplified the staining intensity per antigen, and made the technique generic in that one batch labeled secondary antibody (i.e., goat anti rabbit) could be used to detect many different primary antibodies on different specimens (i.e., rabbit anti-pneumococcus, rabbit anti-streptococcus). A key advance when using formalin-fixed tissue sections for either immunohistochemistry with chromogenic subtracts, or immunofluorescence, was the development of antigen retrieval (Shi, Gu, & Taylor, 2000). A recent development may have further improved antigen retrieval (Vollert, Moree, Gregory, Bark, & Eriksen, 2015).

Figure 4.4.1 *(image appears on previous page)* Tiki_Goddess. Example of scanning an entire tissue section. This Masson trichrome stained mouse tissue section was scanned in "one click" using a Meyer Instruments Pathscan Enabler microscope slide scanner. The tissue section is 40 × 14 mm (~10 μm thick), and the scan dimension length limit is 36 mm, so really a click, rotate slide, click, open in Adobe Photoshop, and a few more clicks and drags to merge, rotate vertically, white balance to taste, and save. The entire process took under five minutes. We emphasize here the value of having "the whole story" in one image.

In 1924, Feulgen and Rossenbeck reported on their use of pararosaniline, a close relative of Perkin's mauve, and their use of a quantitative depurination reaction to make a Schiff's base, to produce a reliable way to quantify DNA in cell nuclei and bacteria. This ultimately led to the discovery of distinct stages of eukaryotic cell cycle, constancy of DNA in most mammalian cell lineages, proved that gametogenesis involves a reduction division, and stimulated many developments in the 1930s to 1950s of quantitative microscopy by Caspersson and others.

Waldeyer's colored bodies were subdivided in the 1930s by Bridge's observation of chromosome banding in *Drosophila* chromosomes. Hsu (1952), capitalizing on a serendipitous buffer dilution error, invented a chromosome spreading technique based on hypotonic swelling of metaphase cells. Tjio and Levan (1956) used the hypotonic swelling/cell dropping method to correctly enumerate the 46 human chromosomes. Lejeune, Gautier, and Turpin (1959) quickly discovered trisomy 21 in (most) Down syndrome patients. Caspersson et al. (1968) published their method of fluorescently banding chromosomes using quinacrine mustard to uniquely identify each of the 23 pairs of human chromosomes. Historically, clinical chromosome banding was done with the Perkin era nonfluorescent dye Giemsa (G-banding). Using an A:T specific fluorescent DNA dye, with digital acquisition by sCMOS, charge-coupled device (CCD), or confocal microscopy, enables a similar banding image, after digital inverse contrast in the computer. Such images can be improved further by either fast unsharp masking (Adobe Photoshop or FIJI ImageJ) or quantitative spatial deconvolution (e.g., *www.microvolution.com*) to obtain higher spatial resolution and contrast. A key advantage of using DAPI over Giemsa is that fluorescence further enables—using multiple probe fluorescence hybridization, such as specific DNA FISH probe sets, or whole genome—spectral karyotyping.

MICROSCOPY IN MODERN HUMAN GENETICS

Microscopy currently plays a crucial role in both research and diagnostic aspects of modern genetics. This typically involves the use of light microscopes for the analysis of microbiological, cytological, and pathological specimens, as well as the cytogenetic analysis of metaphase and interphase chromosomes (*APPENDIX 3N*; Salmon & Canman, 2003). With recent advances in fluorescence technology, there has been growth, even in clinical laboratories, in the use of fluorescence microscopy. Spectral karyotyping and Multiplex-FISH instruments have made their way into many clinical labs, but in narrow niches. Confocal microscopy was invented by Minsky (1957, 1988), and re-invented by Eggar and Petran (1967), but their achievements were not widely appreciated. The first successful confocal microscope was developed around the confocal laser scanning microscope introduced by White, Amos, and Fordham (1987). The history of MRC confocal microscopes, and context of cell analysis and antibody developments, has been reviewed by the inventors, Amos and White (2003). Confocal microscopy improves lateral resolution by a factor of $\sqrt{2}$, that is, by 1.414, but more importantly, provides optical sectioning by blocking out of focus light from reaching the detector. The downside is that some of the in-focus light is also blocked. Most of the fluorescence microarray readers, i.e., Affymetrix, now found in clinical core labs, are based around confocal scanner designs. Denk, Strickler, and Webb, (1990) introduced multi-photon excitation microscopy (MPEM). MPEM is an intrinsically optical sectioning technique, where fluorescence only occurs in a diffraction-limited spot where a high intensity near infra-red laser comes to a focal point. Although most MPEM microscopes are based on, and can be used as, confocal microscopes, the pinhole is typically kept open to collect more light. A few confocal microscopes are within the budget range of a well-endowed clinical lab, but commercial multiphoton microscopes currently use expensive Ti:Sapphire pulsed lasers. The biomedical optics community is busy pushing the limits of microscopy into nanoscopy, a field reviewed by Garini, Vermolen, and Young (2005), and awarded the 2014 Nobel Prize in Chemistry to Eric Betzig, Stefan W. Hell, and William E. Moerner.

Analysis of cell types in blood and biopsy specimens, apoptosis assays in diseased tissue, cytogenetic analysis, and even surgical procedures using fluorescence have all been reported. Because this unit deals primarily with the use of microscopy and contemporary image analysis in mammalian cytogenetics, a brief explanation of some of the applications of fluorescence microscopy in this field is relevant. The ability to label nucleic acids with fluorescent molecules and detect them in situ was developed in the early 1980s (Langer-Safer, Levine, & Ward, 1982;

Manuelidis, Langer-Safer, & Ward, 1982). Fluorescence in situ hybridization (FISH; *UNIT 4.3*; Knoll & Lichter, 2005) technology has been applied to many different areas of cytogenetic investigation (Lichter & Ward, 1990). The first use involved determination of chromosome copy number in interphase nuclei using centromere-specific fluorescent probes (Cremer et al., 1986; Devilee et al., 1988; Manuelidis, 1985). This was later extended to the identification of aberrant or marker chromosomes (Blennow et al., 1995; Taniwaki et al., 1993; Thangavelu, Pergament, Espinosa, & Bohlander, 1994), or microdeletions (Ried et al., 1990) using chromosome painting probes or single-copy probes known to map to specific chromosomes. Giemsa banding was not compatible with fluorescence hybridization techniques, thereby making it difficult to obtain simultaneous identification of the chromosomes. Methods were soon developed, however, whereby banding patterns could be obtained through the hybridization of fluorescently labeled repetitive sequences in both humans (Baldini & Ward, 1991) and mice (Arnold, Bhatt, Ried, Wienberg, & Ward, 1992; Boyle, Ballard, & Ward, 1990). Concurrent with these advances came the start of the Human Genome Project and the application of FISH to gene mapping (Lichter et al., 1990, 1992; Otsu et al., 1993; Ried, Baldini, Rand, & Ward, 1992; Trask et al., 1993; Ward et al., 1991). FISH mapping is a useful technique for the identification of other genes in a gene family, including functional and non-functional genes (Giordano et al., 1993), and for the mapping of genes across species barriers, a technique referred to as Zoo-FISH (Chowdhary, Raudsepp, Fronicke, & Scherthan, 1998; Fronicke & Scherthan, 1997; O'Brien et al., 1997; Raudsepp, Fronicke, Scherthan, Gustavsson, & Chowdhary, 1996; Wienberg, Jauch, Stanyon, & Cremer, 1990).

The fluorescent labeling and hybridization of entire genomes is useful for a number of different areas of investigation. Somatic cell hybrid lines (see Chapter 3; Haines et al., 2017) were historically very useful for isolating and mapping disease genes in both mice and humans (Harris, 1995). Comparative genome hybridization (CGH) is another technique involving the fluorescent labeling of entire genomes. In this instance, the genomes may be from karyotypically normal reference and mutant (i.e., tumor) populations. The genomes, labeled with different fluorophores, are pooled prior to hybridization. The hybridization ratio of the two fluorophores along the length of each chromosome is calculated to determine the gain or loss of chromosomal regions in the mutant cells (*UNIT 4.6*; DeVries, Gray, Pinkel, Waldman, & Sudar, 1995; Forozan, Karhu, Kononen, Kallioniemi, & Kallioniemi 1997; Kallioniemi et al., 1992; Ried et al., 1997). This technique is extremely useful in cases involving multiple chromosomal rearrangements for which specific bands cannot be identified by Giemsa staining, or for detecting small insertions or deletions (larger than 1 Mb). Comparative cytogenetics is the study of changes in chromosome number and composition in different species as a function of their evolutionary divergence from one another. Chromosome painting has proved very useful in identifying homologous chromosome regions between species and has led to a better understanding of the evolutionary rearrangement of genomes (Wienberg et al., 1990). Many fluorescent dyes have now been created, each with different excitation and emission characteristics. This has allowed for the simultaneous hybridization and discernment of multiple probes on a single slide (Johnson, McNeil, Carter, & Lawrence, 1991; Ried et al., 1992). A natural extension of this procedure involves the labeling of different probes with various combinations of fluorophores, thereby enabling the hybridization of more probes than there are distinguishable dyes. With N fluorophores, the number of possible labeling combinations is given by $2N - 1$. This combinatorial labeling of individual chromosomes using five different fluorophores is used for spectral karyotyping (SKY; *UNIT 4.9*; Lee, Rens, & Yang, 2000; Garini et al., 1996; Liyanage et al., 1996; Schröck et al., 1996) and M-FISH (Azofeifa et al., 2000; Jentsch, Geigl, Klein, & Speicher, 2003; Karhu et al., 2001; Speicher, Ballard, & Ward, 1996) analysis of mouse and human metaphase chromosomes. $2^5 - 1 = 31$ combinations are more than the 24 human or 21 types of mouse chromosomes. This technique has proved very useful for the identification of chromosome aberrations in human tumors and mouse models of tumorigenesis (Barlow et al., 1996; Coleman et al., 1997; Ghadimi et al., 1999; Veldman, Vignon, Schröck, Rowley, & Ried, 1997). SKY analysis has also been applied to evolutionary studies and will improve the analysis of genomic relationships (Schröck et al., 1996). Another approach has been to label probes not only by using combinations of dyes, but also by

varying the ratios in which they are used (Nederlof, van der Flier, Vrolijk, Tanke, & Raap, 1992). If K different concentrations are used for each fluorophore, and if the highest concentration used is 1 and the other concentrations are defined as $(1/2)^1$, $(1/2)^2 \ldots .(1/2)^{K-2}$ and 0, the total number of possible valid combinations as described by (Garini, Gil, Bar-Am, Cabib, & Katzir, 1999) is given by:

$$K^N - (K-1)^N$$

where "valid" refers to combinations that have different fluorophore-concentration ratios. In other words, ratios of (1,1) and (0.5,0.5) for a two dye scheme have identical concentration ratios of 1. Extending Nederlof's method to enough dyes and ratios to paint each human chromosome uniquely is called combined binary ratio labeling fluorescence in situ hybridization (Tanke et al., 1999). The method has been used for adding a unique gene (HPV) FISH probe (Szuhai et al., 2000), painting p versus q arms (Wiegant et al., 2000), and a total of 49 colors for all chromosome arms (48 combinations involving 6 fluorophores) plus an HPV genome-specific FISH probe with a long Stokes shift dye that did not cross-talk with the other fluorophores (Brink et al., 2002). Using subtelomeric COBRA-labeled BAC and PAC FISH probes, all 41 unique subtelomeres have been imaged on single human metaphase spreads (Engels et al., 2003).

Fluorescence technology is also contributing to advances in the areas of cell biology, and in studies to determine nuclear topography (Carter et al., 1993; Lawrence, Carter, & Xing, 1993; Lawrence, Singer, & Marselle, 1989; Xing, Johnson, Dobner, & Lawrence, 1993) and chromatin organization (Sachs, van den Engh, Trask, Yokota, & Hearst, 1995; Yokota, Singer, van den Engh, & Trask, 1997; Yokota, van den Engh, Hearst, Sachs, & Trask, 1995). Studies designed to analyze gene function also incorporate advances in fluorescence microscopy, but the fluorescence in this case is not from a fluorophore conjugated to a nucleic acid, but from a green fluorescent protein (GFP) isolated from jellyfish. By making constructs encoding the gene of interest fused to the GFP gene, researchers are able to determine the cellular sub-localization of their "glowing" gene product (Chalfie, Tu, Euskirchen, Ward, & Prasher, 1994). GFP revolutionized biology and was justly awarded the Nobel Prize in Chemistry in 2008 to Osamu Shimomura, Roger Y. Tsien, and Martin Chalfie. GFP has also been used as a reporter gene in transgenic mice to determine the developmental stage and tissue specific transcriptional activation of promoters (Fleischmann et al., 1998). The fusion of GFP to the CENPB gene, the product of which is known to localize to all human centromeres, has been used in conjunction with time-lapse fluorescence microscopy to follow the movement of centromeres throughout the cell cycle (Sullivan & Shelby, 1999).

Subsequent in vitro modifications of the *Aequorea* GFP gene protein sequence have resulted in the development of other fluorescent proteins, including blue, cyan, and yellow whereby enabling the simultaneous use of multiple fluorescently tagged proteins in the same living cell (reviewed by Tsien, 1998, 2005). A key discovery was made by a Russian group that cloned, from *Discosoma* coral, the isolate of a red fluorescent protein (DsRed; Matz et al., 1999). This was followed by characterization of the genetic diversity of the colorful fluorescent protein family (Labas et al., 2002), isolation of more useful mutants of DsRed, such as "Timer" (Terskikh et al., 2000), a monomeric version, mRFP1 (Campbell et al., 2002), and mRFP1's fruity spectrum of mutants from orange through far-red mPlum derivatives (Shaner et al., 2004; Wang, Jackson, Steinbach, & Tsien, 2004). Niu et al. (2016) used spectral karyotyping and FUCCI cell cycle specific fluorescent protein reporters to produce better insight into tumor DNA ploidy changes ("giant cell cycle" hypothesis).

The ability to fuse cDNAs of fluorescent proteins with proteins of interest and/or with other fluorescent proteins, has been the enabling technology for many localization and colocalization studies at the cell and organismal level. The majority of fluorescent protein fluorescence resonance energy transfer (FRET) papers now use 37°C stable versions of cyan (Heim, Prasher, & Tsien, 1994) and yellow (Ormö et al., 1996) fluorescent proteins, with some biosensors switching to state-of-the-art green (mNeonGreen or mClover3) and red (mScarlet or mRuby3; Bajar et al., 2016; Bindels et al., 2017; McNamara & Boswell, 2007; Newman, Fosbrink, & Zhang, 2011; Okumoto, Jones, & Frommer, 2012; Tewson, Martinka, Shaner, Hughes, & Quinn, 2016; see Table 4.4.1 at end of article). At the cell level, the interaction of cyan fluorescent protein (CFP)-sensor-yellow fluorescent protein (YFP) fusion with a molecule of interest, or CFP-protein1 plus YFP-protein2 interactions, can answer questions with

nanometer precision. These studies take advantage of FRET in which the energy released by the excitation of one fluorescent molecule in the cell can directly cause the excitation of a different fluorescent molecule if they are in close enough proximity to one another. The effective range of Förster-type energy transfer is less than 10 nm, making FRET an excellent spectroscopic ruler for molecular interactions in cells (Stryer & Haugland, 1967). For example, Miyawaki and colleagues used CFP-calmodulin-M13-YFP as a calcium sensor, called CaMeleon. In the absence of calcium, the CFP and YFP were far enough apart and/or oriented such that little FRET occurred from CFP to YFP. In the presence of calcium, the binding of four calcium ions to the calmodulin component resulted in a specific interaction between calmodulin and the M13 peptide, which resulted in CFP and YFP becoming close enough and/or orienting their dipole moments such that FRET increased (Miyawaki et al., 1997).

FRET is an excellent imaging tool when large changes occur as in the binding or unbinding of calcium and CaMeleon, or the loss of FRET on cleavage of a protease substrate in a CFP-substrate-YFP protein fusion. However, subtle features of the sensor module and/or the fluorescent protein(s) can have an enormous impact on success or failure. Making the effort to optimize the FRET system can pay off with large dynamic range sensor responses, as in the outstanding twenty times dynamic range for a FRET CFP-caspase substrate-YFP sensor found by mutagenesis and flow sort screening for color derivatives of the two fluorescent proteins (Nguyen & Daugherty, 2005). This methodology has been utilized to identify in vivo molecular interactions between different proteins in transgenic organisms, such as cell-type and temporal-specific expression of calcium ion sensing CaMeleons (Hasan et al., 2004) or calpain protease activation (Stockholm et al., 2005) in mice. A comprehensive review of FRET methods and calculations has been published by Jares-Erjiman and Jovin (2003). Fluorescent protein biosensors are reviewed by Newman et al. (2011); Frommer (*http://biosensor.dpb.carnegiescience.edu*); McNamara (*http://www.geomcnamara.com/fluorescent-biosensors*); and Table 4.4.1.

Fluorescent proteins have also been fused with, or otherwise made to interact with, recombinant luciferases. These recombinants recapitulate the native system of *Aequorea*, in which the calcium-activated blue emitting photoprotein aequorin (a one shot luciferase), excites non-covalently bound GFP by bioluminescence resonance energy transfer (BRET), to produce predominantly green light. Researchers have made use of BRET specifically, and luciferases in general, to monitor protein-protein interactions in homogeneous biochemical assays, live cells, and from cells inside mice (e.g., Contag et al., 1995; Ray, De, Min, Tsien, & Gambhir, 2004; Takai et al., 2015; Waud et al., 2001; Xu, Piston, & Johnson, 1999). While luciferase and GFP labeled cells are not going to become general clinical tools, the ability to look at scales from molecules to mice, from nanoseconds to weeks, is called molecular imaging. For example, the ability of study transplanted stem cells, and their progeny, to differentiate in mouse models, is greatly facilitated by luciferase and/or fluorescent protein tagging. Stem cell progeny can be tracked non-invasively by bioluminescence imaging (Wang et al., 2003). At the end of the experiment, the proof of identify, and presence or lack of fusion with host cells, ideally needs to be proven by combined GFP fluorescence, cell type marker-specific fluorescence immunocytochemistry and sex chromosome and species-specific fluorescence in situ hybridization.

TYPES OF MICROSCOPY

One source for an excellent and detailed discussion of microscopy and live cell analysis (in addition to other topics) is *Cells: A Laboratory Manual* (Spector, Goldman, & Leinwand, 1998), or, in its condensed form, *Live Cell Imaging* (Goldman & Spector, 2004). In general, the ability to generate a clear image is dependent on magnification, contrasts between internal and external milieu, and the ability to resolve discrete objects. There are many different microscope arrangements that can be used to enhance the contrast of specimens. The major imaging modes are epi-fluorescence, transmitted brightfield (*APPENDIX 3N*; Salmon & Canman, 2003), phase contrast (*APPENDIX 3N*; Salmon & Canman, 2003), polarized light, Nomarski, or differential interference contrast (DIC; *APPENDIX 3N*; Salmon & Canman, 2003), darkfield illumination, and reflected light illumination. Most of these configurations are used in conjunction with fluorescence microscopy.

With respect to fluorescence, the older literature referred to "diascopic" fluorescence in the case of transmitted light fluorescence, or trans-fluorescence, and

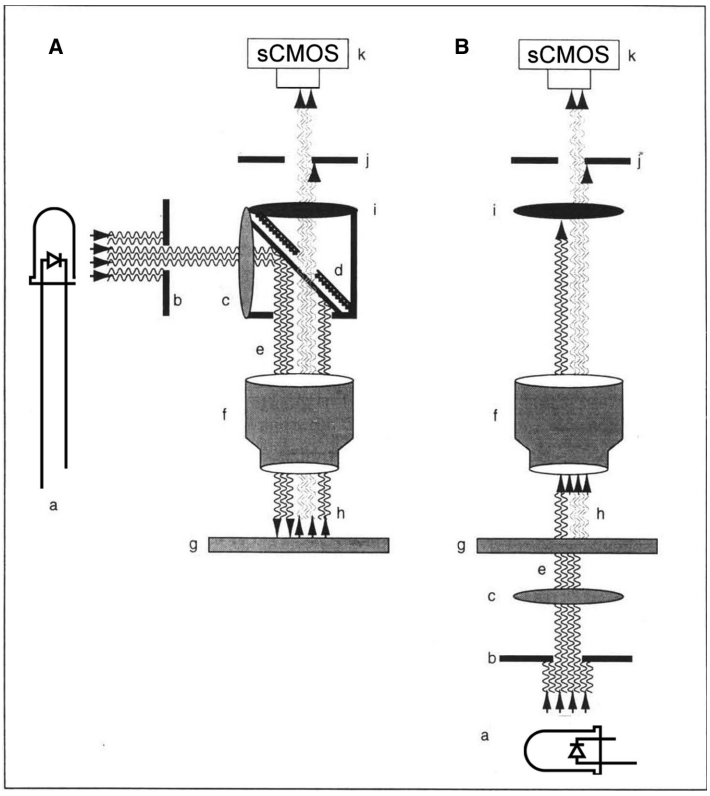

Figure 4.4.2 The concepts of (**A**) epi-illumination (incident), and (**B**) transmitted light as applied to fluorescence microscopy. Many of the major components are similar to those used with either type of brightfield microscopy (with the elimination of the filters which are labeled c and i here). Indicated in the diagrams are the (a) light source, now should be light emitting diode(s) (LEDs) or for specialty research microscopes, lasers, (b) stage condenser, (c) excitation filter, (d) dichroic mirror, (e) selected excitation wavelength, (f) objective, (g) microscope slide with specimen, (h) epi-illumination (in A) or transmitted (in B) illumination (short wave; darker) and emitted fluorescence (long wave; lighter), (i) barrier or emission filter, (j) eyepiece condenser, and (k) eyepiece or camera. In 2016, the standard monochrome digital camera should be a 4.2 or 5.5 megapixel scientific CMOS camera (sCMOS). These are available from Andor, Hamamatsu, PCO, and Photometrics. USB3 interface enables full chip imaging at 30 frames per second (fps); more expensive interfaces enable 100 fps. 30 fps is fine for "real-time" focusing by eye. Exposure time for acquisition of a single fluorophore might be a few milliseconds for DAPI interphase nuclei or metaphase chromosomes; 10s of milliseconds for bright immunofluorescence or overexpressed state of the art fluorescent proteins (e.g., mNeonGreen-Histone H2B), 100 milliseconds for "typical" immunofluorescence or DNA or single molecule RNA FISH on a current generation research or cytogenetics microscope, 1000 milliseconds (1 sec) for dim fluorescence such as single molecule RNA FISH with a non-optimized microscope.

episcopic, incident light fluorescence, or epi-fluorescence (*APPENDIX 3N*, Salmon & Canman, 2003), in the case of reflected light excitation. In incident light microscopy, the incoming light is first reflected down through the specimen and then back up through it into the objective (Fig. 4.4.2). Note that reflected light is useful for imaging thick objects that cannot be trans-illuminated (such as skin tumors, cells in live mice, or circulating blood cells using the handheld CytoScan, CapiScope HVCS Handheld Video Capillaroscopy System), or on microscope slides with monochromatic polarized illumination and a crossed polarizer for imaging highly scattering silver grains or immunogold. This latter configuration has high contrast and is commercially available from microscope and filter companies as an IGS filter cube (immunogold/silver staining). Since the excitation side polarizer only reduces excitation by 50%, a custom IGS cube has been made for the authors by Chroma Technology that has UV-green excitation + polarizer, a 10% reflection/90% transmission 45 degree beamsplitter, and green-near-infrared (NIR) + cross-polarizer emission filter. This custom

IGS can be used in standard IGS mode with green (546 nm) exciter, or with UV exciter for quantum dot fluorescence, or with Nomarski differential interference contrast (DIC) transmitted light where the emission polarizer serves as the DIC analyzer. This has the additional advantage of automating the DIC system on the authors' Leica RMRXA/RF8 (8-filter cube turret) microscope while eliminating the many-micrometer pixel shift introduced by the standard Leica DIC analyzer slider. The single-pass exciter filters were chosen to also enable single channel imaging with a triple DAPI/fluorescein/Cy3 filter set in the same microscope. The custom IGS cube was inspired by the non-reflective reflector fluorescence filter cube of Sawano, Hama, Saito, and Miyawaki (2002).

Oblique illumination, common on stereomicroscopes with a ring light or fiber optic gooseneck, is also possible for microscope slides, using the DarkLite illuminator (Micro Video Instruments) to illuminate through the edges of the slide. The DarkLite illuminator provides barely enough light for imaging silver particles and tissue by scattered light, but is not suitable for fluorescence when used with its standard light bulb. A special type of fluorescence excitation, total internal reflection fluorescence (TIRF), uses the glass surface the cells or molecules are on as a light guide. Essentially, the light is trapped in the high refractive index glass: The same principle is used in fiber optics in the communication industry. In TIRF, the light is trapped, propagating parallel to the glass surface, but fluorophores within ~100 nm in the low refractive index mounting media (i.e., cell culture fluid) are excited by the evanescent wave in the latter media. The advantage of TIRF is that only fluorophores very close to the glass-mounting medium interface are excited. This can include the basal plasma membrane of cells in close apposition to the interface. The evanescent wave energy falls off exponentially with distance into the mounting medium, and the depth can be controlled by adjusting the angle of light entering the glass slide. TIRF can be set up using a prism to couple the excitation light into the glass, or a high numerical aperture objective lens can be used, with the illumination restricted to the high NA portion. Special TIRF lenses are commercially available from Zeiss (NA = 1.45) and Olympus (NA = 1.45 or, with special expensive coverglass and toxic immersion media, NA = 1.65). See reviews by Oheim (2001); Axelrod, Burghardt, and Thompson (1984); Axelrod, (2003, 2013); or Jaiswal and Simon (2003) for additional details on TIRF.

Köhler illumination (*APPENDIX 3N*; Salmon & Canman, 2003) results in an evenly lit field of view and is used for all light microscopy. Epi-fluorescence microscopes use the objective lens for both excitation and emission. The excitation optical path of current fluorescence microscopes are equipped with field and numerical apertures, which are placed at appropriate conjugate optical planes for imaging. As long as they are reasonably well centered, and the numerical aperture fully opened to maximize brightness, epi-Köhler illumination is assured. For a few specific applications, such as high magnification, high numerical aperture imaging of single metaphase spreads or interphase nuclei for FISH, the field aperture can and should be reduced to just outside the diameter of the object of interest. This will reduce glare arising from excitation of auto-fluorescent mounting media in the area around the object, dramatically improving contrast. Using fresh mounting medium and optimizing FISH wash steps, will also reduce autofluorescence.

With respect to trans-Köhler illumination, there are many terms associated with microscopy that indicate the direction of the incoming light with respect to the angle at which it intercepts the sample and the side of the sample through which it first passes (Fig. 4.4.2). Brightfield microscopy (*APPENDIX 3N*; Salmon & Canman, 2003) is the most commonly used light-microscopic technique, and is the basis for phase contrast, polarization, and Nomarski DIC contrast methods. As the name indicates, in brightfield, the surrounding background is bright and the object is dark. The objects may be dark because of their scattering properties, endogenous pigments, or exogenous dyes. Light from the illumination source is transmitted along a pathway parallel to the optical axis directly through the sample into the objective. As light encounters the specimen, the intensity (or amplitude) is reduced compared to its surroundings, resulting in a darker appearance. The location of the illumination source defines the two types of brightfield microscopy. In transmitted light brightfield microscopy, the illumination source is directly below the sample for an upright microscope. As such, the light passes through the sample only once on its way from the source to the objective. Köhler illumination is the standard configuration for transmitted illumination of nearly all biomedical microscopes. However, because the

condenser can be lowered or raised, and moved laterally, it is up to the user to adjust the condenser field aperture centration and focus and numerical aperture setting. Because many samples do not contain sufficient absorption properties to be discerned with normal brightfield microscopy, one can generate contrast and reveal structures with low resolution by slightly rotating the condenser turret. This technique is referred to as oblique, anaxial, or asymmetric illumination contrast (Kachar, 1985).

Both transmitted illumination and incident illumination (epi-illumination) can be used for fluorescence. Older microscopes may use transmitted fluorescence illumination (trans-fluorescence), as in its pioneering use a century ago by Köhler and von Rohr. Trans-fluorescence with a bright arc lamp could be hazardous to the user if full intensity, unfiltered light were transmitted through the eyepieces. Trans-fluorescence went out of fashion in the decades after Bas Ploem introduced the Ploem-pak filter cube (Ploem, 1967), using a wavelength selective excitation filter, 45 degree angle dichroic beamsplitter, and emission filter. However, with modern interference filters acting as exciter and emission—eliminating the need for a beamsplitter or cube assembly—trans-fluorescence has uses, especially with a high numerical aperture condenser (Tran & Chang, 2001). Trans-fluorescence may be particularly useful on microscopes that have an arc lamp with a wavelength controller, i.e., filter wheel, shutter, and the Ellis light scrambler (fiber optic or liquid light guide to homogenize illumination) for DIC or other high resolution microscopies (Inoué & Spring, 1997; Reitz & Pagliaro, 1994). With a high sensitive CCD or sCMOS camera, and interference filters, even a standard tungsten-halogen lamp could serve as a light source for visible and near infrared excitation (these lamps produce little UV however, making them practically useless for DAPI or blue fluorescent protein [BFP] excitation). Trans-fluorescence may be particularly useful for thick specimens, such as mouse brain slices, combined with large Stokes shift dyes, the idea being that the shorter wavelength excitation light may penetrate through only part of the specimen, whereas the longer wavelength NIR fluorescence emission may get through the specimen to the objective lens and detector. This could complement the infrared DIC-videomicroscopy method of Dodt and Zieglgansberger (1994). Fluorescence microscopy is dominated by fluorophores that emit in the visible, since "seeing is believing." With the increasing use of "no eyepiece" microscopes and high content imaging systems, and especially to increase multiplexing, expanding the wavelength range is becoming more popular. We discuss later both UV and NIR fluorescence applications.

Darkfield microscopy can be used to obtain resolution of objects or features that are normally below the resolution of the light microscope. This is only possible with transmitted illumination because no direct light is allowed to enter the objective. Only incoming light diffracted, refracted, or reflected by the specimen enters the objective, resulting in bright objects on a dark background. One note of importance is that the numerical aperture of the condenser must be higher than that of the objective. This technique is incompatible with the use of phase contrast microscopy in association with fluorescence. Darkfield microscopy also requires scrupulously clean optics and slides, because any dirt will cause light to be scattered into the objective and mar the image quality. This is because darkfield has an effectively large depth of field and many microscope optics accumulate dust and dander because the microscopes are not sealed to allow heat to escape. Conversely, the large depth of field could be useful for tracking objects in relatively large volume, though most of the objects will appear out of focus (making them larger, which could in turn improve the centroid XY location precision by image measurement of the larger object).

Differential interference contrast (DIC; *APPENDIX 3N*; Salmon & Canman, 2003; Allen, David, & Nomarski, 1969) can be performed at high numerical apertures, gives better resolution than darkfield microscopy, and can be used in conjunction with fluorescence microscopy and live-cell imaging. DIC is referred to as an optical sectioning technique, because for transparent objects, soon after it leaves the focal plane it disappears. The DIC technique involves polarized light plus a pair of matched Wollaston prisms (Nomarski DIC) or similar light path splitters (Smith DIC). The incoming light is first passed through a polarizing filter that only allows waves oriented in the same direction to pass through the filter. Each plane-polarized light beam is then split into two separate beams containing perpendicularly oscillating components with a Wollaston prism (composed of two quartz prisms cemented together with their optical angles

oriented at 90 degrees with respect to each other). Thickness and refractive index differences within the specimen generate opposing phase shifts in the two halves of the split beam. A second Wollaston prism placed after the objective recombines the halves of each split beam. Constructive or destructive interference occurs as a result of the phase shift between the two separate beams. The light then passes through another polarizing filter (analyzer) and is visualized as differences in gray-scale levels across the specimen. The bas-relief of DIC is due to differences in refractive index, and not the three-dimensional topography of the specimen. Allen and coworkers (Allen, Travis, Allen, & Yilmaz 1981a; Allen, Allen, & Travis, 1981b), and Inoué (1981) independently introduced the advantages of video enhanced polarization (VEC-Pol) and differential interference contrast (VEC-DIC) for imaging unstained cells. Holzwarth and coworkers (Holzwarth, Webb, Kubinski, & Allen 1997; Holzwarth, Hill, & McLaughlin, 2000) have described polarization-modulation DIC hardware that switches the bas-relief with each image, followed by an image difference (plus offset) mathematical operation to double the edges. As anyone who has worn polarized sunglasses knows, polarizers can reduce glare. In light microscopy, polarized light is used for imaging birefringent structures such as chromosomes and/or mitotic spindles (Inoué & Dan, 1951; see also Inoué & Spring, 1997).

Phase contrast microscopy (*APPENDIX 3N*; Salmon & Canman, 2003) is an alternative to DIC that converts normally invisible phase changes as light propagates into and out of interfaces of different refractive indices (culture media-plasma membrane, plasma membrane-cytoplasm, cytoplasm-organelle membrane, organelle membrane-contents, and back out) or through thick slabs of such contents (thin versus thick cytoplasm). Phase contrast is an excellent mode for reviewing metaphase spreads on microscope slides before deciding what areas on what slides to carry out FISH or Giemsa staining. The invention was justly honored with a Nobel Prize (Zernike, 1955). Zernike pointed out the irony that when brightfield imaging ultra-thin, transparent objects, the best focus makes the object invisible. He recognized that the light propagating through the object would delay (or advance) the wave, and worked out a way to convert phase to intensity. The firm of Carl Zeiss famously exhibited a lack of interest, initially, but eventually reversed itself. A phase annulus (ring) in the condenser only allows a ring of light to reach the condenser. Focusing of this ring by the condenser lens generates a hollow cone of light that is projected onto the back focal plane of the objective. Some of the light waves are retarded as they pass through the sample. This is due to absorptive differences among cellular structures and differences in refractive index or thickness. As a result, their phase is shifted relative to those waves from the original light source, which have not encountered phase dense objects. These phase shifts are usually not sufficient, however, to generate full constructive or destructive interference visible with normal brightfield microscopy. The standard dark-light (DL) phase ring in the back focal plane of the objective absorbs 70% to 80% of the non-diffracted rays. In the absence of an object, this only has the effect of reducing brightness slightly. The phase ring crucially shifts the phase by one quarter of the wavelength for the diffracted rays. This arrangement alters the amplitude and phase relationships of the diffracted versus non-diffracted light, thereby enhancing the contrast. Regions with a higher refractive index usually appear darker, with the standard DL design. Objects with too high a refractive index or thickness can result in a rather large phase shift and cause a contrast reversal (i.e., a positive phase shift of 1.5 λ would appear identical to a negative phase shift of 0.5 λ). The phase ring is optimized for monochromatic light of 546 nm (a mercury arc lamp line), so best results are achieved with a monochromatic green filter, though satisfactory results are obtained with a fairly broad pass green interference filter (GIF, or fluorescein emission filter, 510 to 540 nm). Either green filter will also enhance contrast of Giemsa stained chromosomes or nuclei, and can be useful for imaging hematoxylin and other absorption dyes.

Microscope manufacturers also offer limited numbers of special phase contrast lenses, such as the dark-medium (DM) design. A key advantage for phase contrast when imaging single cells by eye is that, with the DL design, a bright phase halo surrounds the dark cell, making the invisible angelic. However, the same halo results in difficulties for precise image analysis of the cells, especially in ultra-thin regions such as lamellipodia or filopodia, where the contrast of edge of the cell and halo disappear due to the weakness of the phase difference. The phase ring in the objective lens absorbs some of light. This is not an issue for phase contrast brightfield illumination, where

even a tungsten-halogen lamp provides plenty of light, but the ring does reduce somewhat the intensity of fluorescence.

In 2002, quantitative phase amplitude microscopy (QPm), a mathematical method using three (or more) brightfield images of different focus positions, was described by Barone-Nugent, Barty, and Nugent (2002). QPm can be performed in software with either conventional brightfield microscope images or with the "free" (but not confocal optical sectioning) transmitted light image of a confocal microscope (Cody et al., 2005). QPm can be done as an off-line post processing, and produces quantitative phase maps that are independent of any absorbing features present in the specimen (provided the entire specimen is not black). Source code for a version of QPm was posted in the supplemental files of Phillips, Baker-Groberg, and McCarty (2014). The phase maps can be used directly (refractive index measurement) or can be recombined in a user-adjustable manner with the absorbing features. The phase maps can also be digitally converted into Nomarski DIC or phase contrast like images, with or without absorbing features. We have not seen QPm used on metaphase chromosomes or cell nuclei, but the method may produce interesting chromosome maps or a novel form of nuclear texture analysis. Hopefully, in the future, the refractive index measurements can be combined with digital deconvolution algorithms to improve 3D deconvolution fluorescence microscopy.

There are many occasions when it is useful to follow the movement of cells or their organelles as a function of time. Studies of cell division, movement of chromosomes and centrosomes, and the polymerization of mitotic tubules are a few examples. Such analysis involves the successive microscopic imaging of live cells, rather than a single image of a fixed specimen. There are two different methods for accomplishing such an analysis. The first, time-lapse microscopy, involves the acquisition of individual images at distinct time points or intervals (e.g., every 10 min over an 8 hr period). These images can then be integrated into a single composite image and displayed simultaneously for an easy comparison of changes as a function of time. Video microscopy, however, involves near-continuous imaging over a prolonged time period, as one would do with a standard video camera that has a rate of 30 frames/sec. If continuous observation is not required, a computer controlled shutter can be added to the system, and a few video images may be captured and averaged, or a single exposure with a digital CCD camera, can be captured on demand. A thorough treatment of this technique, which is beyond the scope of this chapter, can be found in Spector et al. (1998), Goldman and Spector (2004) or Yuste and Konnerth (2005).

MICROSCOPE OBJECTIVES AND EYEPIECE LENSES

The compound light microscope must be equipped with the highest-quality optics (objectives and eyepieces), must be precisely aligned, and must have the proper filters installed to observe and record all relevant information from the objects under study. A detailed manual outlining the steps required to align the microscope is available from the manufacturer of the respective microscope and is discussed in *APPENDIX 3N* (Salmon & Canman, 2003). The importance of proper alignment cannot be overstated. An excellent discussion of microscopy and photography is presented in *The ACT Cytogenetics Laboratory Manual* (Barch, Knutsen, & Spurbeck, 1997) and in *Human Cytogenetics: A Practical Approach* (Rooney & Czepulkowski, 1992). Both references are invaluable resources for the cytogenetics laboratory. High-quality objective lenses are critical for obtaining maximum information in the study of biological specimens. Lenses condense light and magnify the image. The objective lens system must have high resolving power and correction for lens aberrations. The resolving power, R, of a lens is defined as the minimum distance by which two luminous points can be separated and still be discerned as distinct objects using that objective. R is described by the theory of optical diffraction as:

$$R = 1.22\lambda/(2 \times \mathrm{NA})$$

where λ is equal to the wavelength of the incident light and NA is the numerical aperture, a measure of the light cone entering the objective at the fixed objective distance (James & Tanke, 1991; Rawlins, 1992). The value of NA is given by:

$$\mathrm{NA} = \mathrm{n} \sin \alpha$$

with n equal to the refractive index of the medium between the objective and the sample and α equal to half the vertical angle of the light cone (Fig. 4.4.3). The NA is restricted for technical reasons to a maximum of 1.35 to 1.44 for glass objectives and oil immersion media (refractive index 1.515) and is usually indicated

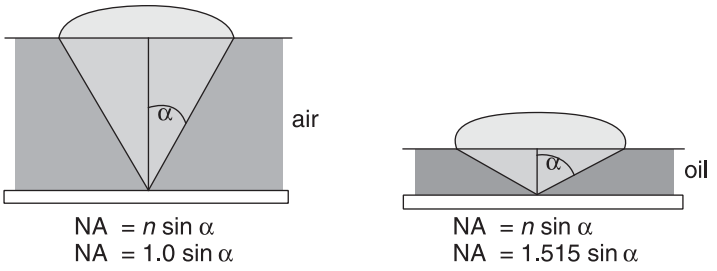

Figure 4.4.3 Diagrammatic explanation of numerical aperture. As α approaches 90 degrees, sin α approaches 1.0. The refractive index of the medium between the sample and the objective is designated as *n*. Standard fluorescence microscopes use epi-illumination and detection through a common path (see Fig. 4.4.2A). Epi-illumination is superior for fluorescence than transmitted light (Fig. 4.4.1). Some applications benefit from total internal reflection fluorescence (TIRF) excitation, through the coverglass, or "light sheet" illumination from the side(s) of the specimen. The light is still collected the same way—numerical aperture applies to emission with TIRF or light sheet enabling new applications. TIRF is briefly described in Appendix 4.4.2 (see Supporting Materials): Total Internal Reflection Fluorescence (TIRF) Microscopy. Light sheet applications are briefly described in the text along with a major opportunity to synergize with expansion microscopy for single cells, optically cleared tumor masses, and developing whole organisms (worms, zebrafish, and whole mice).

on the side of the objective. Special objective lenses in the NA 1.42 to 1.47 NA range are available for the conditions and applications of total internal reflection fluorescence (TIRF), for fluorescence at a coverglass-aqueous solution interface, discussed in Appendix 4.4.2 (see Supporting Materials). High NA results in the smallest lateral resolution, smallest axial resolution, and maximum capture of light photons. This is particularly important in fluorescence microscopy, where the amount of emitted light is often very small. The brightness of the captured light is affected by many different parameters, including the concentration of the fluorophore, the transmission of light through the optics, the total magnification, and the numerical aperture of the objective (and the condenser, in the case of transmitted fluorescence). The relative image brightness in epi-fluorescence microscopy is given by the equation:

$$B = \left(\text{N.A.}_{\text{obj}}\right)^4 \ \text{Mag}^2$$

when the so-called "object space" between the objective and coverglass contains air (as with a "dry" objective), the numerical aperture cannot exceed 0.95. However, when immersion oil with a refractive index of 1.515 is used between the two surfaces, an NA of 1.35 to 1.40 can be obtained. This is because the refractive index of the oil is identical to that of the glass slide, coverglass and objective. This prevents the light from being refracted as it passes from the specimen through these other materials. Immersion media include various natural and synthetic oils (with varying *n* values), water ($n = 1.333$), and glycerol ($n = 1.466$ for 100% glycerol, 1.391 for 40% glycerol:60% water, at 23°C). Immersion objectives are usually produced for use with a specific type of immersion medium and are so indicated on the side of the objective; "dry" objectives will not function as immersion objectives. Immersion oil with low fluorescence is required for fluorescence microscopy, and the objective manufacturer can help obtain the proper type.

In addition to resolving power, which is a function of both magnification and numerical aperture, modern light microscope objectives must correct for problems of spherical and chromatic aberration. Spherical aberration is produced by failure of the curved surface(s) of a lens to direct all light rays passing through the lens to the same focal point. A coverglass of the incorrect thickness or a refractive-index mismatch (i.e., wrong immersion oil) can also cause spherical aberration and an inability to focus. Early microscopes (single or compound lenses) suffered from loss of fine detail due to chromatic aberration that resulted in rings of color around small objects. White light passing through the lens is broken up into its constituent colors. Different wavelengths are diffracted to different extents, and hence have different focal points. After 1820, achromatic lenses were developed, allowing great advances in biology and medicine (Inoué & Spring, 1997; Kapitza, 1996). Achromatic objectives are rather simple in that spherical aberration is corrected for the middle range of the light spectrum,

thereby directing all broken-up wavelengths to the same focal point. Plan-achromatic objectives are more complex and have the advantage of less curvature-of-field aberration than ordinary achromatic objectives. Curvature of field is caused when light passing through the periphery of the objective is focused closer to the back focal plane of the lens than light passing through the center. The result is a discrepancy in focal plane between the center and periphery of the field of view. Plan-apochromatic objectives are costly, complex, flat-field objectives that offer the greatest correction for chromatic and spherical aberration. The type of correction supplied by the objective is also indicated on its side. In the past, fluorite (synthetic quartz) and plan-fluorite lenses were required for deep UV excitation, for example, for 340 nm excitation of Fura-2, because apochromat lenses had many UV-absorbing glass components. Modern (post 1997) plan-apochromat lenses often, but not always, transmit light down to 300 nm. If this may be important, as in Fura-2 or to truly maximize quantum dot excitation, transmission curves should be obtained from the manufacturer, or several lenses should be tested in the lab. As biologists expand our color palette, wanting to use our microscopes for imaging specimens from UV (<380 nm) to near infra-red (e.g., Cy5.5, Cy7, NIR quantum dots), and excite with UV lasers (337 nm nitrogen laser dissection) to NIR (two-photon and three-photon excitation, 600 to 1200 nm), we are discovering that apochromat often means visible light only. Manufacturers are starting to supply lenses that match our expanded palette. The addition of special accessories, such as the Neil, Juskaitis, and Wilson (1997) "structured illumination grid," commercialized in OptiGrid (Thales Optem), Apotome (Zeiss), and "electronic light modulator" (Keyence) that project a grid pattern (placed at the epi-illumination field aperture) onto the specimen, quickly reveal how un-chromatic most current research epi-illumination light paths are.

FLUORESCENCE MICROSCOPY

Many molecules, especially those with conjugate planar rings (e.g., benzene) absorb light. The larger the planar ring structure, the longer the wavelengths of light that can be absorbed. At room temperature, the molecules are at various vibration energies, which result in broadening of the spectra. Some molecules absorb light, boosting an outer shell electron from its ground state (S_0) to the first excited singlet state (S_1) and efficiently lose the acquired energy to surrounding molecules, such as water, and thus return to the ground state (S_0). Other molecules, absorb light energy at one wavelength and either lose all the energy to surrounding molecules or lose a part of the energy to the surroundings but emit most of the energy as light (fluorescence) at a longer wavelength. Considering one photon and one molecule, the absorption event (now also referred to as excitation) occurs in femtoseconds (10^{-15} sec), the initial vibration energy loss occurs in picoseconds (10^{-12} sec), while fluorescence occurs in the nanosecond range (10^{-9} sec). All compounds that absorb in the visible light range, such as Perkin's mauve, are called chromophores. Those molecules that efficiently emit photons, whether in the UV (tryptophan), visible (fluorescein), or near infra-red (Cy5.5) are termed fluorochromes or fluorophores. The efficiency with which molecules absorb light is characterized by the extinction coefficient, ε, whose units are $M^{-1}cm^{-1}$. The efficiency of fluorescence is the ratio of light emitted divided by light absorbed, which is termed quantum yield (QY). A convenient way to compare fluorophores is to calculate the brightness index (BI), of each, where $BI = \varepsilon \times QY / 1000$. For green fluorescing dyes, the xanthene dye, fluorescein, $\varepsilon = 90{,}000\ M^{-1}cm^{-1}$ and QY = 0.92 (both for pH ≥8), resulting in $BI_{fluorescein} = 82.8$. The cyanine dye, Cy2, has a higher extinction coefficient, $\varepsilon = 150{,}000\ M^{-1}cm^{-1}$ and QY = 0.12 (relatively pH independent), resulting in $BI_{Cy2} = 18$. A more useful cyanine dye is the orange fluorescing Cy3, with $\varepsilon = 150{,}000\ M^{-1}cm^{-1}$ and QY = 0.15 (relatively pH independent), resulting in $BI_{Cy3} = 22.5$. A newer, rigidized cyanine dye, Cy3B has a very similar extinction coefficient of $\varepsilon = 120{,}000\ M^{-1}cm^{-1}$ but with a QY = 0.67, Cy3B's $BI_{Cy3B} = 87.1$. Table 4.4.2 (at end of article) summarizes the performance of many useful fluorophores.

Of the conventional fluorophores, B- and R-phycoerythrin and allophycocyanin stand out. These molecules are very useful in flow cytometry, because of their brightness, they excite well with the typical 488 nm laser line, and can serve as efficient FRET donors to near-infrared dyes. However, all three are based on multiple dyes in protein complexes and photobleach very rapidly in fluorescence microscopy. DAPI and Hoechst 33258 (H33342 is similar) fluoresce poorly as free dyes in aqueous media—a good property to keep the background low—and have substantially higher brightness indices in non-aqueous solvents. Both of these

dyes bind well to DNA, resulting in high local concentrations, and the DNA shields these two fluorophores from water, enhancing fluorescence. As a consequence, while not having exceptional photophysics, DAPI and the Hoechst dyes are brilliant DNA counterstains. DAPI only fluoresces in AT-rich DNA, which results in the characteristic R-banding pattern.

A new class of products—fluorescent nanocrystals, or quantum dots—are highly photostable, high absorbing, good quantum yield molecules (typically CdSe, CdS, CdTe, and/or ZnS) encased in a bio-compatible coating that enable coupling to streptavidin, antibodies, other proteins, and haptens such as biotin (Bruchez, Moronne, Gin, Weiss, & Alivisatos, 1998; Chan & Nie, 1998). In 2016, Qdots have not taken over any fluorescence microscopy market niche (i.e., cell biology, cytogenetics, flow cytometry, or pathology). A combination of "old school is good enough," aggregation issues with some (maybe many) production lots, atypical excitation → emission requirements (405 or 488 nm excitation, Qdot### specific emission wavelengths), lack of synergy between Qdot reagent vendors, microscope vendors, and spectral imager vendors, and lack of enthusiasm of those who owned spectral imagers, may have each contributed. The new "great bright hope" are the Brilliant polymers (BD Biosciences, BioLegend), based on the Nobel Prize in Chemistry (2000) work on conductive polymers by Alan J. Heeger, Alan MacDiarmid, and Hideki Shirakawa (and colleagues and competitors). Both Qdots and Brilliants are tabulated with key photophysics parameters, in Table 4.4.2, along with an extensive, though not exhaustive, list of conventional fluorescent dyes.

In order to grasp the principles of fluorescence, it is necessary to further understand the laws describing light. Energy behaves in accordance with Planck's law, which states:

$$E = h\nu = hc/\lambda$$

where E is energy, h equals Plank's constant, ν equals light frequency, c equals light velocity, and λ equals light wavelength. Thus, energy is linearly proportional to the light frequency and inversely proportional to its wavelength. The quantum of energy (E) is greater for radiations of shorter wavelengths, such as UV, than for radiations of longer wavelength, such as infrared. Wavelengths in the UV spectrum (300 to 380 nm), visible light spectrum (380 to 700 nm), and near infrared (700 nm to 1000 nm) are nowadays used in fluorescence. The spectral characteristics of individual fluorophores and fluorescent proteins are dependent upon the regions of the light spectrum where absorption (excitation) and emission of light energy occur. Stokes' law states that the average wavelength of emitted fluorescence is longer than the average excitation wavelength for any given fluorophore. The longer wavelength of the emitted light is due to the rapid loss of some vibration energy in the first picoseconds post-absorption (with a spectral confocal microscope and bright fluorescent objects, the anti-Stokes emission can be detected—however this is a small fraction of the Stokes emission). Multi-photon excitation fluorescence works by having two low energy photons, for example 800-nm wavelength each, reach the molecule at the same time (femtoseconds). This results in an excitation event equivalent to absorbing an ~400-nm photon, and fluorescence practically identical to that of 1-photon excitation. At the quantum mechanical level, the selection rules for 1-, 2- and 3-photon excitation do differ, which leads to some dyes working poorly, and others—such as quantum dots—exceptionally well, for multi-photon excitation.

We use as an example, DAPI (4,6- diamino-2-phenylindole), a fluorescent dye with affinity for A-T residues in DNA. This is often used to give a chromosome banding pattern (R-banding) complementary to that obtained with Giemsa staining (*UNIT 4.2*; Schreck & Distèche). A simple digital image-processing step, "inverse contrast," is thus able to transform a DAPI-stained metaphase spread into a Giemsa-like staining pattern. An additional sharpening step then improves the banding to near G-band quality. It is also useful as a DNA counterstain for interphase nuclear studies, where, for example, flat tissue culture cell nuclei can be identified as human or mouse on the basis of dark nucleoli versus bright centromeres, respectively (the comparison only works for human versus *Mus musculus* nuclei; e.g., bovine, other mice have other structures). The energy absorbed at 350 nm raises an electron to a higher excitation state. Some of the energy is then lost to vibration. When the electron falls back to its starting, or ground, state the energy is released as fluorescent light. Because the amount of energy is less than the input, the emitted light has a longer wavelength (the mode being 470 nm) and is said to be red-shifted. With fluorescence lifetime spectral imaging it is possible to measure that the molecules that emit rapidly (1 nsec) tend to emit shorter wavelengths (higher

energies) than those that emit slowly (5 nsec). The latter are red-shifted because they have had more time to lose more vibration energy to the surrounding molecules. Fluorophores can also give up some or all of their energy to other molecules. Many excited fluorophores can have the excited electron transition from the first excited singlet state (S_1) to the slightly lower energy first triplet state (T_1). This is referred to as intersystem crossing. The triplet state can be very long-lived, microseconds (10^{-6} sec) to milliseconds (10^{-3} sec), after which delayed fluorescence (if it flips back to the S_1 state) or phosphorescence (emission directly from the T_1 to the ground state) can occur. However, when in the T_1 state, the energy may be transferred to a nearby normally triplet state oxygen molecule ($O_2{}^3$), which flips to the highly reactive singlet state ($O_2{}^1$). The singlet oxygen molecule can convert to oxygen radicals, all of which are highly reactive. Since the fluorophore and the reactive oxygen molecule are in close proximity, they often react, resulting in destruction of the fluorophore. Sometimes the reaction can be taken advantage of, as in the in the reaction of superoxide with non-fluorescent hydroethidine to make a fluorescent ethidium dye (Haugland, 2004 and *http://www.probes.com/handbook/*). More generally, an excited fluorophore may donate its energy to another molecule, the acceptor, which if it is an efficient fluorophore, may then emit at its characteristic wavelength. This process, is non-radiative (the light is not emitted and then re-absorbed), and when the transfer occurs with an efficiency that falls off as distance to the sixth power, is termed Förster-type fluorescence resonance energy transfer (FRET; Förster, 1965; Jares-Erijman & Jovin, 2003).

Some fluorophores, however, may require an excitation energy that overlaps with the emission energy of another fluorophore. This fact must be considered when setting up an experiment involving the simultaneous use of more than one fluorophore. It is crucial to note that spectral properties of some fluorophores are subject to significant environmental effects and vary depending on measuring conditions, e.g., medium, pH, and substrate (Haugland, 1996; Mason, 1993).

Understanding the spectral properties of various fluorophores is important when choosing components of the microscope used in fluorescence microscopy. This includes the light source (Xe or Hg) as well as the filter(s). To generate and observe fluorescence requires a fluorophore bound to a molecule. This can be a fluorophore bound either directly to a nucleic acid probe or indirectly, through the use of haptens (such as biotin and digoxigenin) and fluorescently conjugated moieties with which they interact (avidin and anti-digoxigenin antibodies, respectively). Another source of fluorescence tagging is fusion of the GFP or any of its many derivatives directly to a protein of interest. A light source and optical filters are required to produce the correct wavelength(s) of light energy required for excitation of the fluorescent moiety. The light passing through or being emitted by the sample must then pass through another set of optical filters, such that emitted light energy of only the desired wavelength reaches the detection system (i.e., eye or another detector; Fig. 4.4.2). Details of these requirements are elaborated in the following sections.

LIGHT SOURCES

Old School

The standard light source for brightfield microscopy has been a tungsten-filament bulb. Bulbs are now losing favor thanks to the improvements in white light light-emitting diodes (LEDs). The intensity of a bulb is controlled by changing the amount of current flowing to the lamp via a rheostat dial; this has the undesirable effect of changing the color temperature. The use of white light LEDs ensures consistent color balance at any light level.

The light sources used in fluorescence microscopy used to be mercury or xenon arc lamps, or metal-halide lamp. These are now being superceded by high intensity LEDs or lasers (discussed below). The choice of whether mercury or xenon arc lamp was determined by the wavelengths of excitation energy needed to excite the fluorescent molecule being used as a probe. In turn, this limited useful fluorophores to those that worked well with the mercury or xenon lamp and filter sets on hand. Mercury lamps have three main peaks of excitation light around 440, 550, and 580 nm, whereas xenon lamps are more uniform in their intensity across this range. An additional mercury peak around 365 nm in the UV range is important for the imaging of DAPI-stained objects (i.e., DNA). Both types of bulbs have been available in a number of different wattages. Brighter lamps result in more intense fluorescence and therefore a shorter exposure time is required. A 100-W bulb also has a longer operating life than a 50-W bulb (200 hr versus 100 hr). LEDs have 10,000+ hr!

Solid state lasers (diodes) have similarly long lifespans to LEDs, and laser light is monochromatic (single nm wavelength, e.g., 488 nm). LEDs and lasers are discussed further below. Another important parameter is the gap between the anode and cathode in the bulb itself. This is known as the arc gap. Small gaps provide a small arc that can emulate a point source for epi-Köhler illumination.

It is important to monitor the bulb use because older bulbs result in weaker fluorescence signals. This will affect exposure settings, which is more important when using photographic film, because it is easier to retake the image with a digital-imaging device. Also, mercury bulbs should not be used >200 hr because there is a risk of explosion that can damage the microscope. Changing and aligning the bulb requires patience and skill and is often best performed by the microscope service representative.

New School and Why You Should Switch

When purchasing a new light microscope, the transmitted light should now (i.e., 2017) be LED based. Fluorescence cost-benefit and performance, are now favoring LED or laser over mercury, xenon, or Hg-Xe arc lamps, or metal halide lamps. Besides being energy inefficient (heat more than light), requiring replacement every 100 to 1000 hr (typical rating is 300 hr), high pressure Hg arc lamps sometimes explode. This is most likely to happen when someone is trying to adjust the lamp. While most lamps have some safety protections so glass shards do not blast into your face, why take the risk anymore. Even without an explosion and medical costs, the total cost of ownership now favors LEDs or lasers for fluorescence illumination. High intensity epi-fluorescence LED lamps are now as bright as arc lamps or metal halide. Combined with LED optimized filter set(s), these greatly outperform every lab's "old" illumination setup. A basic fluorescence four-wavelength LED with liquid light guide is available for under $3,000 (*https://www.thorlabs.com/newgrouppage9.cfm?objectgroup_id=3836*; the microscope-specific adapter cost depends on the microscope, usually under $200), with more and brighter LEDs and computer control adding to the price.

We are especially excited by recent developments in laser light sources for fluorescence microscopy. Each modern laser is monochromatic (1 to 3 nm full width at half maximum and the same as full width at 5% maximum), providing a big "effective power per nm" advantage over LEDs (10 to 30 nm band full width at half maximum, but much wider full width at 5% maximum, requiring a bandpass filter to cut off these tails). Modern hard coated filter sets can in turn be optimized for the laser lines, and then the emission light path can be optimized to take advantage of essentially all emission photons. For example, with a six laser line system, say 405, 440, 488, 514, 550, 633 nm, with 5-nm blocking for each wavelength, the emission range from 410 to 810 nm, would have 25 nm blocked by the laser safety emission bandpass (so for a 400 nm range—25 nm = 375 nm collectible photons—the dichroic would also help make the light path safer; a typical dichroic reflects 99%, so it transmits ~1% [1e-2], whereas an optimized emission filter blocks 1e-6. A key issue is the price point of this "laser stack": Imagine if it is under $20,000). Conceivably, one filter cube could serve all six laser lines, then an emission filter (or six or more cameras with appropriate image splitters), would enable multiple wavelengths acquired per laser line. Such a setup would decrease the number of moving parts: The upshot is that we expect with LEDs, and especially lasers, and computer processing, to be able to acquire multiple channels in a shorter time than is done now. This will enable light microscopy to compete with both flow cytometry (which needs single cells, so no more spatial information) and other approaches, such as "imaging mass cytometry." Multiplexing with speed and high spatial resolution could enable efficient multiplex single gene DNA FISH, single molecule RNA FISH, and high sensitivity immunofluorescence, to be imaged and quantified simultaneously, on isolated cells, "touch preps," fine needle aspirates, tissue sections, and modestly thick tissues. In 1996 many cytogenetics and pathology labs acquired on film, printed on paper, and cut out chromosomes and cells of interest with scissors; in 2006 CCD cameras and any color you wanted as long as they were DAPI, fluorescein, Cy3, and Cy5 were in vogue. In 2017, sCMOS and LEDs are becoming common in the research setting (although cytogenetics is lagging behind). In 2027, we hope everyone is able to acquire and process all their images in "one click."

Filters

Fluorescence microscopes use filters in several positions in the excitation and emission light paths to select specific wavelengths. Modern microscope filters use an

interference coating, with the glass substrate carrying vacuum-deposited thin layers of metallic salt compounds (see *http://micro.magnet.fsu.edu/primer/java/filters/interference* for tutorial).

These filters maximize the advantage of fluorescent reagents: The excitation wavelengths and emission wavelengths are different. Under almost all conditions the emission is longer than the excitation. For example, fluorescein is typically excited ~488 nm, close to its excitation spectrum peak, and emission wavelengths ≥500 nm directed to the detector (eye, camera, photomultiplier tube). Traditional mercury arc lamps, or a similar LED, might use a 480 to 500 nm excitation filter (Fig. 4.4.2A, component c) and 510 to 540 nm bandpass emission filter (Fig. 4.4.2A, component i). A key component in an epi-illumination microscope is the dichroic beamsplitter (Fig. 4.4.2A, component d): Dichroic is two colors; in this configuration, short wavelengths (<500 nm in our fluorescein example) are reflected down (Fig. 4.4.2A, e) to the objective lens (Fig. 4.4.2A, f) and specimen (Fig. 4.4.2A, h), the emitted fluorescence light is collected by the objective lens, and since the longer wavelength is transmitted through the dichroic (Fig. 4.4.23A, d, again), through the emission filter (Fig. 4.4.2A, i)—optionally conditioned by an aperture (Fig. 4.4.2A, j, not required)—to the detector (Fig. 4.4.2A, k). The dichroic and emission filter collaborate to block unwanted excitation light that may be reflected from the specimen (coverglass and slide each reflect ~3% of light back). The use of a bandpass emission filter (510 to 540 nm here for fluorescein) also helps select against autofluorescence (typically very broad), and other fluorophores that are excited by the current excitation wavelength (490 to 500 nm in this example). The other fluorophores can be best imaged with optimized filter sets for each.

The key to successful fluorescence microscopy is effective selection of excitation and emission wavelength ranges that (1) enable efficient fluorescence of one fluorophore at a time, and (2) prevent fluorescence, or at least minimize detection of fluorescence, from the other fluorophores and autofluorescence of the specimen. Good filters are the critical to success. We suggest that the "priority list" of improvements to be made to upgrade an old fluorescence microscope would be new filters > new sCMOS camera > new objective lens(s). Any list of available filters and/or filter sets would be incomplete and therefore misleading to anyone getting started with fluorescence microscopy. A list of vendors and their Web sites has therefore been included at the end of this unit (Table 4.4.3 at end of article) and a continually updated version will be maintained on our Web site (*http://www.geomcnamara.com/light-microscopy-websites*). A discussion with each manufacturer stating the nature of the experiment, illumination source available, and fluorophores to be used (particularly for samples labeled with multiple dyes) is highly recommended prior to the purchase of any filter or filter set. Fluorophores commonly used in fluorescence microscopy and for which filters are typically needed are DAPI, Hoechst, quinacrine, or propidium iodide as DNA counterstains, as well as fluorescein isothiocyanate (FITC), Texas red, rhodamine, and other fluorophores emitting in the far-red portion of the spectrum as probe-specific labels (see Table 4.4.2 for an extensive list of fluorophores). Filters are usually supplied in sets, and consist of an excitation filter, a dichroic mirror, and an emission filter. These are often contained within a device known as a filter cube, which are pre-aligned, easy to handle, and go easily into the filter holder or turret of the microscope.

Filter sets also differ in the amount of light they permit to pass. There is usually a trade-off between brightness and selectivity. Short-pass filters allow all light shorter than a particular wavelength to pass through to the specimen, while long-pass filters only allow the passage of longer wavelengths. These types of filters are therefore not very restrictive in their transmission range. Band-pass filters are more selective in that they transmit one (or more) particular region(s) or band(s) of the light spectrum. This means that wavelengths both shorter and longer than the excitation wavelength are blocked. Narrowband-pass filters have a much more restricted range of transmitted wavelengths compared to wide-pass (or broad-pass) filters. Broad-pass filters, because they allow more light through, result in a brighter image but include a broader spectrum of wavelengths. Band-pass filters now have high light transmission values (>90%) and very narrow band characteristics that allow selective excitation of one or more fluorophores. The use of lasers (confocal microscopes, flow cytometers, some widefield research microscopes), simplify the excitation side: Each laser line is an ~1 nm wide wavelength. The newest solid-state lasers (often

laser diodes) are electronically controlled and "instant" on and off, enabling use of a single laser line at a time. An all solid-state laser excitation microscope would eliminate the need for excitation filters (Fig. 4.4.2A, c), simplify and make more efficient the dichroic filter position to be a notch or multi-notch filter (Fig. 4.4.2A, d) to simply reflect the laser lines (on excitation, to the specimen; on the return, unwanted reflections would be directed back along the excitation path, that is, away from the emission path). Such a "laser dichroic" or "laser multichroic notch filter" would transmit more emission wavelengths, for example, for fluorescein 488 nm excitation, "all but 488 nm" through the dichroic; 490 to 540 nm through the emission filter (Fig. 4.4.2A, i). Optionally, the emission filter could be fixed in place (with a multi-line notch filter, "one filter cube to use them all") and an emission filter wheel could handle the emission wavelength selection (the wheel might be inside the microscope, or mounted between the microscope camera port and camera).

Dual- and triple-band-pass filters, which permit concurrent visualization of two or three fluorophore combinations, are available. These are mostly for use by eye, since the best cameras are monochrome and are best used to image one fluorophore at a time. These are useful for the simultaneous excitation and detection of multiple fluorophores immunostained or DNA or RNA probes hybridized to the same sample and abrogate the need to change filters between imaging each fluorophore. The simplest application is the imaging of two gene-specific probes for mapping. To take advantage of these filter sets, one needs a means of imaging that distinguishes the different colors. An advanced example of a triple-pass filter cube is the one used for spectral karyotyping (SKY). This contains filters that allow alternating regions of excitation and emission wavelengths. This is necessary due to the overlapping excitation and emission spectra of the five fluorophores used in the hybridization. Quadruple-pass filters do have some compromises, however, in that the brightness may be affected (P. Millman, Chroma Technology, pers. comm.). Filters and filter sets can be purchased from microscope companies or directly (and usually at a reduced cost) from filter manufacturers (e.g., Chroma Technology and Semrock are the two leading fluorescence microscope filters companies—the microscope manufacturers now mostly sell filters manufactured by these or similar companies). Other filters are important for altering the intensity of light entering the system. Neutral density filters decrease the overall amount of transmitted light without altering the intensity ratios of different wavelengths—mostly of use for color balancing tungsten-halogen transmitted light images (Fig. 4.4.2B), with such lamps now being superceded by white light LEDs. This may be desired if the signal intensity is strong and the fluorophore is particularly sensitive to photobleaching. Heat filters can be extremely important in removing excessive heat radiating from lamps (especially arc and metal halide lamps for fluorescence, also useful for tungsten-halogen lamps for transmitted light; LEDs and lasers usually handle heat dissipation at the source). KG-1, BG-38, and Hot-Mirrors are some examples of heat filters. Each has a different wavelength at which it reduces the transmitted heat. Choosing the correct heat filter depends on the wavelengths one needs for excitation of the sample. Requiring shorter excitation wavelengths allows one to choose a heat filter that prevents a larger portion of the spectrum from reaching the sample. Heat filters protect not only the specimen from damage, but are also useful for protecting sensitive elements such as polarizers and other filters.

FROM FLUORESCENT DYES, QDOTS, AND POLYMERS TO FLUORESCENT PROTEINS

Fluorophores are available as small organic dyes, various types of nanoparticles, including quantum dots (Qdots; Bruchez et al., 1998, Chan & Nie, 1998), organic polymers (based on the 2000 Nobel Prize in Chemistry on electron conduction of organic plastic wires), and even single walled carbon nanotubes (SWCNT, related to the famous Buckyballs; O'Connell et al., 2002). Table 4.4.2 lists many fluorescent dyes and these newer compositions of bright matter.

Chalfie et al. (1994) ushered in a revolution in cell imaging by the cloning and expression of green fluorescent protein (GFP), enabling easy DNA construction of gene cassettes of GFP tagged protein, optionally with specific expression promoters (now $65 per plasmid, *http://www.addgene.org/fluorescent-proteins*). An explosion of colors and biosensors has followed. Table 4.4.1 lists many fluorescent proteins (FP) and their basic photophysical properties. Table 4.4.3 lists many of the published fluorescent protein biosensors and what they measure (see Frommer, 2016; Newman et al., 2011, for references and background). We envision that 96-well plate(s), 384-well

plate, or single "well" reverse transfection cell microarrays (*www.persomics.com*) could be used to transfect or transduce FP localization reporters, transcriptional activity reporters (e.g., promoter response elements → FP or FPB), or constitutive or linearizer-inducible promoter → FP or FPB, to comprehensively characterize control and patient-derived cells. We further suggest that localizing FPs or FPBs would enable better signal-to-noise ratio (e.g., nucleolus is smaller volume than nucleus, which is smaller volume than nucleoplasm + cytosol), multimerizing (mNeonGreen-mNeonGreen-mNeonGreen is three times brighter than single mNeonGreen, which in turn is over three times brighter than the 1996 enhanced GFP), and enable multiplexing. FPs can also add value to FPBs. For example, if a panel of dark-to-bright green FPBs were expressed from different plasmids, other 5 color × 5 locations, would enable marking 25 populations. If using combinatorial 5 × 5 pairs, or triplets, this would greatly expand the number of cell populations that could be marked (i.e., green FPB, with $25^2 = 625$, or $25^3 = 16{,}525$, recognizing that quantitative fluorescence microscopy could be used to separate one times, two times, and three times brightness at the same location—much as done in the past for COBRA-FISH on metaphase chromosome spreads).

IMAGE ACQUISITION

After identifying an object that is worthy of documenting, an image must be acquired, particular portions of the object resolved and defined, and a careful analysis performed to generate useful information. In the past, images were photographed or studied directly at the microscope. Photographic film was high resolution, but low quantum efficiency (at best ~3% of photons contributed to data). High-technology image analysis systems are now available that allow computerized image capture, image enhancement, manipulation of captured images, mass storage, retrieval, and computer analysis. Imaging systems are now commercially available for storage and analysis of DNA gels and autoradiograms, cell morphometry and motion analysis, and interphase and metaphase cytogenetic studies. These systems have found their places in clinical diagnostic laboratories as well as in basic research laboratories. Preparation of the mammalian karyotype has always been a time-consuming and labor intensive process. Significant strides have been made in automating cytogenetic analysis and now several commercial imaging systems are available that offer either semiautomatic or interactive karyotyping capabilities. These systems save time because they eliminate the darkroom work required to make photographic prints and the physical cutting and pasting of chromosomes to produce a karyotype. We predict that the combination of automated labeling ("autostainers"), image acquisition (automated microscopes, high content screening instruments, digital pathology/cytogenetics acquisition stations) and "machine learning" (also known as artificial intelligence) will exceed the performance of human operators. In the lab, we are not there yet, with the microscopy lab not being that far behind the Tesla self-driving car. This will liberate lab staff from tedious, repetitive, error-prone, wet lab and microscope bench tasks, to much higher value tasks of evaluating the specimens before automation, and reviewing and acting on the data and automated interpretation that comes out. A famous computer saying: "Garbage in, garbage out" applies: Human lab staff will remain critical. For now (2017 and the next decades) we are in transition to automation.

Each imaging system is composed of the following basic components: A microscope with a charge-coupled device (CCD) or scientific CMOS (sCMOS) camera, a computer monitor to view the image, a computer with the appropriate image capture and storage capabilities, and a high-resolution printer for generating a copy of the image. Because the metaphases and karyotypes are digital images, long-term storage and fading of photographs is avoided, and quick transmission of high-quality data is possible via computer networks and, if there are no Health Insurance Portability and Accountability Act of 1996 (HIPAA) compliance issues, "the Cloud." Many research examples of cloud-based microscopy image data are available at The Cell Image library (*http://www.cellimagelibrary.org*).

The light microscope is useful for imaging metaphase cells, cell morphology, expression of proteins (e.g., GFP-fusion proteins) in transfected tissue culture cells, and stained histological specimens. The following section will therefore cover some of the essentials.

Previous versions of this unit discussed photographic film. For 2017 we are going "all digital." Digital cameras detect 30 to 90 times more photons than film, and convert the intensity information of the scene into a computer-ready format for quantitation and display (Inoué & Spring, 1997).

Digital Image Acquisition

Instead of traditional photographic cameras, CCD cameras, developed in the 1970s and 1980s, or sCMOS cameras (developed in 2000s and mature in 2017) are used in digital-imaging systems. The sCMOS cameras take advantage of the semi-conductor manufacturing processes that enable your smartphone to have a pretty good 10+ megapixel camera(s) inside, while keeping the entire phone at an affordable price. The price:performance of the sCMOS camera has been outstanding. The newest (2017) sCMOS, such as the Hamamatsu ORCA-FLASH 4.2 v3 (version 3) and PCO pco.panda are around $7,000 and outperform the previous generation sCMOS ($12,000, circa 2014!) and high performance CCDs (also $12,000). Advantages of sCMOS include more pixels (4.2 or 5.5 megapixels versus 1.3 megapixel CCD, for sensors with $\sim 7 \times 7$ μm pixel size, so sCMOS cameras have an approximately three times or four times bigger field of view), high quantum efficiency (82% peak quantum efficiency sCMOS, ~70% for CCD), and especially fast readout (100 frames per second sCMOS, ~14 fps CCD, even though sCMOS delivers a lot more pixels in each frame). For our discussion here we will ignore exotic variants, such as back-illuminated sCMOS and CCD (~90% quantum efficiency, expensive because low yield of usable sensors), and electron multiplication CCDs (EMCCDs), which are CCD variants that excel at very low photon flux (0 to 4 photons per pixel per exposure), but usually have large pixels (e.g., 16×16 μm pixel size). We briefly discuss the history of digital cameras.

Modern high-performance CCD cameras were originally used in quantitative astronomy, where CCDs revolutionized the field (e.g., Hubble Space Telescope). They are currently used in the security and surveillance industry, military installations, airports, banks, radar tracking, and in quality-control applications. CCDs are much smaller and more robust that the old tube cameras and have become ubiquitous at home in both hand-held video camcorders and digital "photography." One-dimensional CCD arrays are also the enabling technology for the flat-bed scanners used to digitize photographs and printed pages. These CCD cameras are used increasingly in image processing and image analysis. Several companies now market CCD cameras for diverse applications in video microscopy. CCD cameras have been developed using various technologies for specific functions.

Most CCD cameras sample an image approximately fourteen times per second, but integrating CCD cameras have the ability to delay the readout for several seconds rather than milliseconds, thus offering good performance in low-light applications such as fluorescence microscopy. One-chip color CCD cameras are available for fluorescence microscopy. A red, green, or blue filter (striped filters) is placed in front of each pixel. These are broad-band filters and are not perfectly spectrally matched to the fluorophores. Three-chip color CCD cameras, with one color per chip, are sometimes used in pathology applications. These are more expensive (three CCD sensors instead of one, plus more elaborate wavelength separation), with better spatial resolution that only sometimes is taken advantage of. Digital pathology slide scanners are more expensive than a typical pathology microscope, but since the slide scanner can operate 24/7, the investment in purchasing a high quality instrument is enabling of greatly improved workflows and economies of scale. Brightfield color histology digital slide scanners have been available since the early 2000s, and special niche fluorescence scanners have existed almost as long (e.g., 3DHistech Pannoramic scanners with ten fluorescence channels available, *http://www.3dhistech.com/systems*). In 2017 there is more interest in multiplexing, driven in part from the needs of immune-oncology (anti-PD-L1 and other immune checkpoint biomarkers) and in part by the availability of new technologies and multiplex data analysis.

The CCD or sCMOS is an array of individual light sensors, each of which is a linear photometer (Aikens, 1990; Photometrics, 1995) that use silicon semi-conductors whose covalent bonds are broken by incoming photons, thereby liberating electrons and generating electron hole pairs. The CCD itself contains a rectangular array (or matrix) of wells where the liberated electrons are collected and stored until their quantity (i.e., charge) is measured. The capacity of each well may vary in accordance with the manufacturer, with capacities that can range up to 1 million electrons per well. Each well represents a pixel of digital information, the size of which is related to the magnification of the objective and the size of the array. A typical research microscope CCD or sCMOS camera uses $\sim 7 \times 7$ μm microlenses in front of somewhat smaller light sensitive areas. The microlenses determine the pixel size; the light sensitive area determines

the dynamic range (e.g., a 4 × 4 μm silicon square for a 7 × 7 μm pixel has 1% of the "full well" capacity that a 40 × 40 μm silicon square does). Other energy sources, such as heat, can generate charge not related to the electromagnetic energy released by the fluorophore. This "dark current" can be reduced through cooling of the silicon array and by improvements in electronics.

We briefly discuss here the evolution of CCD cameras, while strongly lobbying for a future that is mostly sCMOS cameras, since sCMOS hit a sweet spot of performance and price.

The signal output of a CCD array is a voltage that is linearly proportional to the charge present in each pixel. But how is the charge in each well, hereafter referred to as a charge packet, measured? Think of the array as being divided into rows and columns (Fig. 4.4.4). Once the CCD is exposed to the emitted light, charge accumulates in each of the wells. The information in each well is shifted by one row, with the first row being transferred to an output node (i.e., an extra row outside the array used for the transfer of information to the signal-processing device). The packets in the node are then shifted column by column to the processor and counted. Once all the wells in the node have been measured, the next row is transferred and the process repeated until the entire array has been read. The matrix is then capable of being exposed again to the light. The charge packets can be transferred thousands of times without significant loss of charge. This charge transfer efficiency (CTE) measurement is an important factor in choosing a camera, especially where the charge packets are small and any loss may result in significant image degradation. Because this is a complex process, methods have been established for reducing the readout time. One such technique, called binning, combines the charge from adjacent pixels; readout time is reduced as this effectively reduces the number of pixels that must be read. This comes at the price of reduced spatial resolution, however. One can control the amount and direction of binning. For example, 2 × 2 binning combines the energy packets of 4 pixels; 2 pixels in the horizontal direction and 2 pixels in the vertical direction (Fig. 4.4.4, panels D to F). CCD performance is affected by a number of factors including linearity, charge-transfer efficiency, resolution, noise, dynamic range, quantum efficiency, and signal-to-noise ratio (Aikens, 1990; Photometrics, 1995).

Spurred by penetration into the manufacturing machine vision market, and consumer demand for all things digital, scientific digital cameras and other detectors have come a long way in the past decade. Circa 1995, most light microscopes captured images on 35-mm film or on commercial video standards. Film was processed in specialty photo stores or using an in-lab darkroom. Video was saved to the relatively new video cassette recorder, analog optical memory disk recorder, or digitized to a computer using an expensive frame grabber card. Computer memory was over $50/Mb, with personal computers (PCs) supporting 64 Mb of memory and a 75 MHz Pentium (586 chip) was the fastest central processor unit (CPU). 100 Mb hard drives were rare. Scientific digital cameras typically used a cooled Kodak-1400 full frame CCD sensor with 1317 × 1035 pixels (1.3 megapixels), 12-bit dynamic range (4096 intensity levels), a readout rate of 500 Kpixels/sec and a mechanical shutter. Fortunately, binning was available! The Kodak-1400 CCD had a maximum quantum efficiency of 35% (green light), and over 10% from 400 to 700 nm. Specialty back-thinned CCD cameras, whose sensors were illuminated from the non-gate side—which was thinned in a costly and inefficient process—were available in large pixel (25 × 25 μm), 512 × 512 pixel (262,144 pixels), 16-bit dynamic range (65,536 intensity levels), 50,000 pixel/sec readout, so 0.2 frames per second—5 sec to read out one frame! The advantage of back-thinned cameras is that the sensors that survive the thinning manufacturing process had quantum efficiencies of 80% to 90% from 400 to 800 nm. The back-illuminated CCDs have been the mainstay of major astronomy telescopes where the camera is a fraction of the total instrument price, but were rare in light microscopy facilities where such a camera might cost more than the rest of the instrument. An alternative approach to high sensitivity was to combine an image intensifier ("night vision unit") with a video or binned digital camera. At the time, the Gen II intensifier with video CCD was still the preferred method for physiological imaging of probes such as Fura-2, in spite of the "chicken wire" appearance of the images through the multichannel plate.

In 2005, a plethora of fast camera-computer interfaces became available, such as USB2, Firewire, and Cameralink, although some specialty cameras still use proprietary digitizer cards. Standard CCD cameras have

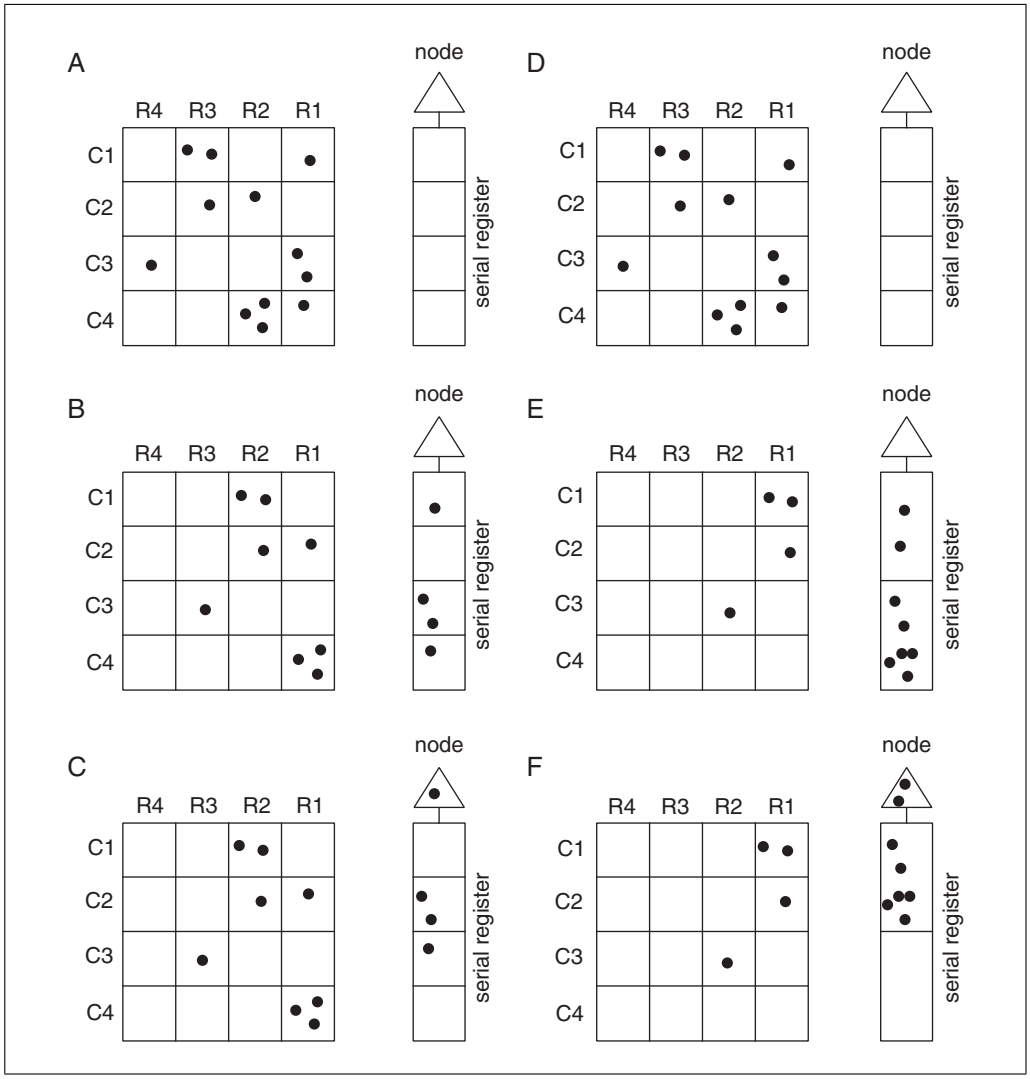

Figure 4.4.4 The 4 × 4 pixels CCD array illustrated above (**A**) has accumulated energy packets in several of the wells. (**B**) The energy packets are transferred one row at a time to the serial register. (**C**) They are then shifted into the output node one pixel at a time and on to the processor where they are counted and recorded. The concept of 2 × 2 pixel binning is demonstrated in panels **D** to **F**. Modified with permission from Photometrics (1995). CCD binning happens before the readout register, which is a source of noise. The sCMOS sensor data can be binned, but this is after digitization, so noise from each pixel is added together; fortunately the current (2017) sCMOS cameras have such low readout noise (~1 electron/pixel) that this is not critical. Binning in the camera is good for both CCD and sCMOS in that less data is transferred, enabling higher frame rate, at the cost of lower spatial resolution.

lost the mechanical shutter in favor of using interline CCD readout. Computer memory is $280/Gb ($0.27/Mb), with PCs supporting 4 Gb (4096 Mb) of memory (more with Windows Server) and dual 3.6 GHz Pentium 4 CPUs are the fastest chips. Terabyte disk arrays for user desktops are available for under $2000. Gigapixel images have been assembled by consumer digital photographers (*http://www.tawbaware.com/maxlyons/gigapixel.htm*). These 2005 camera-computer interfaces and computer performance specifications are now (2017) mostly obsolete, with USB3.1 interface and NVidia Pascal GPU cards ($1000 for 11 teraflops!) leading the way.

In front of the CCD sensor is an array of microlenses that gather the light into the photosensitive pixel areas. In the past, the electronic gates of front-illuminated CCDs blocked some of the light, especially in the blue spectral range. Kodak invented a transparent tin oxide electronic gate that improved sensitivity in the blue. The combination of the lenslets and the Kodak blue-enhanced gate resulted in front-illuminated cameras with quantum efficiencies

of 60%, at a fraction of the cost of somewhat faster back-thinned CCDs. The standard sensors are now 1600 × 1200 or 2048 × 2048 pixels, though the smaller pixels, often only 5 × 5 μm, still limits the useful dynamic range of most scientific cameras to 12 bits (4096 intensity levels). The sensors have increased in pixel number by two times to three times, but the readout speed has increased faster, to 10 or 20 Mb/sec. Binning is still available, to further improve signal-to-noise ratio. The hyperHAD lenslets can also be dyed to transmit red, green, or blue, and laid out in a regular pattern on the CCD (most commonly the Bayer mask of 2 × 2 units of B, G, G, R) to produce one-chip color cameras. For high sensitivity, electron multiplication (EMCCD), electron bombardment (EBCCD), and high resolution Gen IV photon counting intensifiers are combining signal amplification, low noise, and fast readout for photon counting imaging. These can be combined with spectral imagers and/or spinning disk confocal microscopes, OptiGrid, Apotome, or a digital micromirror device to provide fast, 3D optical sectioning. Confocal microscopes are available from several vendors, and the patent holder for sub-picosecond pulsed multiphoton microscopes has agreed to not enforce their patent against do-it-yourself academic researchers. The pulsed lasers are still expensive but now have spectral tuning in software, are fiber-optic coupled to the microscope(s), and no longer require a Ph.D. physicist attendant. Even the photomultiplier tubes that are the detectors of laser scanning confocal and multiphoton microscopes have improved quantum yield or have been packaged as spectral emission detectors (e.g., Zeiss Quasar spectral detector based on 32-channel GaAsP photomultiplier tube).

Image Analysis

After the photons in a scene are collected on the CCD sensor, the number of electrons present at each picture element (pixel) is then quantified and read out as a signal whose intensity is proportional to the number of electrons, and hence to the number of photons. For video cameras, the data are reformatted to a broadcast standard so that it can be displayed on a television monitor. This video signal is then digitized to an 8-bit dynamic range (256 intensity level) image by using a video frame grabber in the computer. Some video cameras and frame grabbers can handle color video capture and transfer ("24-bit color"). For digital cameras, the camera electronics convert the number of electrons into a digital value that is sent directly to a custom board in the computer, where the value is deciphered by a custom driver. Most digital cameras read out 12-bit (4096 intensity level) image data, because this is a good combination of cost and dynamic range. Three sequential red, green, and blue images acquired with a monochrome digital camera can be merged to give a better color image than possible with color video cameras, though with image processing, the quality but not sensitivity of a Bayer mask microlense color CCD digital camera is often "good enough." Often the same software can be used for acquiring video or digital images (assuming appropriate frame grabber or digital camera drivers), as well as image processing, analysis, color merging, and storage. Typical configurations include a PC running any of Microsoft Windows, Linux, or Mac OS 10 and a graphics card that allows multiple image displays on a single monitor, networking capabilities for multiple workstations, choice of printers (including color), full-image contrasting, and, for FISH, hybridization spot enhancement and image sharpening.

Computerized imaging systems for cytogenetic applications vary in the extent of automation. Some possess slide-scanning and metaphase finding capabilities, some identify specific chromosomes, while others require the user to point to each chromosome with a mouse or other pointing device and assign it a number (see Table 4.4.4 at end of article). The software then places each chromosome onto a standard karyotype template. The chromosome images can be rotated, trimmed, inverted, labeled, and, in some systems, straightened. There are also variations in the degree of image enhancement or manipulation available. Software is available for the quantification of FISH signals, measurement analysis for gene mapping and spot-counting analysis for aneuploidy detection. Color image ratio measurement is a feature of software developed for comparative genomic hybridization technology (*UNIT 4.6*; DeVries, Gray, Pinkel, Waldman, & Sudar, 1995). Similarly, sophisticated software is available for spectral karyotyping (SKY). This technique employs a labeling scheme (discussed earlier in Microscopy in Modern Human Genetics section, above) in which different chromosome painting probes are labeled with various combinations of five different fluorophores. The software is able to identify each chromosome based on the different fluorescent-label-dependent patterns of the chromosomes, and arrange them in a karyotype. It is also capable of quantitative

analysis for hybridization intensity and simultaneous display of fluorescent, DAPI-banded, and classification of chromosomes, along with an idiogram. Image annotation and zooming are features on many software programs, and case and patient databases are available for importing image files and compiling data for statistical and epidemiologic studies. Image analysis systems, both for routine karyotyping and for FISH applications, are undergoing constant improvement. Because price and features continue to change, manufacturers should be contacted directly for current information.

Spectral Imaging Systems

Spectral karyotyping (SKY) and various forms of multiplex FISH (M-FISH) have taken cytogenetics labs beyond monochrome, beyond RGB color, and even beyond the visible spectrum. The primary uses of SKY and M-FISH systems are to use five fluorescent dyes in combinations, on unique chromosome DNA, to paint by FISH each human or mouse chromosome uniquely (described in detail in Microscopy in Modern Human Genetics section, above). However, the question can be asked, like confocal microscopy (Amos & White, 2003): Is spectral imaging underutilized in cytogenetics and pathology? A few articles have been published in spectral pathology, including Ornberg, Woerner, and Edwards (1999), Tsurui et al. (2000), Rothmann et al. (2000), Macville et al. (2001), Farkas and Becker (2001), Schultz et al. (2001), Greenspan et al. (2002), and Jaganath, Angeletti, Levenson, and Rimm (2004). Of these, the 7-color immunofluorescence histology images of Tsurui et al. (2000) provides a way to maximize the immuno-information from a pathology specimen. The work of Dickinson, Bearman, Tille, Lansford, and Fraser (2001) on the Zeiss META emission spectral detector for multiphoton/confocal microscopes, shows what is possible for those who have enough money. By 2005, spectral detectors were available from all of the major confocal microscope manufacturers. The PARISS imaging spectrometer from Lightform, can be operated as a spectral linescan confocal tissue section mapper by simply replacing the epi-illumination field aperture with a slit (linescan, or slit scan, confocal light paths are often disrespected in reviews touting other technologies; for many applications, in particular multiplex fluorescence digital slide scanning, they perform well; light sheet imagers are in a sense an orthogonal configuration of the same intent). The SKY system, and several other commercial spectral imagers (Table 4.4.4) could be made confocal by combining with a CREST X-Light or Yokogawa spinning disk confocal unit. The plethora of point scanning spectral confocal microscopes from the big four microscope companies could also be used.

Spectral imaging in cytogenetics and pathology can be used with any or all of standard histology dyes, immunohistochemical dyes, conventional fluorophores, and fluorescent nanocrystal quantum dots (Table 4.4.2).

Valm, Oldenbourg, and Borisy (2016) established 115-plex imaging of microbes. Please recall that one *Escherichia coli* cell is approximately the volume of a human metaphase chromosome ($\sim$1 μm^3) so this technology could be translated to human cell DNA FISH, single molecule FISH, or RNA intron FISH (Levesque & Raj, 2013), especially when combined with expansion microscopy (see Expansion Microscopy section). Using spectral confocal microscopes with sequential laser line acquisition (633 nm, 594 nm, 561 nm, 512 nm, 488 nm, 405 nm, 32 channel PMT Nikon A1 or Zeiss LSM710 confocal microscopes), they labeled bacterial cells with a single fluorescent-labeled oligonucleotide to the highly expressed ribosomal 16 S rRNA, with each of sixteen fluorophores. Their "simple spectral" matrix unmixing algorithm converts the 115 channel data (every pixel 115 plex) to a sixteen-fluorophore channel image, a seven-fold reduction in data. We suggest that the Scott and Hoppe (2016) joint spatial deconvolution and spectral unmixing would result in better data, and porting to NVidia GPU(s) would provide (near) instant gratification, with better signal-to-noise ratio. We further suggest that if the noise is minimal—as it would be performing this labeling and imaging on expansion microscopy specimens—that all background pixels could be "zeroed out" enabling compact storage of image data as either lossless LZW compression (massive number of zeros contribute little to file storage space) or as "single molecule" x, y, z (16 intensities) points in space (with each spot at super-resolution centroid coordinates).

Image Measurements

The cytogenetic microscope/imaging systems described above for FISH and G-banding cytogenetics are essentially the same as that needed in a pathology lab to document hematoxylin and eosin (H&E) slides, immunohistochemistry, chromogenic in situ hybridization, and DNA ploidy. Most clinical DNA ploidy assays have moved to flow cytometers because

of high throughput, hands-off operation, and instrument purchases leveraged through the need for $CD4^+$ cell counting in HIV patient testing. There are still opportunities to use image cytometry in DNA ploidy, especially to exploit the feasibility of imaging nuclear texture on small numbers of cells ($n < 100$) with good statistics (small coefficient of variation). A good review on the image parameters that can be measured on a cytogenetics/pathology microscope imaging system are reviewed by Rodenacker and Bengtsson (2003). Uses in cell biology are reviewed by Price et al. (2002).

More generally, image measurements can be divided into tasks such as FISH spot counting, nuclear and/or cell area, and fluorescence intensity or dye absorption. Using a digital camera and microscope enable image analysis and measurements to be done quickly and reproducibly. Automated image acquisition and measurements are becoming important in drug discovery and cell biology research, as discussed by Carpenter and Sabatini (2004). Tissue microarrays, invented by Kononen et al. (1998), are having an impact in pathology research. Automated metaphase finders, as adjuncts to karyotyping systems, are available from several companies (Table 4.4.4, Karyotype Systems and Digital Pathology section). National Aeronautics and Space Administration (NASA) has had occasional difficulties translating "faster, better, cheaper" into consistently excellent science—hopefully the biomedical microscopy community will do better (Ward, 2010).

Image Storage

With the increase in information per image and the decreasing cost of computer memory and storage space, image files have become larger—gigapixel, multi-gigabyte, digital slide images are now commonplace in pathology workflows. The easiest way to store files is on an external hard drive or server. Many universities and corporations have information service departments that can provide long-term archiving of data (for a price). Make sure to save data in a broadly compatible file format so that any of the software you may use for image acquisition, enhancement, manipulation, and presentation can read the data. The almost-universal standard is uncompressed or lossless LZW compression tagged image file format (TIFF) images. Image acquisition software is often specific to the microscope/camera system being used and the type of analysis to be performed (e.g., FISH, immunocytochemistry, CGH, SKY, microarray analysis, spectral imaging, multidimensional imaging). Careful consideration is therefore recommended when purchasing software from a company other than that from which the hardware was obtained. At a minimum, be sure that the imaging software can save the images in the industry standard TIFF, so that one can share the data with colleagues. The JPEG and graphics interchange format (GIF) file formats use data compression and are useful formats for displaying image data on Web pages but should not be relied on to maintain scientific and clinical data. Most of the multidimensional and spectral imaging systems save data in their own proprietary formats. Before purchasing such equipment you should make sure that the data—preferably all the data—can be exported to a universal format, i.e., wavelength named TIFF files, so that other software products can read the data and you can access the information even if the company's product is discontinued or you move to a location that does not have a software license.

Optical Clearing

Most organisms and organs are opaque to the human eye. Exceptions like zebrafish embryos or *Caenorhabditis elegans* worms are among the reasons some model organisms become useful and popular. Imaging in the near-infrared with digital cameras is useful, though removes the direct eye-to-brain "seeing is believing" option. Dodt and Zieglgansberger (1994) made excellent use of infrared videomicroscopy to image thick brain slices. Bioluminescence of firefly luciferase, other beetle luciferases, and to a lesser extent other luciferases have become useful tools for tracking cells by in vivo imaging (Contag et al., 1995, 1997; Zhang, 2003; recent reviews by Sharkey et al., 2016; Xu et al., 2016).

Dent, Polson, and Klymkowsky (1989), crediting Andrew Murray and Marc Kirschner, (unpublished; see also Zucker, 2006; Zucker & Jeffay, 2006), used a mixture of benzyl alcohol/benzyl benzoate (BABB) and initiated the modern era to optically clear thick specimens for imaging. Azaripour et al. (2016) and Lee, Kim, and Sun (2016) review the use of BABB and a plethora of newer optical clearing reagents.

Illumination of the specimen from the side(s) with a light sheet has created a new niche for microscopes. Names of these technologies and products include Ultramicroscopy (Dodt et al., 2007, 2015), selective plane illumination (Huisken, Swoger, Del Bene, Wittbrodt, & Stelzer, 2004),

digital scanned laser light sheet fluorescence microscopy (Keller, Schmidt, Wittbrodt, & Stelzer, 2008; see Table 4.4.5 at end of article). Historical publications include Siedentopf and Zsigmondy (1902; Richard Zsigmondy was awarded the 1926 Nobel Prize), Voie, Burns, and Spelman (1993), Fuchs, Jaffe, Long, and Azam (2002). A nice recent review is Rieckher (2016). In addition to commercial "light sheet" imagers, open plans are available from OpenSPIM and OpenSpinMicroscopy consortia. Please refer to these publications, consortia, and vendors' Web sites for additional details. For those who have instruments available, light sheet imaging techniques are especially advantageous when used with our final topic: Expansion microscopy.

Expansion Microscopy

Users of optical clearing agents have remarked for many years on expansion or shrinkage of specimens as they pass through the clearing reagents and are then mounted in either buffer (e.g., PBS, pH 7.4), glycerol (80% with PBS buffering), or other media. Specimen size changes were usually considered a hassle (i.e., reviewers questioning distances and volume measurements). Ed Boyden and colleagues changed expansion from being a hassle to a "killer feature" (Chen, Tillberg, & Boyden, 2015; commentary by Dodt, 2015). They developed, "By covalently anchoring specific labels located within the specimen directly to the [swellable] polymer network, labels spaced closer than the optical diffraction limit can be isotropically separated and optically resolved, a process we call expansion microscopy (ExM)." A typical expansion protocol results in a four times expansion per axis, so $4^3 = 64$ times greater volume, very low background from autofluorescence or non-specific binding. Expansion microscopy further improved by Chen et al. (2016) to enable "ExFISH" nanoscale imaging, by crosslinking RNA directly to the polymer matrix, expansion, then sequential hybridization and imaging of single molecules of six different RNA species at greater than three times expansion per axis. Expansion, then imaging, enables complete control over the refractive index and antifade reagent properties of the mounting medium; by using a water immersion objective lens with aqueous mounting medium (specimen side of coverglass) and immersion medium (lens side), aberrations and autofluorescence are minimized, transparency is maximized, for optimal image quality. Water and aqueous buffers are refractive index 1.333, which limits the numerical aperture to 1.2 NA. A pair of silicon oil objective lenses optimized for refractive index 1.404 have been produced (Olympus), which enables 1.3 NA (that is 1.404 refractive index mounting medium and silicone oil immersion medium). It may be possible to develop 1.515 refractive index mounting media compatible with immunofluorescence and RNA and DNA FISH probes, and perfusion to enable sequential reiterative labeling/imaging/stripping cycles with 1.4 NA oil immersion lenses—the main challenge may be to limit viscosity of the mounting medium to make perfusion of sequential reagents tolerably fast. With expansion microscopy, it may be much simpler to use aqueous media and matched optics (water immersion lens) and expand more.

The four times expansion per axis when used with a high resolution or even modest resolution, microscope optical train, enables super-resolution with current optics. For example, a 100×/1.4 NA oil immersion objective lens has XY resolution of 214 nm, and Z resolution of 600 nm (calculations with 500 nm light). Four times per axis expansion results in effective resolution of 54 and 150 nm, when relating back to the original cell size (we use 1.4 NA here because most DNA FISH and cytogenetics labs are more likely to use oil immersion lenses). The practically zero background, and sparse nature of the expanded specimen, also makes even more useful than usual quantitative spatial deconvolution processing of the resulting image data from either widefield or confocal or light sheet microscopes. The Moore's Law increase in computing power for the same price, compared to our 2005 Unit (*UNIT 4.4*, McNamara, Difilippantonio, & Ried, 2005), shows itself in the current generation NVidia GPU graphics cards (10 teraflops on a $1000 card), which drive 4 K HD computer monitors (3840 × 2160 pixels) and enable (practically) instant gratification quantitative deconvolution with current commercial GPU enabled deconvolution software (*www.microvolution.com*; *www.svi.nl*; *http://www.mediacy.com/autoquantx3*). We anticipate in the near future such software will take advantage of spectral data for "joint" spatial deconvolution and spectral unmixing (Hoppe, Shorte, Swanson, & Heintzmann, 2008; Scott & Hoppe, 2016), with a large improvement in signal-to-noise ratio for multichannel images. Expansion with joint processing in turn will facilitate going to even higher multiplexing, since expansion specimens

have low autofluorescence and low nonspecific binding fluorescence. For more on spatial deconvolution, see Appendix 4.4.3 (see Supporting Materials). Chozinski et al. (2016) describe how to use expansion microscopy to expand and image tissue sections. This has great implications for pathology applications, both immunofluorescence and single molecule RNA FISH (Chen et al., 2016).

Cytogenetics applications can benefit from expansion microscopy, and "joint" digital processing, at the single cell level. We suggest this can be done with current microscopes, with modest investment in new optics, microscope automation, and software, having the potential for having an outsize positive impact on the practice of DNA FISH, DAPI chromosome banding, and bringing on clinical single molecule RNA FISH (most genes are either not expressed, so no RNA molecules, or the RNAs are expressed at much greater copy number than the one to four gene copies of a single diploid cell; the RNA also contains the relevant splicing and proximity, or not, to polyribosomes). Ideally the expansion, imaging, and "joint" processing—and some of the analysis—will become "one click" automation, enabling the cytogenetics lab operators to oversee and troubleshoot the workflow and data output. To take maximum advantage of expansion microscopy, one would like to operate at the limits of resolution of the optics. This results in a lot of data—and even greater when multiplexing, and especially with iterative cycles of labeling/imaging/de-labeling (facilitated by the specimen being embedded in the polymer matrix). Boyden and colleagues have lectured on much greater than four times per axis expansion: Ten times per axis, so 10^3 = 1000 times volume, would be equivalent to 21 XY and Z 60 nm resolution, equivalent to state-of-the-art single molecule superresolution techniques. The raw data may push the limits of current imaging systems and network and storage. Instead of saving the raw and joint processed data as volumes, efficient storage of single-molecule-like output is possible and likely to result in a great deal of both storage space and network time. The data can then be rendered in appropriate fashion on analysis workstation 4 K HD monitors, or using augmented reality/virtual reality displays (Facebook/Oculus Rift, Google Cardboard VR, Google Daydream View, Google Glass, HTV Hive, Microsoft HoloLens, Samsung Gear VR, or Magic Leap; Magic Leap is still in development in mid-2016) or even outdoors (Pokemon Go Genes, Cells and Molecules).

The expansion microscopy field is new enough as we write this, to enable comprehensive citations: Chen et al. (2015, 2016), Dodt (2015), Chozinski et al. (2016), Geertsema and Ewers (2016), Ku et al. (2016), Tillberg et al. (2016), Tsanov et al. (2016), and Zhang et al. (2016). An opportunity to obtain optically cleared tissues in "one click" is with the MesoLens (McConnell et al., 2016; *http://www.mesolens.com*). We also note that reiterative cycles of FISH labeling with multiple fluorophore probe sets enables a high degree of multiplex reporting such as MERFISH (Frieda et al., 2017; Moffitt et al., 2016a, 2016b).

In Gulliver's Travels, the protagonist experienced expansion as well as shrinkage. Shrinkage microscopy is also in play in biomedical imaging. Pan et al. (2016) reported that the uDISCO optical clearing method enables consistent shrinkage of specimens to one-half or one-third their original volume. Because the specimen is (almost) transparent, and with careful control (or correction) of autofluorescence, the same specimen can be imaged in proportionally less time and fewer data storage requirements. They report useful shrinkage microscopy with both confocal microscopy and light sheet microscopy.

Ultraviolet and Near-Infrared Windows of Opportunity

In Gulliver's Travels, the young girl threading an invisible needle with invisible silk may have been precision localizing the eye of the needle with ultraviolet (UV) or near-infrared photons—perhaps with fluorescent silk. Light interacting with molecules may be absorbed, scattered, or phase shifted (anyone wearing polarized sunglasses will appreciate other uses). If absorbed, the energy may be re-emitted at a longer wavelength, which is variously referred to as luminescence (any), fluorescence (if emitted in the first few nanoseconds from a singlet state), delayed fluorescence (if emitted after more than a few nanoseconds from a singlet state), or phosphorescence (very late, depopulation from a triplet state), or transferred to another molecule (Dexter or Förster energy transfer, the latter enabling use as a molecular ruler, also known as FRET; the energy may be transferred to a quencher or, commonly, to oxygen, O_2, from which good or bad chemical reactions may occur). Without chlorophyll absorbing and transferring (by carefully organized FRET handoffs) photons to enable specific chemical reactions at photosystems

in photosynthetic organisms (bacteria, algae, and plants), life on earth would likely solely consist of microscopic organisms at or near hydrothermal vents.

Light scattering is inversely proportional to the fourth power of the wavelength. This means that relatively speaking, 250 nm, 500 nm, and 1000 nm photons scatter in tissue at sixteen times, one time, and one-sixteenth times. Scattering is not in itself good or bad, useful or useless—understanding what is going on can help or hurt you (note: UV light sources such as mercury or xenon arc lamps give off UV light that may illuminate your skin in bad ways—probably more likely is a high pressure bulb exploding and the glass shards hurting you or a colleague: We recommend in 2016 and beyond to switch to LEDs or lasers for fluorescence microscopy).

The 250 nm photons are also absorbed by various molecules. Ultraviolet light is commonly used for sterilization or for quantifying nucleic acids versus protein concentrations and purity (e.g., 260/230 nm ratio, *https://en.wikipedia.org/wiki/Nucleic_acid_quantitation*, which also mentions other molecules can contribute to absorption at one or both wavelengths). This is possible because the nucleobases absorb UV, as do tryptophan, tyrosine, and phenylalanine (Trp is the major contributor to fluorescence). UV ranges are provided in Table 4.4.6 (at end of article).

The absorbance at these wavelengths can be used directly, provided a suitable light source (e.g., Energetiq EQ lamp), microscope optics (Ultrafluar or reflection type objective lens), and camera (typically the faceplate requires a UV sensitive phosphor) are available (Cheung, Evans, McKenna, & Ehrlich, 2011; Cheung et al., 2013), or a lot of patience (Caspersson, 1979, 1989, 2016). From a historic perspective, we also note that august Kohler and Moritz von Rohr (working at Carl Zeiss) developed an ultraviolet microscope in 1904 (see Kohler, 2016). Recently, Demos, Levenson, and colleagues have shown the value of using the very shallow penetration of UV light into tissue sections (or whole mounts), which they call microscopy with ultraviolet surface excitation (MUSE) microscopy (Fong & Levenson, 2016; Lin, Urayama, Saroufeem, Matthews, & Demos, 2009; Raman et al., 2009). Many UV (and visible) fluorophores had low quantum yields and photostabilities. Grimm et al. (2015) invented four-membered (square) azetidine rings that appended onto a chemically diverse set of fluorophores, improve both quantum yields and photostability in aqueous media. For example, a UV excitation, blue emission coumarin with quantum yield 0.19 was improved to 0.96 (see Janelia Fluor, fluorophores in Table 4.4.2). The azetidine rings improved a wide range of fluorophores from UV through NIR, and the same authors have published on bright photoactivatable fluorophores for use in PALm/STORM type single molecule localization fluorescence microscopy (Grimm et al., 2016).

Near-infrared (NIR) light has been used for many years for the low scattering and absorption properties of tissues. With video enhancement, Dodt and Zieglgansberger (1994) nicely showed the advantages of NIR contrast microscopy of thick (~300 μm) brain slices. Denk et al. (1990) pioneered the use of multiphoton excitation fluorescence microscopy to likewise image deeper into tissue. Light scattering ($1 / \text{wavelength}^4$) results in a gradual decrease in scattering, through the visible (i.e., 400 versus 500 versus 600 versus 700 nm). Tissue is not uniform: Hemoglobin, myoglobin, cytochrome, and specific other molecules dominate absorption at particular wavelength ranges. This results in several wavelength bands that are ideal for quantifying hemoglobin. (Oxyhemoglobin and deoxyhemoglobin have somewhat different absorption spectra, though somewhat complicated by red blood cell plasma membrane light scattering and potentially red blood cell density, packing, and orientation in specific blood vessels.) For imaging with minimal absorption, and progressively less scattering, four near-infrared windows have been defined for tissue: NIR windows I (650 to 950 nm); II (1100 to 1350 nm); III (1600 to 1870 nm); and IV (2100 to 2300 nm); transmittance and depth attenuation were measured in a freshly sacrificed rat brain by Shi et al. (2016). They flushed out the red blood cells (hemoglobin absorbance and membrane scattering) and white blood cells (scattering, potentially cytochrome absorbance) first (see also Boden et al., 2012; Li et al., 2008; McNamara et al., 2014, for a generalizable protocol and $0.50 per animal DiI blood vessel labeling). We see great opportunities in extending the useful wavelength ranges of light microscopes further into the UV and NIR than are commonly used now. One advantage of near-infrared windows is that most tissue and common lab materials have very low (practically nil) autofluorescence in the near-infrared. A key exception

is plant-based material containing chlorophyll, such as mouse chow in the digestive tract of a mouse or rat in an IVIS imaging system or microscope system. (This could be considered an advantage for providing tissue contrast—if this is desired, you may want to feed the animal a near-infrared fluorescent molecule with optimal photophysics, photochemistry, and biology for your application.) The NIR I window (650 to 950 nm) has been used for several years for low background Western blotting (LI-COR Biosciences, *www.Li-Cor.com*, two color NIR fluorescence Odyssey product line) and for in vivo bioluminescence imaging (IVIS product line, now part of PerkinElmer). Table 4.4.2 Fluorophores Photophysics Data, tabulates the Brilliant Ultraviolet (BUV) and Brilliant Violet (BV) product lines, as well as a prototype series of bacteriochlorins (relatives of chlorophyll), each of which have product family members that excite in the UV or violet, and emit in the NIR. (The bacteriochlorins also have small Stokes shift excitation peaks close to their respective emission peaks.) Additional families of NIR fluorophores are becoming available in NIR window II, e.g., single wall carbon nanotubes (SWCNT; Cherukuri, Bachilo, Litovsky, & Weisman, 2004; Cherukuri, Tsyboulski, & Weisman, 2012; Jena et al., 2016; O'Connell et al., 2002; Pansare, Hejazi, Faenza, & Prud'homme, 2012; Roxbury et al., 2015; Tao et al., 2013), and NIR III (stay tuned). We note that Roxbury et al. (2015) achieved 17plex SWCNT types across NIR I and II (900 to 1400 nm), and NIR cameras with InGaAs sensors are available (e.g., First Light Imaging, C-RED 2, *http://www.first-light.fr/products*; Photon Etc, ZEPHYR, *http://www.photonetc.com/products*). One near-infrared fluorescent dye, indocyanine green (ICG) is used as a fluorescent contrast agent in humans—typically fluorescence angiography as an alternative to fluorescein. An example of whole human bodies fluorescence angiography is Piper et al. (2013; supplemental video *https://doi.org/10.1371/journal.pone.0083749.s003*).

CONCLUSIONS

As light microscopy moves into the twenty-first century, improvements in reagents, protocols, microscopes, imaging systems, and user's knowledge are being used in research and clinical labs to better understand Waldeyer's chromosomes and their role in biology and medicine.

SUPPORTING MATERIALS

All supporting material text files discussed in this article can only be accessed from the online version of this article.

ACKNOWLEDGMENTS

Dr. McNamara thanks the vendors, colleagues, and customers, Confocal Listserv online community and LinkedIn microscopy, biosensors, and image analysis groups for interactions. Thanks to Jeremy Sanderson for permission to use his imaging facility checklist as an appendix (see Appendix 4.4.1 in Supporting Materials); to Dr. Alex Asanov, President, TIRF Labs, for permission to re-use his TIRF figure; to Dr. Jahan Khalili for discussions about T-cells, multiplexing fluorescent protein biosensors, Tableau visualization, and developing *http://www.GeoMcNamara.com*.

CONFLICT OF INTEREST STATEMENT

Dr. McNamara is or has been a consultant/advisor to several companies mentioned in this Unit. We plan to update resources/vendors table, fluorophores, fluorescent proteins, and fluorescent protein biosensors at *http://www.GeoMcNamara.com* as freely accessible data.

For the 2016 update we have cited "Gold" (immediate) open access articles whenever possible. Some literature becomes open access at the publishers' platform after six or twelve months; other publications become available at PubMed Central.

LITERATURE CITED

Aikens, R. (1990). CCD cameras for video microscopy. In B. Herman & K. Jacobson (Eds.), *Optical microscopy for biology* (pp. 85-110). New York: John Wiley & Sons.

Allen, R. D., Allen, N. S., & Travis, J. L. (1981b). Video-enhanced contrast, differential interference contrast (AVEC-DIC) microscopy: A new method capable of analyzing microtubule-related motility in the reticulopodial network of *Allogromia laticollaris*. *Cell Motility*, *1*, 291–302. doi: 10.1002/cm.970010303.

Allen, R. D., David, G. B., & Nomarski, G. (1969). The Zeiss-Nomarski differential interference equipment for transmitted-light microscopy. *Zeitschrift fur Wissenschaftliche Mikroskopie und Mikroskopische Technik*, *69*, 193–221.

Allen, R. D., Travis, J. L., Allen, N. S., & Yilmaz, H. (1981a). Video-enhanced contrast polarization (AVEC-POL) microscopy: A new method applied to the detection of birefringence in the motile reticulopodial network *of Allogromia laticollaris*. *Cell Motility*, *1*, 275–289. doi: 10.1002/cm.970010302.

Amos, W. B., & White, J. G. (2003). How the confocal laser scanning microscope entered biological research. *Biology of the Cell*, *95*, 335–342. doi: 10.1016/S0248-4900(03)00078-9.

Arnold, N., Bhatt, M., Ried, T., Wienberg, J., & Ward, D. C. (1992). Fluorescence *in situ* hybridization on banded chromosomes. In C. Kessler (Ed.), *Techniques and methods in molecular biology: Nonradioactive labeling and detection of biomolecules* (pp. 324-326). Heidelberg: Springer-Verlag.

Axelrod, D. (2003). Total internal reflection fluorescence microscopy in cell biology. *Methods in Enzymology*, *361*, 1–33. doi: 10.1016/S0076-6879(03)61003-7.

Axelrod, D. (2013). Evanescent excitation and emission in fluorescence microscopy. *Biophysical Journal*, *104*, 1401–1409. doi: 10.1016/j.bpj.2013.02.044.

Axelrod, D., Burghardt, T. P., & Thompson, N. L. (1984). Total internal reflection fluorescence. *Annual Review of Biophysics and Bioengineering*, *13*, 247–268. doi: 10.1146/annurev.bb.13.060184.001335.

Azaripour, A., Lagerweij, T., Scharfbillig, C., Jadczak, A. E., Willershausen, B., & Van Noorden, C. J. (2016). A survey of clearing techniques for 3D imaging of tissues with special reference to connective tissue. *Progress in Histochemistry and Cytochemistry*, *51*, 9–23. doi: 10.1016/j.proghi.2016.04.001.

Azofeifa, J., Fauth, C., Kraus, J., Maierhofer, C., Langer, S., Bolzer, A., ... Speicher, M. R. (2000). An optimized probe set for the detection of small interchromosomal aberrations by use of 24-color FISH. *American Journal of Human Genetics*, *66*, 1684–1688. doi: 10.1086/302875.

Bajar, B. T., Wang, E. S., Lam, A. J., Kim, B. B., Jacobs, C. L., Howe, E. S., ... Chu, J. (2016). Improving brightness and photostability of green and red fluorescent proteins for live cell imaging and FRET reporting. *Scientific Reports*, *6*, 20889. doi: 10.1038/srep20889.

Baldini, A., & Ward, D. C. (1991). *In situ* hybridization of human chromosomes with Alu-PCR products: A simultaneous karyotype for gene mapping studies. *Genomics*, *9*, 770–774. doi: 10.1016/0888-7543(91)90374-N.

Barch, M., Knutsen, T., & Spurbeck, J. (Eds.). (1997). *The AGT cytogenetics laboratory manual*. New York: Raven Press.

Barlow, C., Hirotsune, S., Paylor, R., Liyanage, M., Eckhaus, M., Collins, F., ... Wynshaw-Boris, A. (1996). Atm-deficient mice: A paradigm of ataxia telangiectasia. *Cell*, *86*, 159–171. doi: 10.1016/S0092-8674(00)80086-0.

Barone-Nugent, E. D., Barty, A., & Nugent, K. A. (2002). Quantitative phase-amplitude microscopy I: Optical microscopy. *Journal of Microscopy*, *206*, 194–203. doi: 10.1046/j.1365-2818.2002.01027.x.

Barykina, N. V., Subach, O. M., Doronin, D. A., Sotskov, V. P., Roshchina, M. A., Kunitsyna, T. A., ... Enikolopov, G. N. (2016). A new design for a green calcium indicator with a smaller size and a reduced number of calcium-binding sites. *Scientific Reports*, *6*, 34447. doi: 10.1038/srep34447.

Bindels, D. S., Haarbosch, L., van Weeren, L., Postma, M., Wiese, K. E., Mastop, M., ... Gadella, T. W. Jr. (2017). mScarlet: A bright monomeric red fluorescent protein for cellular imaging. *Nature Methods*, *14*, 53–56. doi: 10.1038/nmeth.4074.

Blennow, E., Nielson, K. B., Telenius, H., Carter, N. P., Kristoffersson, U., Holmberg, E., ... Nordenskjøld, M. (1995). Fifty probands with extra structurally abnormal chromosomes characterized by fluorescence *in situ* hybridization. *American Journal of Medical Genetics*, *55*, 85–94. doi: 10.1002/ajmg.1320550122.

Boden, J., Wei, J., McNamara, G., Layman, H., Abdulreda, M., Andreopoulos, F., & Webster, K. A. (2012). Whole-mount imaging of the mouse hindlimb vasculature using the lipophilic carbocyanine dye DiI. *Biotechniques (Rapid Dispatches)*, *53*, 1–4. doi: 10.2144/000113907.

Boyle, A. L., Ballard, S. G., & Ward, D. C. (1990). Differential distribution of long and short interspersed element sequences in the mouse genome: Chromosome karyotyping by fluorescence *in situ* hybridization. *Proceedings of the National Academy of Sciences of the United States of America*, *87*, 7757–7761. doi: 10.1073/pnas.87.19.7757.

Brink, A. A., Wiegant, J. C., Szuhai, K., Tanke, H. J., Kenter, G. G., Fleuren, G. J., ... Raap, A. K. (2002). Simultaneous mapping of human papillomavirus integration sites and molecular karyotyping in short-term cultures of cervical carcinomas by using 49-color combined binary ratio labeling fluorescence *in situ* hybridization. *Cancer Genetics and Cytogenetics*, *134*, 145–150. doi: 10.1016/S0165-4608(01)00620-3.

Bruchez, M. Jr., Moronne, M., Gin, P., Weiss, S., & Alivisatos, A. P. (1998). Semiconductor nanocrystals as fluorescent biological labels. *Science*, *281*, 2013–2016. doi: 10.1126/science.281.5385.2013.

Campbell, R. E., Tour, O., Palmer, A. E., Steinbach, P. A., Baird, G. S., Zacharias, D. A., & Tsien, R. Y. (2002). A monomeric red fluorescent protein. *Proceedings of the National Academy of Sciences of the United States of America*, *99*, 7877–7882. doi: 10.1073/pnas.082243699.

Carpenter, A. E., & Sabatini, D. M. (2004). Systematic genome-wide screens of gene function. *Nature Reviews Genetics*, *5*, 11–22. doi: 10.1038/nrg1248.

Carter, K. C., Bowman, D., Carrington, W., Fogarty, K., McNeil, J. A., Fay, F. S., & Lawrence, J. B. (1993). A three-dimensional view of precursor messenger RNA metabolism within the mammalian nucleus. *Science*, *259*, 1330–1336. doi: 10.1126/science.8446902.

Caspersson, T., Farber, S., Foley, G. E., Kudynowski, J., Modest, E. J., Simonsson, E., ... Zech, L. (1968). Chemical differentiation along metaphase chromosomes. *Experimental*

Cell Research, *49*, 219–222. doi: 10.1016/0014-4827(68)90538-7.

Caspersson, T. O. (1979). Quantitative tumor cytochemistry-G.H.A. clowes memorial lecture. *Cancer Research*, *39*, 2341–2345.

Caspersson, T. O. (1989). The William Allan memorial award address: The background for the development of the chromosome banding techniques. *American Journal of Human Genetics*, *44*, 441–451.

Chalfie, M., Tu, Y., Euskirchen, G., Ward, W. W., & Prasher, D. C. (1994). Green fluorescent protein as a marker for gene expression. *Science*, *263*, 802–805. doi: 10.1126/science.8303295.

Chan, W. C. W., & Nie, S. (1998). Quantum dot bioconjugates for ultrasensitive nonisotopic detection. *Science*, *281*, 2016–2018. doi: 10.1126/science.281.5385.2016.

Chen, F., Tillberg, P. W., & Boyden, E. S. (2015). Optical imaging. Expansion microscopy. *Science*, *347*, 543–548. doi: 10.1126/science.1260088.

Chen, F., Wassie, A. T., Cote, A. J., Sinha, A., Alon, S., Asano, S., ... Boyden, E. S. (2016). Nanoscale imaging of RNA with expansion microscopy. *Nature Methods*, *13*, 679–684. doi: 10.1038/nmeth.3899.

Cherukuri, T. K., Tsyboulski, D. A., & Weisman, R. B. (2012). Length- and defect-dependent fluorescence efficiencies of individual single-walled carbon nanotubes. *ACS Nano*, *6*, 843–850. doi: 10.1021/nn2043516.

Cherukuri, P., Bachilo, S. M., Litovsky, S. H., & Weisman, R. B. (2004). Near-infrared fluorescence microscopy of single-walled carbon nanotubes in phagocytic cells. *Journal of the American Chemical Society*, *126*, 15638–15639. doi: 10.1021/ja0466311.

Cheung, M. C., Evans, J. G., McKenna, B., & Ehrlich, D. J. (2011). Deep ultraviolet mapping of intracellular protein and nucleic acid in femtograms per pixel. *Cytometry Part A*, *79*, 920–932. doi: 10.1002/cyto.a.21111.

Cheung, M. C., LaCroix, R., McKenna, B. K., Liu, L., Winkelman, J., & Ehrlich, D. J. (2013). Intracellular protein and nucleic acid measured in eight cell types using deep-ultraviolet mass mapping. *Cytometry Part A*, *83*, 540–551. doi: 10.1002/cyto.a.22277.

Chroma Technology Corp. (2017). 5-Channel fluorescence imaging simplified - reliable multiplexing for the non-specialist. Chroma Tech Corp in collaboration with BD Biosciences. Retrieved from https://www.chroma.com/sites/default/files/5-CHANNEL%20FLUORESCENCE%20IMAGING%20SIMPLIFIED%20-%20Reliable%20Multiplexing%20for%20the%20Non-Specialist_New.pdf.

Chowdhary, B., Raudsepp, T., Fronicke, L., & Scherthan, H. (1998). Emerging patterns of comparative genome organization in some mammalian species as revealed by Zoo-FISH. *Genome Research*, *8*, 577–589. doi: 10.1101/gr.8.6.577.

Chozinski, T. J., Halpern, A. R., Okawa, H., Kim, H. J., Tremel, G. J., Wong, R. O., & Vaughan, J. C. (2016). Expansion microscopy with conventional antibodies and fluorescent proteins. *Nature Methods*, *13*, 485–488. doi: 10.1038/nmeth.3833.

Clark, G., & Kasten, F. H. (1983). *History of Staining*. Baltimore: Williams & Wilkins.

Cody, S. H., Xiang, S. D., Layton, M. J., Handman, E., Lam, M. H., Layton, J. E., ... Heath, J. K. (2005). A simple method allowing DIC imaging in conjunction with confocal microscopy. *Journal of Microscopy*, *217*, 265–274. doi: 10.1111/j.1365-2818.2005.01452.x.

Coleman, A. E., Schröck, E., Weaver, Z., du Manoir, S., Yang, F., Ferguson-Smith, M. A., ... Janz, S. (1997). Previously hidden chromosome aberrations in T(12;15)-positive BALB/c plasmacytomas uncovered by multicolor spectral karyotyping. *Cancer Research*, *57*, 4585–4592.

Contag, C. H., Contag, P. R., Mullins, J. I., Spilman, S. D., Stevenson, D. K., & Benaron, D. A. (1995). Photonic detection of bacterial pathogens in living hosts. *Molecular Microbiology*, *18*, 593–603. doi: 10.1111/j.1365-2958.1995.mmi_18040593.x.

Contag, C. H., Spilman, S. D., Contag, P. R., Oshiro, M., Eames, B., Dennery, P., ... Benaron, D. A. (1997). Visualizing gene expression in living mammals using a bioluminescent reporter. *Photochemistry and Photobiology*, *66*, 523–531. doi: 10.1111/j.1751-1097.1997.tb03184.x.

Coons, A. H. (1961). The beginnings of immunofluorescence. *Journal of Immunology*, *87*, 499–503.

Coons, A. H., & Kaplan, M. H. (1950). Localization of antigen in tissue cells. II. Improvements in a method for the detection of antigen by means of a fluorescent antibody. *The Journal of Experimental Medicine*, *91*, 1–13. doi: 10.1084/jem.91.1.1.

Coons, A. H., Creech, H. J., & Jones, R. N. (1941). Immunological properties of an antibody containing a fluorescent group. *Experimental Biology and Medicine*, *47*, 200–202. doi: 10.3181/00379727-47-13084P.

Coons, A. H., Creech, H. J., Jones, R. N., & Berliner, E. (1942). The demonstration of pneumococcal antigen in tissue by the use of a fluorescent antibody. *Journal of Immunology*, *45*, 159–170.

Cranfill, P. J., Sell, B. R., Baird, M. A., Allen, J. R., Lavagnino, Z., de Gruiter, H. M., ... Piston, D. W. (2016). Quantitative assessment of fluorescent proteins. *Nature Methods*, *13*, 557–562. doi: 10.1038/nmeth.3891.

Cremer, T., Landegent, J. E., Bruckner, A., Scholl, H. P., Schardin, M., Hager, H.-D., ... van der Ploeg, M. (1986). Detection of chromosome aberrations in the human interphase nucleus by visualization of specific target DNAs with radioactive and nonradioactive *in situ* hybridization techniques: Diagnosis of trisomy 18 with probe L1.84. *Human Genetics*, *74*, 346–352. doi: 10.1007/BF00280484.

Denk, W., Strickler, J. H., & Webb, W. W. (1990). Two-photon laser scanning fluorescence microscopy. *Science*, *248*, 73–76. doi: 10.1126/science.2321027.

Dent, J. A., Polson, A. G., & Klymkowsky, M. W. (1989). A whole- mount immunocytochemical analysis of the expression of the intermediate filament protein vimentin in *Xenopus*. *Development*, *105*, 61–74.

Devilee, P., Thierry, R. F., Kievits, T., Kolluri, R., Hopman, A. H. N., Willard, H. F., ... Cornelisse, C. J. (1988). Detection of chromosome aneuploidies in interphase nuclei from human primary breast tumors using chromosome specific repetitive DNA probes. *Cancer Research*, *48*, 5825–5830.

DeVries, S., Gray, J. W., Pinkel, D., Waldman, F. M., & Sudar, D. (1995). Comparative genomic hybridization. *Current Protocols in Human Genetics*. *6*, 4.6.1–4.6.18. doi: 10.1002/0471142905.hg0406s06.

Diaspro, A. (Ed). (2001). *Confocal and two-photon microscopy; foundations, applications and advances*. New York: Wiley-Liss.

Dickinson, M. E., Bearman, G., Tille, S., Lansford, R., & Fraser, S. E. (2001). Multi-spectral imaging and linear unmixing add a whole new dimension to laser scanning fluorescence microscopy. *BioTechniques*, *31*, 1272, 1274–6, 1278.

Dodt, H. U. (2015). Microscopy. The superresolved brain. *Science*, *347*, 474–475. doi: 10.1126/science.aaa5084.

Dodt, H.-U., & Zieglgansberger, W. (1994). Infrared videomicroscopy: A new look at neuronal structure and function. *Trends in Neurosciences*, *17*, 453–458. doi: 10.1016/0166-2236(94)90130-9.

Dodt, H. U., Saghafi, S., Becker, K., Jährling, N., Hahn, C., Pende, M., ... Niendorf, A. (2015). Ultramicroscopy: Development and outlook. *Neurophotonics*, *2*, 041407. doi: 10.1117/1.NPh.2.4.041407.

Dodt, H.-U., Leischner, U., Schierloh, A., Jährling, N., Mauch, C. P., Deininger, K., ... Becker, K. (2007). Ultramicroscopy: Three-dimensional visualization of neuronal networks in the whole mouse brain. *Nature Methods*, *4*, 331–336. doi: 10.1038/nmeth1036.

Egger, M. D., & Petran, M. (1967). New reflected-light microscope for viewing unstained brain and ganglion cells. *Science*, *157*, 305–307. doi: 10.1126/science.157.3786.305.

Einstein, A. (1905). Über die von der molekularkinetischen Theorie der Wärme geforderte Bewegung von in ruhenden Flüssigkeiten suspendierten Teilchen. "[Investigations on the theory of Brownian Movement]". *Annalen der Physik*, *322*, 549–560. doi:10.1002/andp.19053220806.

Engels, H., Ehrbrecht, A., Zahn, S., Bosse, K., Vrolijk, H., White, S., ... Raap, A. K. (2003). Comprehensive analysis of human subtelomeres with combined binary ratio labelling fluorescence *in situ* hybridisation. *European Journal of Human Genetics*, *11*, 643–651. doi: 10.1038/sj.ejhg.5201028.

Evanko, D. (2012, December 12). Our reporting standards for fluorescent proteins - Feedback wanted [Web log post]. Retrieved from http://blogs.nature.com/methagora/2012/12/our-reporting-standards-for-fluorescent-proteins-feedback-wanted.html.

Farkas, D. L., & Becker, D. (2001). Applications of spectral imaging: Detection and analysis of human melanoma and its precursors. *Pigment Cell Research*, *14*, 2–8. doi: 10.1034/j.1600-0749.2001.140102.x.

Feulgen, R., & Rossenbeck, H. (1924). Mikroskopisch-chemischer nachweis einer nucleisäure vom typus der thymonucleinsäure und die darauf beruhende elektive Färburg von Zellkernen in mikroskopischen präparaten. [Microscopic chemical detection of a nucleic acid of the thymonucleic acid family and the elective dye of cell nuclei based on microscopic preparations]. *Hoppe-Seyler's Zeitschrift fur physiologische Chemie*, *135*, 203–248. doi: 10.1515/bchm2.1924.135.5-6.203.

Fleischmann, M., Bloch, W., Kolossov, E., Andressen, C., Muller, M., Brem, G., ... Fleischmann, B. K. (1998). Cardiac specific expression of the green fluorescent protein during early murine embryonic development. *FEBS Letters*, *440*, 370–376. doi: 10.1016/S0014-5793(98)01476-8.

Fong, A., & Levenson, R. M. (2016). MUSE: Slide-free microscopy. *Optics & Photonics News*, *June 2016*, 16-18.

Forozan, F., Karhu, R., Kononen, J., Kallioniemi, A., & Kallioniemi, O.-P. (1997). Genome screening by comparative genomic hybridization. *Trends in Genetics*, *13*, 405–409. doi: 10.1016/S0168-9525(97)01244-4.

Förster, T. (1965). Delocalized excitation and excitation transfer. In O. Sinanoglu (Ed.), *Modern quantum chemistry part III: Action of light and organic crystals* (pp. 93-137). New York: Academic Press.

Frieda, K. L., Linton, J. M., Hormoz, S., Choi, J., Chow, K. K., Singer, Z. S., ... Cai, L. (2017). Synthetic recording and in situ readout of lineage information in single cells. *Nature*, *541*, 107–111. doi: 10.1038/nature20777.

Frommer, W. (2016). *Biosensor*. Retrieved from https://codex.dpb.carnegiescience.edu/db/biosensor.

Fronicke, L., & Scherthan, H. (1997). Zoo-fluorescence *in situ* hybridization analysis of human and Indian muntjac karyotypes (*Muntiacus muntjac vaginalis*) reveals satellite DNA clusters at the margins of conserved syntenic segments. *Chromosome Research*, *5*, 254–261. doi: 10.1023/B:CHRO.0000032298.22346.46.

Fuchs, E., Jaffe, J., Long, R., & Azam, F. (2002). Thin laser light sheet microscope for microbial oceanography. *Optics Express*, *10*, 145–154. doi: 10.1364/OE.10.000145.

Garfield, S. (2001). *Mauve: How one man invented a color that changed the world*. New York: W.W. Norton & Company.

Garini, Y., Gil, A., Bar-Am, I., Cabib, D., & Katzir, N. (1999). Signal to noise analysis of multiple color fluorescence imaging microscopy. *Cytometry*, *35*, 214–226. doi: 10.1002/(SICI)1097-0320(19990301)35:3%3c214::AID-CYTO4%3e3.0.CO;2-D.

Garini, Y., Vermolen, B. J., & Young, I. T. (2005). From micro to nano: Recent advances in high-resolution microscopy. *Current Opinion in Biotechnology*, *16*, 3–12. doi: 10.1016/j.copbio.2005.01.003.

Garini, Y., Macville, M., du Manoir, S., Buckwald, R. A., Lavi, M., Katzir, N., ... Ried, T. (1996). Spectral karyotyping. *Bioimaging*, *4*, 65–72. doi: 10.1002/1361-6374(199606)4:2%3c65::AID-BIO4%3e3.3.CO;2-4.

GE Healthcare Life Sciences. (2017). Imaging Principles and Methods. Retrieved from http://www.gelifesciences.com/file_source/GELS/Service%20and%20Support/Documents%20and%20Downloads/Handbooks/pdfs/Molecular%20Imaging.pdf.

Geertsema, H., & Ewers, H. (2016). Expansion microscopy passes its first test. *Nature Methods*, *13*, 481–482. doi: 10.1038/nmeth.3872.

Ghadimi, B. M., Schröck, E., Walker, R. L., Wangsa, D., Jauho, A., Melzer, P., & Ried, T. (1999). Specific chromosomal aberrations and amplification of AIB1 nuclear receptor coactivator gene in pancreatic carcinomas. *The American Journal of Pathology*, *154*, 525–536. doi: 10.1016/S0002-9440(10)65298-4.

Ghosh, S., Yu, C. L., Ferraro, D. J., Sudha, S., Pal, S. K., Schaefer, W. F., ... Ramaswamy, S. (2016). Blue protein with red fluorescence. *Proceedings of the National Academy of Sciences of the United States of America*, *113*, 11513–11518. doi: 10.1073/pnas.1525622113.

Giordano, S. J., Yoo, M., Ward, D. C., Bhatt, M., Overhauser, J., & Steggles, A. W. (1993). The human cytochrome b5 gene and two of its pseudogenes are located on chromosomes 18q23, 14q31-32.1 and 20p11.2, respectively. *Human Genetics*, *92*, 615–618. doi: 10.1007/BF00420948.

Goldman, R. D., & Spector, D. K. (Eds.). (2004). *Live cell imaging*. Cold Spring Harbor, NY: Cold Spring Harbor Press.

Greenspan, H., Rothmann, C., Cycowitz, T., Nissan, Y., Cohen, A. M., & Malik, Z. (2002). Classification of lymphoproliferative disorders by spectral imaging of the nucleus. *Histology and Histopathology*, *17*, 767–773.

Grimm, J. B., English, B. P., Choi, H., Muthusamy, A. K., Mehl, B. P., Dong, P., ... Lavis, L. D. (2016). Bright photoactivatable fluorophores for single-molecule imaging. *Nature Methods*, *13*, 985–988. doi: 10.1038/nmeth.4034.

Grimm, J. B., English, B. P., Chen, J., Slaughter, J. P., Zhang, Z., Revyakin, A., ... Lavis, L. D. (2015). A general method to improve fluorophores for live-cell and single-molecule microscopy. *Nature Methods*, *12*, 244–250, 3 p following 250. doi: 10.1038/nmeth.3256.

Haines, J. L., Korf, B. R., Morton, C. C., Seidman, C. E., Seidman, C. E., & Smith, D. R. (Eds.) (2017). *Current Protocols in Human Genetics*. Hoboken, NJ: John Wiley & Sons.

Harris, H. (1995). *The cells of the body. A history of somatic cell genetics*. Cold Spring Harbor, NY: Cold Spring Harbor Press.

Hasan, M. T., Friedrich, R. W., Euler, T., Larkum, M. E., Giese, G. G., Both, M., ... Denk, W. (2004). Functional fluorescent Ca2+ indicator proteins in transgenic mice under TET control. *PLoS Biology*, *2*, E163. doi: 10.1371/journal.pbio.0020163.

Haugland, R. (2004). *The handbook — a guide to fluorescent probes and labeling technologies*. Eugene, OR: Molecular Probes (Invitrogen).

Haugland, R. P. (1996). *Handbook of fluorescent probes and research chemicals*. Eugene, OR: Molecular Probes.

Heim, R., Prasher, D. C., & Tsien, R. Y. (1994). Wavelength mutations and posttranslational autoxidation of green fluorescent protein. *Proceedings of the National Academy of Sciences of the United States of America*, *91*, 12501–12504. doi: 10.1073/pnas.91.26.12501.

Holzwarth, G., Hill, D. B., & McLaughlin, E. B. (2000). Polarization-modulated differential-interference contrast microscopy with a variable retarder. *Applied Optics*, *39*, 6268–6294. doi: 10.1364/AO.39.006288.

Holzwarth, G., Webb, S. C., Kubinski, D. J., & Allen, N. S. (1997). Improving DIC microscopy with polarization modulation. *Journal of Microscopy*, *188*, 249–254. doi: 10.1046/j.1365-2818.1997.2500807.x.

Hooke, R. (1665). *Micrographia. Or, Some physiological descriptions of minute bodies made by magnifying glasses, with observations and inquiries thereupon*. London: Royal Society.

Hoppe, A. D., Shorte, S. L., Swanson, J. A., & Heintzmann, R. (2008). Three-dimensional FRET reconstruction microscopy for analysis of dynamic molecular interactions in live cells. *Biophysical Journal*, *95*, 400–418. doi: 10.1529/biophysj.107.125385.

Hsu, T. C. (1952). Mammalian chromosomes *in vitro*. I. The karyotype of man. *The Journal of Heredity*, *43*, 167–172. doi: 10.1093/oxfordjournals.jhered.a106296.

Huisken, J., Swoger, J., Del Bene, F., Wittbrodt, J., & Stelzer, E. H. (2004). Optical sectioning deep inside live embryos by selective plane illumination microscopy. *Science*, *305*, 1007–1009. doi: 10.1126/science.1100035.

Inoué, S. (1981). Video image processing greatly enhances contrast, quality, and speed in polarization-based microscopy. *The Journal of Cell Biology*, *89*, 346–356. doi: 10.1083/jcb.89.2.346.

Inoué, S., & Dan, K. (1951). Birefringence of the dividing cell. *Journal of Morphology*, *89*, 423. doi: 10.1002/jmor.1050890304.

Inoué, S., & Spring, K. R. (1997). *Video microscopy* (2nd ed.). New York: Plenum.

Ishikawa-Ankerhold, H. C., Ankerhold, R., & Drummen, G. P. (2012). Advanced fluorescence microscopy techniques-FRAP, FLIP, FLAP, FRET and FLIM. *Molecules*, *17*, 4047–4132. doi: 10.3390/molecules17044047.

Jaganath, R., Angeletti, C., Levenson, R., & Rimm, D. L. (2004). Diagnostic classification of urothelial cells in urine cytology specimens using exclusively spectral information. *Cancer*, *102*, 186–191. doi: 10.1002/cncr.20302.

Jaiswal, J. K., & Simon, S. M. (2003). Total internal reflection fluorescence microscopy for high-resolution imaging of cell-surface events. *Current Protocols in Cell Biology*, *20*, 4.12.1–4.12.15. doi: 10.1002/0471143030.cb0412s20.

James, J., & Tanke, H. (1991). *Biomedical light microscopy*. Boston: Kluwer Academic Publishers.

Jardine, L. (2004). *The curious life of Robert Hooke: The man who measured London*. New York: HarperCollins.

Jares-Erijman, E. A., & Jovin, T. M. (2003). FRET imaging. *Nature Biotechnology*, *21*, 1387–1395. doi: 10.1038/nbt896.

Jena, P. V., Shamay, Y., Shah, J., Roxbury, D., Paknejad, N., & Heller, D. A. (2016). Photoluminescent carbon nanotubes interrogate the permeability of multicellular tumor spheroids. *Carbon*, *97*, 99–109. doi: 10.1016/j.carbon.2015.08.024.

Jentsch, I., Geigl, J., Klein, C. A., & Speicher, M. R. (2003). Seven-fluorochrome mouse M-FISH for high-resolution analysis of interchromosomal rearrangements. *Cytogenetic and Genome Research*, *103*, 84–88. doi: 10.1159/000076294.

Johnson, C. V., McNeil, J. A., Carter, K. C., & Lawrence, J. B. (1991). A simple, rapid technique for precise mapping of multiple sequences in two colors using a single optical filter set. *Genetic Analysis, Techniques and Applications*, *8*, 24–35. doi: 10.1016/1050-3862(91)90052-S.

Kachar, B. (1985). Asymmetric illumination contrast: A method of image formation for video light microscopy. *Science*, *227*, 766–768. doi: 10.1126/science.3969565.

Kallioniemi, A., Kallioniemi, O.-P., Sudar, D., Rutovitz, D., Gray, J. W., Waldman, F., & Pinkel, D. (1992). Comparative genomic hybridization for molecular cytogenetic analysis of solid tumors. *Science*, *258*, 818–821. doi: 10.1126/science.1359641.

Kapitza, H.-G. (1996). Modern microscope objectives. *Proceedings of the Royal Society of Medicine*, *31*, 24–27.

Karhu, R., Ahlstedt-Soini, M., Bittner, M., Meltzer, P., Trent, J. M., & Isola, J. J. (2001). Chromosome arm-specific multicolor FISH. *Genes Chromosomes Cancer*, *30*, 105–109. doi: 10.1002/1098-2264(2000)9999:9999%3c::AID-GCC1068%3e3.0.CO;2-9.

Keller, P. J., Schmidt, A. D., Wittbrodt, J., & Stelzer, E. H. (2008). Reconstruction of zebrafish early embryonic development by scanned light sheet microscopy. *Science*, *322*, 1065–1069. doi: 10.1126/science.1162493.

Knoll, J. H. M., & Lichter, P. (2005). In situ hybridization to metaphase chromosomes and interphase nuclei. *Current Protocols in Human Genetics*, *45*, 4.3.1–4.3.31. doi: 10.1002/0471142905.hg0403s45.

Kohler, A. (2016). August Kohler. Retrieved from http://micro.magnet.fsu.edu/optics/timeline/people/kohler.html.

Kononen, J., Bubendorf, L., Kallioniemi, A., Bärlund, M., Schraml, P., Leighton, S., ... Kallioniemi, O. P. (1998). Tissue microarrays for high-throughput molecular profiling of tumor specimens. *Nature Medicine*, *4*, 844–847. doi: 10.1038/nm0798-844.

Ku, T., Swaney, J., Park, J. Y., Albanese, A., Murray, E., Cho, J. H., ... Chung, K. (2016). Multiplexed and scalable super-resolution imaging of three-dimensional protein localization in size-adjustable tissues. *Nature Biotechnology*, *34*, 973–981. doi: 10.1038/nbt.3641.

Labas, Y. A., Gurskaya, N. G., Yanushevich, Y. G., Fradkov, A. F., Lukyanov, K. A., Lukyanov, S. A., & Matz, M. V. (2002). Diversity and evolution of the green fluorescent protein family. *Proceedings of the National Academy of Sciences of the United States of America*, *99*, 4256–4261. doi: 10.1073/pnas.062552299.

Lambert, T., & Thorn, K. (2016). *Interactive visualization fluorescent protein properties*. San Francisco: University of California. Retrieved from http://nic.ucsf.edu/FPvisualization

Langer-Safer, P. R., Levine, M., & Ward, D. C. (1982). Immunological method for mapping genes on *Drosophila* polytene chromosomes. *Proceedings of the National Academy of Sciences of the United States of America*, *79*, 4381–4385. doi: 10.1073/pnas.79.14.4381.

Lawrence, J. B., Singer, R. H., & Marselle, L. M. (1989). Highly localized tracks of specific transcripts within interphase nuclei visualized by *in situ* hybridization. *Cell*, *57*, 493–502. doi: 10.1016/0092-8674(89)90924-0.

Lawrence, J. B., Carter, K. C., & Xing, X. (1993). Probing functional organization within the nucleus: Is genome structure integrated with RNA metabolism? *Cold Spring Harbor Symposia on Quantitative Biology*, *58*, 807–818. doi: 10.1101/SQB.1993.058.01.088.

Lee, E., Kim, H. J., & Sun, W. (2016). See-through technology for biological tissue: 3-dimensional visualization of macromolecules. *International Neurourology Journal*, *20*(Suppl 1), S15-S22. doi: 10.5213/inj.1632630.315.

Lee, C., Rens, W. and Yang, F. (2000). Multicolor fluorescence in situ hybridization (FISH) approaches for simultaneous analysis of the entire human genome. *Current Protocols*

in Human Genetics. *24*, 4.9.1–4.9.11. doi: 10.1002/0471142905.hg0409s24.

Leewenhoeck, A. (1683). An abstract of a letter from Mr. Anthony Leewenhoeck writ to sir C. W. Jan. 22. 1682/3 from Delft. *Philosophical Transactions*, *13*, 74–81. doi: 10.1098/rstl.1683.0013.

Lejeune, J., Gautier, M., & Turpin, R. (1959). Etude des chromosomes somatiques de neuf enfants mongoliens. [Study of somatic chromosomes nine-Mongolian children]. *Comptes Rendus Hebdomadaires des Séances de l'Académie des Sciences (Paris)*, *248*, 1721–1722.

Levesque, M. J., & Raj, A. (2013). Single-chromosome transcriptional profiling reveals chromosomal gene expression regulation. *Nature Methods*, *10*, 246–248. Erratum in: *Nature Methods*, *10*, 445. doi: 10.1038/nmeth.2372.

Li, Y., Song, Y., Zhao, L., Gaidosh, G., Laties, A. M., & Wen, R. (2008). Direct labeling and visualization of blood vessels with lipophilic carbocyanine dye DiI. *Nature Protocols*, *3*, 1703–1708. doi: 10.1038/nprot.2008.172.

Lichter, P., & Ward, D. C. (1990). Is non-isotopic *in situ* hybridization finally coming of age? *Nature*, *345*, 93–95. doi: 10.1038/345093a0.

Lichter, P., Chang Tang, C.-J., Call, K., Hermanson, G., Evans, G. A., Housman, D., & Ward, D. C. (1990). High resolution mapping of human chromosome 11 by *in situ* hybridization with cosmid clones. *Science*, *247*, 64–69. doi: 10.1126/science.2294592.

Lichter, J. B., Difilippantonio, M., Wu, J., Miller, D., Ward, D. C., Goodfellow, P. J., & Kidd, K. K. (1992). Localization of the gene for MEN 2A. *Henry Ford Hospital Medical Journal*, *40*, 199–204.

Lin, B., Urayama, S., Saroufeem, R. M., Matthews, D. L., & Demos, S. G. (2009). Real-time microscopic imaging of esophageal epithelial disease with autofluorescence under ultraviolet excitation. *Optics Express*, *17*, 12502–12509. doi: 10.1364/OE.17.012502.

Liu, P., Ahmed, S., & Wohland, T. (2008). The F-techniques: Advances in receptor protein studies. *Trends in Endocrinology and Metabolism*, *19*, 181–190. doi: 10.1016/j.tem.2008.02.004.

Liyanage, M., Coleman, C., du Manoir, S., Veldman, T., McCormack, S., Dickson, R. B., ... Ried, T. (1996). Multicolour spectral karyotyping of mouse chromosomes. *Nature Genetics*, *14*, 312–315. doi: 10.1038/ng1196-312.

Macville, M. V., Van Der Laak, J. A., Speel, E. J., Katzir, N., Garini, Y., Soenksen, D., ... Ried, T. (2001). Spectral imaging of multi-color chromogenic dyes in pathological specimens. *Analytical Cellular Pathology*, *22*, 133–142. doi: 10.1155/2001/740909.

Manuelidis, L. (1985). Individual interphase chromosome domains revealed by *in situ* hybridization. *Human Genetics*, *71*, 288–293. doi: 10.1007/BF00388453.

Manuelidis, L., Langer-Safer, P. R., & Ward, D. C. (1982). High-resolution mapping of satellite DNA using biotin-labeled DNA probes. *The Journal of Cell Biology*, *95*, 619–625. doi: 10.1083/jcb.95.2.619.

Marrack, J. (1934). Nature of antibodies. *Nature*, *133*, 292. doi: 10.1038/133292b0.

Mason, W. (1993). *Fluorescent and luminescent probes for biological activity: A practical guide to technology for quantitative real-time analysis*. San Diego: Academic Press.

Matsumoto, B. (Ed). (2002). *Cell biological applications of confocal microscopy* (2nd ed.). New York: Academic Press.

Matz, M. V., Fradkov, A. F., Labas, Y. A., Savitsky, A. P., Zaraisky, A. G., Markelov, M. L., & Lukyanov, S. A. (1999). Fluorescent proteins from nonbioluminescent *Anthozoa* species. *Nature Biotechnology*, *17*, 969–973. Erratum 17. (1227). doi: 10.1038/13657.

McConnell, G., Trägårdh, J., Amor, R., Dempster, J., Reid, E., & Amos, W. B. (2016). A novel optical microscope for imaging large embryos and tissue volumes with sub-cellular resolution throughout. *Elife*, *5*, pii: e18659. doi: 10.7554/eLife.18659.

McNamara, G. (2005). Multi-Probe Microscopy. Retrieved from http://home.earthlink.net/~mpmicro.

McNamara, G. (2016). GEOMCNAMARA (updates of tables). Retrieved from http://www.GeoMcNamara.com.

McNamara, G., & Boswell, C. A. (2007). A thousand proteins of light: 15 years of advances in fluorescent proteins. In A. Méndez-Vilas & J. Díaz (Eds.), *Modern research and educational topics in microscopy*, *Vol. 3*, (pp. 287-296). Badajoz, Spain: FORMATEX Microscopy.

McNamara, G., Difilippantonio, M. J., & Ried, T. (2005). Microscopy and image analysis. *Current Protocols in Human Genetics*, *46*, 4.4.1-4.4.34. doi: 10.1002/0471142905.hg0404s46.

McNamara, G., Yanai, A., Khankaldyyan, V., Laug, W. E., Boden, J., Webster, K., ... Wen, R. (2014). Low magnification confocal microscopy of tumor angiogenesis. *Methods in Molecular Biology*, *1075*, 149–175. doi: 10.1007/978-1-60761-847-8_6.

Minsky, M. (1957). Microscopy apparatus. U.S. Patent 3013467.

Minsky, M. (1988). Memoir on inventing the confocal scanning microscope. *Scanning*, *10*, 128–138. doi: 10.1002/sca.4950100403.

Miyawaki, A., Llopis, J., Heim, R., McCaffery, J. M., Adams, J. A., Ikura, M., & Tsien, R. Y. (1997). Fluorescent indicators for Ca^{2+} based on green fluorescent proteins and calmodulin. *Nature*, *388*, 882–887. doi: 10.1038/42264.

Moffitt, J. R., Hao, J., Wang, G., Chen, K. H., Babcock, H. P., & Zhuang, X. (2016a). High-throughput single-cell gene-expression profiling with multiplexed error-robust fluorescence in situ hybridization. *Proceedings of the National Academy of Sciences of the United States of America*, *113*, 11046–11051. doi: 10.1073/pnas.1612826113.

Moffitt, J. R., Hao, J., Bambah-Mukku, D., Lu, T., Dulac, C., & Zhuang, X. (2016b). High-performance multiplexed fluorescence in situ hybridization in culture and tissue with matrix imprinting and clearing. *Proceedings of the National Academy of Sciences of the United States of America*, *113*, 14456–14461. doi: 10.1073/pnas.1617699113.

Nakahata, Y., Nabekur, A. J., & Murakoshi, H. (2016). Dual observation of the ATP-evoked small GTPase activation and Ca^{2+} transient in astrocytes using a dark red fluorescent protein. *Science Reports*, *6*, 39564. doi: 10.1038/srep39564.

Nederlof, P. M., van der Flier, S., Vrolijk, J., Tanke, H. J., & Raap, A. K. (1992). Fluorescence ratio measurements of double-labeled probes for multiple *in situ* hybridization by digital imaging microscopy. *Cytometry*, *13*, 839–845. doi: 10.1002/cyto.990130806.

Neil, M. A. A., Juskaitis, R., & Wilson, T. (1997). Method of obtaining optical sectioning by using structured light in a conventional microscope. *Optics Letters*, *15*, 1905–1907. doi: 10.1364/OL.22.001905.

Newman, R. H., Fosbrink, M. D., & Zhang, J. (2011). Genetically encodable fluorescent biosensors for tracking signaling dynamics in living cells. *Chemical Reviews*, *111*, 3614–3666. doi: 10.1021/cr100002u.

Newton, I. (1672). A series of quere's propounded by Mr. Isaac Netwon, to be determin'd by experiments, positively and directly concluding his new theory of light and colours; and here recommended to the industry of the lovers of experimental philosophy, as they were generously imparted to the publisher in a letter of the said Mr. Newton of July 8, 1672. *Philosophical Transactions*, *7*, 4004–5007.

Newton, I. (1730). *Optiks; or, a treatise of the reflections, refractions, inflections & colours of light* (4th ed.). London: Dover Publications.

Nguyen, A. W., & Daugherty, P. S. (2005). Evolutionary optimization of fluorescent proteins for intracellular FRET. *Nature Biotechnology*, *23*, 355–360. doi: 10.1038/nbt1066.

Niu, N., Zhang, J., Zhang, N., Mercado-Uribe, I., Tao, F., Han, Z., ... Liu, J. (2016). Linking genomic reorganization to tumor initiation via the giant cell cycle. *Oncogenesis*, *5*, e281. doi: 10.1038/oncsis.2016.75.

Nobelprize.org. (Eds.) (2014). *The Nobel Prize in Chemistry 2014*. Nobel Media AB 2014. Retrieved from https://www.nobelprize.org/nobel_prizes/chemistry/laureates/2014/.

O'Brien, S., Cevario, S., Martenson, J., Thompson, M., Nash, W., Chang, E., ... Lyons, L. (1997). Comparative gene mapping in the domestic cat (*Felis catus*). *The Journal of Heredity*, *88*, 408–414. doi: 10.1093/oxfordjournals.jhered.a023127.

O'Connell, M. J., Bachilo, S. M., Huffman, C. B., Moore, V. C., Strano, M. S., Haroz, E. H., ... Smalley, R. E. (2002). Band gap fluorescence from individual single-walled carbon nanotubes. *Science*, *297*, 593–596. doi: 10.1126/science.1072631.

Oheim, M. (2001). Imaging transmitter release. II. A practical guide to evanescent-wave imaging. *Lasers in Medical Science*, *16*, 159–170. doi: 10.1007/PL00011350.

Okumoto, S., Jones, A., & Frommer, W. B. (2012). Quantitative imaging with fluorescent biosensors. *Annual Review of Plant Biology*, *63*, 663–706. doi: 10.1146/annurev-arplant-042110-103745.

Ormö, M., Cubitt, A. B., Kallio, K., Gross, L. A., Tsien, R. Y., & Remington, S. J. (1996). Crystal structure of the Aequorea victoria green fluorescent protein. *Science*, *273*, 1392–1395. doi: 10.1126/science.273.5280.1392.

Ornberg, R. L., Woerner, B. M., & Edwards, D. A. (1999). Analysis of stained objects in histological sections by spectral imaging and differential absorption. *The Journal of Histochemistry and Cytochemistry*, *47*, 1307–1314. doi: 10.1177/002215549904701010.

Otsu, K., Fujii, J., Periasamy, M., Difilippantonio, M., Upender, M., Ward, D. C., & MacLennan, D. H. (1993). Chromosome mapping of five human cardiac and skeletal muscle sarcoplasmic reticulum protein genes. *Genomics*, *17*, 507–509. doi: 10.1006/geno.1993.1357.

Paddock, S. W. (Ed). (1999). *Confocal microscopy methods and protocols*. Totawa, NJ: Humana Press.

Pan, C., Cai, R., Quacquarelli, F. P., Ghasemigharagoz, A., Lourbopoulos, A., Matryba, P., ... Ertürk, A. (2016). Shrinkage-mediated imaging of entire organs and organisms using uDISCO. *Nature Methods*, *13*, 859–867. doi: 10.1038/nmeth.3964.

Pansare, V., Hejazi, S., Faenza, W., & Prud'homme, R. K. (2012). Review of long-wavelength optical and NIR imaging materials: Contrast agents, fluorophores and multifunctional nano carriers. *Chemistry of Materials*, *24*, 812–827. doi: 10.1021/cm2028367.

Pawley, J. B. (Ed.) (2005). *Handbook of biological confocal microscopy* (3rd ed.). New York: Plenum.

Perkin, W. (1906). Address of William Henry Perkin. *Science*, *24*, 488–493. doi: 10.1126/science.24.616.488.

Phillips, K. G., Baker-Groberg, S. M., & McCarty, O. J. (2014). Quantitative optical microscopy: Measurement of cellular biophysical features with a standard optical microscope. *Journal of Visualized Experiments*, *86*, e50988. doi:10.3791/50988.

Photometrics. (1995). *SenSys user manual for windows*. Tuscon, AZ: Photometrics.

Piper, S. K., Habermehl, C., Schmitz, C. H., Kuebler, W. M., Obrig, H., Steinbrink, J., & Mehnert, J. (2013). Towards whole-body fluorescence imaging in humans. *PLoS One*, *8*, e83749. doi: 10.1371/journal.pone.0083749.

Ploem, J. S. (1967). The use of a vertical illuminator with interchangeable dichroic mirrors for

fluorescence microscopy with incidental light. *Zeitschrift fur Wissenschaftliche Mikroskopie und Mikroskopische Technik*, *68*, 129–142.

Price, J. H., Goodacre, A., Hahn, K., Hodgson, L., Hunter, E. A., Krajewski, S., ... Heynen, S. (2002). Advances in molecular labeling, high throughput imaging and machine intelligence portend powerful functional cellular biochemistry tools. *Journal of Cellular Biochemistry*, *87*(Suppl 39), 194–210. doi: 10.1002/jcb.10448.

Prost, S., Kishen, R. E., Kluth, D. C., & Bellamy, C. O. (2017). Working with commercially available quantum dots for immunofluorescence on tissue sections. *PLoS One*, *11*, e0163856.5858. doi: 10.1371/journal.pone.0163856.

Raman, R. N., Pivetti, C. D., Rubenchik, A. M., Matthews, D. L., Troppmann, C., & Demos, S. G. (2009). Evaluation of the contribution of the renal capsule and cortex to kidney autofluorescence intensity under ultraviolet excitation. *Journal of Biomedical Optics*, *14*, 020505. doi: 10.1117/1.3094948.

Raudsepp, T., Fronicke, L., Scherthan, H., Gustavsson, I., & Chowdhary, B. (1996). Zoo-FISH delineates conserved chromosomal segments in horse and man. *Chromosome Research*, *4*, 218–225. doi: 10.1007/BF02254963.

Rawlins, D. (1992). *Light microscopy*. Oxford: BIOS Scientific Publishers.

Ray, P., De, A., Min, J. J., Tsien, R. Y., & Gambhir, S. S. (2004). Imaging tri-fusion multimodality reporter gene expression in living subjects. *Cancer Research*, *64*, 1323–1330. doi: 10.1158/0008-5472.CAN-03-1816.

Regot, S., Hughey, J. J., Bajar, B. T., Carrasco, S., & Covert, M. W. (2014). High-sensitivity measurements of multiple kinase activities in live single cells. *Cell*, *157*, 1724-1734. doi: 10.1016/j.cell.2014.04.039.

Reitz, F. B., & Pagliaro, L. (1994). Fibre optic scrambling in light microscopy: A computer simulation and analysis. *Journal of Microscopy*, *176*, 143–151. doi: 10.1111/j.1365-2818.1994.tb03508.x.

Rieckher. (2016). Light sheet microscopy to measure protein dynamics. *Journal of Cellular Physiology*, *232*, 27–35. doi: 10.1002/jcp.25451.

Ried, T., Baldini, A., Rand, T. C., & Ward, D. C. (1992). Simultaneous visualization of seven different DNA probes using combinatorial fluorescence and digital imaging microscopy. *Proceedings of the National Academy of Sciences of the United States of America*, *89*, 1388–1392. doi: 10.1073/pnas.89.4.1388.

Ried, T., Mahler, V., Vogt, P., Blonden, L., van Ommen, G. J. B., Cremer, T., & Cremer, M. (1990). Direct carrier detection by *in situ* suppression hybridization with cosmid clones for the Duchenne/Becker muscular dystrophy locus. *Human Genetics*, *85*, 581–586. doi: 10.1007/BF00193578.

Ried, T., Liyanage, M., du Manoir, S., Heselmeyer, K., Auer, G., Macville, M., & Schröck, E. (1997). Tumor cytogenetics revisited: Comparative genomic hybridization and spectral karyotyping. *Journal of Molecular Medicine*, *75*, 801–814. doi: 10.1007/s001090050169.

Rodenacker, K., & Bengtsson, E. (2003). A feature set for cytometry on digitized microscopic images. *Analytical Cellular Pathology*, *25*, 1–36. doi: 10.1155/2003/548678.

Rooney, D., & Czepulkowski, B. (1992). *Human cytogenetics. A practical approach*. New York: Oxford University Press.

Rothmann, C., Barshack, I., Gil, A., Goldberg, I., Kopolovic, J., & Malik, Z. (2000). Potential use of spectral image analysis for the quantitative evaluation of estrogen receptors in breast cancer. *Histology and Histopathology*, *15*, 1051–1057.

Roxbury, D., Jena, P. V., Williams, R. M., Enyedi, B., Niethammer, P., Marcet, S., ... Heller, D. A. (2015). Hyperspectral microscopy of near-infrared fluorescence enables 17-chirality carbon nanotube imaging. *Scientific Reports*, *5*, 14167. doi: 10.1038/srep14167.

Ruestow, E. G. (1996). *The microscope in the Dutch Republic*. New York: Cambridge University Press.

Sachs, R. K., van den Engh, G., Trask, B., Yokota, H., & Hearst, J. E. (1995). A random-walk/giant loop model for interphase chromosomes. *Proceedings of the National Academy of Sciences of the United States of America*, *92*, 2710–2714. doi: 10.1073/pnas.92.7.2710.

Salmon, E. D., & Canman, J. C. (2003). Proper alignment and adjustment of the light microscope. *Current Protocols in Human Genetics*, *38*, A.3N.1–A.3N.25. doi: 10.1002/0471142905.hga03ns38.

Sawano, A., Hama, H., Saito, N., & Miyawaki, A. (2002). Multicolor imaging of Ca2+ and protein kinase C signals using novel epifluorescence microscopy. *Biophysical Journal*, *82*, 1076–1085. doi: 10.1016/S0006-3495(02)75467-2.

Schermelleh, L., Heintzmann, R., & Leonhardt, H. (2010). A guide to super-resolution fluorescence microscopy. *The Journal of Cell Biology*, *190*, 165–175. doi: 10.1083/jcb.201002018.

Schröck, E., du Manoir, S., Veldman, T., Schoell, B., Wienberg, J., Ferguson-Smith, M. A., ... Ried, T. (1996). Multicolor spectral karyotyping of human chromosomes. *Science*, *273*, 494–497. doi: 10.1126/science.273.5274.494.

Schultz, R. A., Nielsen, T., Zavaleta, J. R., Ruch, R., Wyatt, R., & Garner, H. R. (2001). Hyperspectral imaging: A novel approach for microscopic analysis. *Cytometry*, *43*, 239–247. doi: 10.1002/1097-0320(20010401)43:4%3c239::AID-CYTO1056%3e3.0.CO;2-Z.

Scott, B. L., & Hoppe, A. D. (2016). Three-dimensional reconstruction of three-way FRET microscopy improves imaging of multiple protein-protein interactions. *PLoS One*, *11*, e0152401. doi: 10.1371/journal.pone.0152401.

Sednev, M. V., Belov, V. N., & Hell, S. W. (2015). Fluorescent dyes with large Stokes shifts for super-resolution optical microscopy of biological objects: A review. *Methods and Applications in Fluorescence*, *3*, 042004.

Shaner, N. C., Campbell, R. E., Steinbach, P. A., Giepmans, B. N., Palmer, A. E., & Tsien, R. Y. (2004). Improved monomeric red, orange and yellow fluorescent proteins derived from *Discosoma sp*. red fluorescent protein. *Nature Biotechnology*, *22*, 1567–1572. doi: 10.1038/nbt1037.

Sharkey, J., Scarfe, L., Santeramo, I., Garcia-Finana, M., Park, B. K., Poptani, H., ... Murray, P. (2016). Imaging technologies for monitoring the safety, efficacy and mechanisms of action of cell-based regenerative medicine therapies in models of kidney disease. *European Journal of Pharmacology*, *790*, 74–82. doi: 10.1016/j.ejphar.2016.06.056.

Shi, S.-R., Gu, J., & Taylor, C. R. (2000). *Antigen retrieval techniques: Immunohistochemistry and molecular morphology*. Biotechniques Books. Natick, MA: Eaton Publishing Company.

Shi, L., Sordillo, L. A., Rodríguez-Contreras, A., & Alfano, R. (2016). Transmission in near-infrared optical windows for deep brain imaging. *Journal of Biophotonics*, *9*, 38–43. doi: 10.1002/jbio.201500192.

Shotton, D. (1993). *Electronic light microscopy: The principles and practice of video-enhanced contrast, digital intensified fluorescence, and confocal scanning light microscopy*. New York: John Wiley & Sons.

Siedentopf, H., & Zsigmondy, R. (1902). Uber sichtbarmachung und größenbestimmung ultramikoskopischer teilchen, mit besonderer anwendung auf goldrubingläser. [About visualization and sizing ultramicroscopic particles, with particular application to gold ruby glasses]. *Annalen der Physik*, *315*, 1–39. doi: 10.1002/andp.19023150102.

Singer, E. (1932). A microscope for observation of fluorescence in living tissue. *Science*, *75*, 289–291. doi: 10.1126/science.75.1941.289-a.

Spector, D., Goldman, R., & Leinwand, L. (Eds.). (1998). Light microscopy and cell structure. In *Cells: A laboratory manual*. Cold Spring Harbor, NY: Cold Spring Harbor Laboratory Press.

Speicher, M., Ballard, S., & Ward, D. (1996). Karyotyping human chromosomes by combinatorial multi-fluor FISH. *Nature Genetics*, *12*, 1–11. doi: 10.1038/ng0496-368.

Stockholm, D., Bartoli, M., Sillon, G., Bourg, N., Davoust, J., & Richard, I. (2005). Imaging calpain protease activity by multiphoton FRET in living mice. *Journal of Molecular Biology*, *346*, 215–222. doi: 10.1016/j.jmb.2004.11.039.

Stryer, L., & Haugland, R. P. (1967). Energy transfer: A spectroscopic ruler. *Proceedings of the National Academy of Sciences of the United States of America*, *58*, 719–726. doi: 10.1073/pnas.58.2.719.

Sullivan, K. F., & Shelby, R. D. (1999). Using timelapse confocal microscopy for analysis of centromere dynamics in human cells. *Methods in Cell Biology*, *58*, 183–202. doi: 10.1016/S0091-679X(08)61956-1.

Swift, J., (1726). *Gulliver's travels into several remote nations of the world*. London: Benjamin Motte.

Szuhai, K., Bezrookove, V., Wiegant, J., Vrolijk, J., Dirks, R. W., Rosenberg, C., ... Tanke, H. J. (2000). Simultaneous molecular karyotyping and mapping of viral DNA integration sites by 25-color COBRA-FISH. *Genes Chromosomes Cancer*, *28*, 92–97. doi: 10.1002/(SICI)1098-2264(200005)28:1%3c92::AID-GCC11%3e3.0.CO;2-2.

Takai, A., Nakano, M., Saito, K., Haruno, R., Watanabe, T. M., Ohyanagi, T., ... Nagai, T. (2015). Expanded palette of Nano-lanterns for real-time multicolor luminescence imaging. *Proceedings of the National Academy of Sciences of the United States of America*, *112*, 4352–4356. doi: 10.1073/pnas.1418468112.

Taniguchi, M., & Lindsey, J. S. (2017). Synthetic chlorins, possible surrogates for chlorophylls, prepared by derivatization of porphyrins. *Chemical Reviews*, *117*, 344–535. doi: 10.1021/acs.chemrev.5b00696

Taniguchi, M., Cramer, D. L., Bhise, A. D., Kee, H. L., Bocian, D. F., Holten, D., & Lindsey, J. S. (2008). Accessing the near-infrared spectral region with stable, synthetic, wavelength-tunable bacteriochlorins. *New Journal of Chemistry*, *32*, 947–958. doi: 10.1039/b717803d.

Taniwaki, M., Speicher, M. R., Lengauer, C., Jauch, A., Popp, S., & Cremer, T. (1993). Characterization of two marker chromosomes in a patient with acute nonlymphocytic leukemia by two color fluorescence *in situ* hybridization. *Cancer Genetics and Cytogenetics*, *70*, 99–102. doi: 10.1016/0165-4608(93)90175-L.

Tanke, H. J., Wiegant, J., Van Gijlswijk, R. P. M., Bezrookove, V., Pattenier, H., Heetebrij, R. J., ... Vrolijk, J. (1999). New strategy for multicolour fluorescence *in situ* hybridisation. COBRA: Combined binary ratio labelling. *European Journal of Human Genetics*, *7*, 2–11. doi: 10.1038/sj.ejhg.5200265.

Tao, Z., Hong, G., Shinji, C., Chen, C., Diao, S., Antaris, A. L., ... Dai, H. (2013). Biological imaging using nanoparticles of small organic molecules with fluorescence emission at wavelengths longer than 1000 nm. *Angewandte Chemie (International ed. in English)*, *52*, 13002–13006. doi: 10.1002/anie.201307346.

Terskikh, A., Fradkov, A., Ermakova, G., Zaraisky, A., Tan, P., Kajava, A. V., ... Siebert, P. (2000). "Fluorescent timer": Protein that changes color with time. *Science*, *290*, 1585–1588. doi: 10.1126/science.290.5496.1585.

Tewson, P. H., Martinka, S., Shaner, N. C., Hughes, T. E., & Quinn, A. M. (2016). New DAG and cAMP sensors optimized for live-cell assays in automated laboratories. *Jour-*

nal of Biomolecular Screening, *21*, 298–305. doi: 10.1177/1087057115618608.

Thangavelu, M., Pergament, E., Espinosa, R. I., & Bohlander, S. K. (1994). Characterization of marker chromosomes by microdissection and fluorescence *in situ* hybridization. *Prenatal Diagnosis*, *14*, 583–588. doi: 10.1002/pd.1970140712.

Tillberg, P. W., Chen, F., Piatkevich, K. D., Zhao, Y., Yu, C. C., English, B. P., ... Boyden, E. S. (2016). Protein-retention expansion microscopy of cells and tissues labeled using standard fluorescent proteins and antibodies. *Nature Biotechnology*, *34*, 987–992. doi: 10.1038/nbt.3625.

Tjio, J. H., & Levan, A. (1956). The chromosome number of man. *Hereditas*, *42*, 1–6. doi: 10.1111/j.1601-5223.1956.tb03010.x.

Tran, P. T., & Chang, F. (2001). Transmitted light fluorescence microscopy revisited. *The Biological Bulletin*, *201*, 235–236. doi: 10.2307/1543340.

Trask, B., Fertitta, A., Christensen, M., Youngblom, J., Bergmann, A., Copeland, A., ... Tynan, K. (1993). Fluorescence *in situ* hybridization mapping of human chromosome, *19*, Cytogenetic band location of 540 cosmids and 70 genes or DNA markers. *Genomics*, *15*, 133–145. doi: 10.1006/geno.1993.1021.

Tsanov, N., Samacoits, A., Chouaib, R., Traboulsi, A. M., Gostan, T., Weber, C., ... Mueller, F. (2016). smiFISH and FISH-quant - a flexible single RNA detection approach with super-resolution capability. *Nucleic Acids Research*, *44*, e165. doi: https://doi.org/10.1093/nar/gkw784.

Tsien, R. Y. (1998). The green fluorescent protein. *Annual Review of Biochemistry*, *67*, 509–544. doi: 10.1146/annurev.biochem.67.1.509.

Tsien, R. Y. (2005). Building and breeding molecules to spy on cells and tumors. *FEBS Letters*, *579*, 927–932. doi: 10.1016/j.febslet.2004.11.025.

Tsurui, H., Nishimura, H., Hattori, S., Hirose, S., Okumura, K., & Shirai, T. (2000). Seven-color fluorescence imaging of tissue samples based on Fourier spectroscopy and singular value decomposition. *The Journal of Histochemistry and Cytochemistry*, *48*, 653–662. doi: 10.1177/002215540004800509.

Turkowyd, B., Virant, D., & Endesfelder, U. (2016). From single molecules to life: Microscopy at the nanoscale. *Analytical and Bioanalytical Chemistry*, *408*, 6885–6911. doi: 10.1007/s00216-016-9781-8.

Urquidi, V., Sloan, D., Kawai, K., Agarwal, D., Woodman, A. C., Tarin, D., & Goodison, S. (2002). Contrasting expression of thrombospondin-1 and osteopontin correlates with absence or presence of metastatic phenotype in an isogenic model of spontaneous human breast cancer metastasis. *Clinical Cancer Research*, *8*, 61–74.

Valm, A. M., Oldenbourg, R., & Borisy, G. G. (2016). Multiplexed spectral imaging of 120 different fluorescent labels. *PLoS One*, *11*, e0158495. doi: 10.1371/journal.pone.0158495.

van der Voort, H., Valkenburg, J., van Spronsen, E., Woldringh, C., & Brakenhoff, G. (1987). Confocal microscopy in comparison with electron and conventional light microscopy. In M. Hayat (Ed.), *Correlative microscopy in biology: Instrumentation and methods* (pp. 23-37). San Diego: Academic Press.

Veldman, T., Vignon, C., Schröck, E., Rowley, J. D., & Ried, T. (1997). Hidden chromosomes: Abnormalities in hematological malignancies detected by multicolour spectral karyotyping. *Nature Genetics*, *15*, 406–410. doi: 10.1038/ng0497-406.

Voie, A. H., Burns, D. H., & Spelman, F. A. (1993). Orthogonal-plane fluorescence optical sectioning: Three-dimensional imaging of macroscopic biological specimens. *Journal of Microscopy*, *170*, 229–236. doi: 10.1111/j.1365-2818.1993.tb03346.x.

Vollert, C. T., Moree, W. J., Gregory, S., Bark, S. J., & Eriksen, J. L. (2015). Formaldehyde scavengers function as novel antigen retrieval agents. *Scientific Reports*, *5*, 17322. doi: 10.1038/srep17322.

von Waldeyer, W. (1888). Über karyokinese und ihre beziehungen zu den befruchtungsvorgängen. [About mitosis and its relationship with the processes of fertilization]. *Archiv Für Mikroskopische Anatomie und Entwicklungsmechanik*, *32*, 1–122. doi: 10.1007/BF02956988.

Wang, L., Jackson, W. C., Steinbach, P. A., & Tsien, R. Y. (2004). Evolution of new nonantibody proteins via iterative somatic hypermutation. *Proceedings of the National Academy of Sciences of the United States of America*, *101*, 16745–16749. doi: 10.1073/pnas.0407752101.

Wang, X., Rosol, M., Ge, S., Peterson, D., McNamara, G., Pollack, H., ... Crooks, G. M. (2003). Dynamic tracking of human hematopoietic stem cell engraftment using in vivo bioluminescence imaging. *Blood*, *102*, 3478–3482. doi: 10.1182/blood-2003-05-1432.

Ward, D. (2010). Faster, better, cheaper revisited - program management lessons from NASA. *Defense AT&L*, 48-52. Retrieved from http://www.thedanward.com/resources/Faster$2C+Better$2C+Cheaper+Revisited.pdf.

Ward, D. C., Lichter, P., Boyle, A., Baldini, A., Menninger, J., & Ballard, S. G. (1991). Gene mapping by fluorescent *in situ* hybridization and digital imaging microscopy. In J. Lindsten & U. Petterson (Eds.), *Etiology of human diseases at the DNA level*. New York: Raven Press.

Waud, J. P., Bermudez Fajardo, A., Sudhaharan, T., Trimby, A. R., Jeffery, J., Jones, A., & Campbell, A. K. (2001). Measurement of proteases using chemiluminescence-resonance-energy-transfer chimaeras between green fluorescent protein and aequorin. *The*

Biochemical Journal, *357*, 687–697. doi: 10.1042/bj3570687.

White, J. G., Amos, W. B., & Fordham, M. (1987). An evaluation of confocal versus conventional imaging of biological structures by fluorescence light microscopy. *The Journal of Cell Biology*, *105*, 41–48. doi: 10.1083/jcb.105.1.41.

Wiegant, J., Bezrookove, V., Rosenberg, C., Tanke, H. J., Raap, A. K., Zhang, H., ... Meltzer, P. (2000). Differentially painting human chromosome arms with combined binary ratio-labeling fluorescence *in situ* hybridization. *Genome Research*, *10*, 861–865. doi: 10.1101/gr.10.6.861.

Wienberg, J., Jauch, A., Stanyon, R., & Cremer, T. (1990). Molecular cytotaxonomy of primates by chromosomal *in situ* suppression hybridization. *Genomics*, *8*, 347–370. doi: 10.1016/0888-7543(90)90292-3.

Wikipedia. (2016). Torbjorn Caspersson Retrieved from https://en.wikipedia.org/wiki/Torbj%C3%B6rn_Caspersson.

Xing, Y., Johnson, C. V., Dobner, P. R., & Lawrence, J. B. (1993). Higher level organization of individual gene transcription and RNA splicing. *Science*, *259*, 1326–1330. doi: 10.1126/science.8446901.

Xu, Y., Piston, D. W., & Johnson, C. H. (1999). A bioluminescence resonance energy transfer (BRET) system: Application to interacting circadian clock proteins. *Proceedings of the National Academy of Sciences of the United States of America*, *96*, 151–156. doi: 10.1073/pnas.96.1.151.

Xu, T., Close, D., Handagama, W., Marr, E., Sayler, G., & Ripp, S. (2016). The expanding toolbox of in vivo bioluminescent imaging. *Frontiers in Oncology*, *6*, 150. doi: 10.3389/fonc.2016.00150.

Yokota, H., Singer, M. J., van den Engh, G. J., & Trask, B. J. (1997). Regional differences in the compaction of chromatin in human G0/G1 interphase nuclei. *Chromosome Research*, *5*, 157–166. doi: 10.1023/A:1018438729203.

Yokota, H., van den Engh, G., Hearst, J. E., Sachs, R. K., & Trask, B. J. (1995). Evidence for the organization of chromatin in megabase pair-sized loops arranged along a random walk path in the human G0/G1 interphase nucleus. *The Journal of Cell Biology*, *130*, 1239–1249. doi: 10.1083/jcb.130.6.1239.

Yuste, R., & Konnerth, A. (2005). *Imaging in neuroscience and development. A laboratory manual*. Cold Spring Harbor, NY: Cold Spring Harbor Press

Zernike, F. (1955). How I discovered phase contrast. *Science*, *121*, 345–349. doi: 10.1126/science.121.3141.345.

Zhang, W., Purchio, A., Chen, K., Burns, S. M., Contag, C. H., & Contag, P. R. (2003). In vivo activation of the human CYP3A4 promoter in mouse liver and regulation by pregnane X receptors. *Biochemical Pharmacology*, *65*, 1889–1896. doi: 10.1016/S0006-2952(03)00188-6.

Zhang, Y. S., Chang, J. B., Alvarez, M. M., Trujillo-de Santiago, G., Aleman, J., Batzaya, B., ... Khademhosseini, A. (2016). Hybrid microscopy: Enabling inexpensive high-performance imaging through combined physical and optical magnifications. *Scientific Reports*, *6*, 22691. doi: 10.1038/srep22691.

Zhao, Y., Araki, S., Wu, J., Teramoto, T., Chang, Y. F., Nakano, M., ... Campbell, R. E. (2011). An expanded palette of genetically encoded Ca^{2+} indicators. *Science*, *333*, 1888–1891. doi: 10.1126/science.1208592.

Zucker, R. M. (2006). Whole insect and mammalian embryo imaging with confocal microscopy: Morphology and apoptosis. *Cytometry. Part A*, *69*, 1143–1152. doi: 10.1002/cyto.a.20343.

Zucker, R. M., & Jeffay, S. C. (2006). Confocal laser scanning microscopy of whole mouse ovaries: Excellent morphology, apoptosis detection, and spectroscopy. *Cytometry Part A*, *69*, 930–939. doi: 10.1002/cyto.a.20315.

KEY REFERENCES

Newman, R. H., Fosbrink, M. D., Zhang, J., (2011). Genetically encodable fluorescent biosensors for tracking signaling dynamics in living cells. *Chemical Reviews*, *111*, 3614-3666. doi: 10.1021/cr100002u.

See supplemental file. An extensive review related to the construction and use of fluorescently tagged proteins for monitoring and measuring proteins and protein-protein interactions in living cells.

Zhang, J., Ni, Q., Newman, R. H. (Eds.) (2014). *Fluorescent protein-based biosensors: methods and protocols, Methods in Molecular Biology 1071*. Totowa, NJ: Humana Press.

Fluorescent biosensor applications for live cell imaging of many biological processes.

INTERNET RESOURCES

http://biosensor.dpb.carnegiescience.edu/biosensors

Contributed by DPB/DGE Codex; see W. B. Frommer entry for molecular sensors.

https://www.addgene.org/fluorescent-proteins/biosensors

Contributed by Addgene; fluorescent protein guide: Biosensors.

http://www.GeoMcNamara.com

Contributed by George McNamara.

Table 4.4.1 Fluorescent Proteins Photophysics Data[a]

Fluorescent protein	Abs or Ex max (nm)	Em max (nm)	Extinction coefficient	Quantum yield	Brightness index	Brightness relative to eGFP
AcS-CFP (acid stable)	440	480	36,700	0.35	13	0.38
Amarillo (GFPmut3*Y203)	514	526	NA	NA	NA	NA
amFP486 Anemonia majano	458	486	40,000	0.24	10	0.29
amilCFP	441	489	29,500	0.90	27	0.79
Aqua (GFPmut3*L64T65W66)	425	450	NA	NA	NA	NA
Aquamarine	430	474	26,000	0.89	23	0.69
Azure (eGFPY66H)	385	450	NA	NA	NA	NA
Azurite	383	447	51,000	0.48	24	0.73
Bronze (GFPmut3*T65W66Y203)	468	507	NA	NA	NA	NA
Celeste (eGFP*66)	456	490	NA	NA	NA	NA
Cerulean	433	475	43,000	0.58	25	0.74
cgreGFP	485	500	63,000	0.86	54	1.61
Chlopsid FP 1 + bilirubin	489	523	77,000	0.47	36	1.08
Chlopsid FP 1-GGG + bilirubin	489	523	77,000	0.11	8	0.25
Chlopsid FP 2 + bilirubin	489	523	77,000	0.37	28	0.85
Clavularia sp.	456	484	35,300	0.48	17	0.50
Clover	505	515	111,000	0.76	84	2.51
CreiLOV	450	495	12,500	0.51	6	0.19
CyOFP1	497	589	40,000	0.76	30	0.90
CyOFP1	497	589	40,000	0.76	30	0.90
CyPet	435	477	35,000	0.51	18	0.53
dLanYFP	513	524	125,000	0.90	113	3.35
dsFP483 Discosoma striata	443	483	23,900	0.46	11	0.33
E2-Crimson	605	646	58,500	0.12	7	0.21
EBFP	377	446	30,000	0.15	5	0.13
EBFP2	383	448	32,000	0.45	14	0.43
EcFbFP (Flavin based)	450	495	12,500	0.39	5	0.15
ECFP	433	475	33,000	0.14	5	0.14
eCGP123	493	504	68,000	0.70	48	1.42
eforCP/RFP (chromoprotein)	589	609	111,300	0.16	18	0.53
eGFP	488	507	56,000	0.60	34	1.00
eqFP611	559	611	78,000	0.45	35	1.04
eqFP650	592	650	65,000	0.24	16	0.46
eqFP670	605	670	70,000	0.06	4	0.13
EYFP	514	526	72,000	0.76	55	1.63
FF-GFP (fast folding)	490	514	71,750	0.64	46	1.37

continued

Table 4.4.1 Fluorescent Proteins Photophysics Data[a], *continued*

Fluorescent protein	Abs or Ex max (nm)	Em max (nm)	Extinction coefficient	Quantum yield	Brightness index	Brightness relative to eGFP
FFTS-YFP (fast folding, thermostable)	510	528	95,000	0.68	65	1.92
FusionRed	580	608	94,500	0.19	18	0.53
gfasCP (chromoprotein)	577		205,200		None	None
GFP Aequorea victoria ("wild-type")	397	509	27,600	0.80	22	0.66
GFPmut3b	500	515	38,520	0.44	17	0.50
HcRed-Tandem	590	637	160,000	0.04	6	0.19
hmKeima4.15	430	612	28,000	0.29	8	0.24
hmKeima8.5	438	612	32,000	0.34	11	0.32
IFP1.4	684	708	92,000	0.07	6	0.19
IFP2.0	690	711	86,000	0.08	7	0.20
iLOV	450	495	12,500	0.34	4	0.13
iRFP670	643	670	114,000	0.11	13	0.37
iRFP670	643	670	114,000	0.11	13	0.37
iRFP670	663	682	90,000	0.11	10	0.29
iRFP682	663	682	90,000	0.11	10	0.29
iRFP702	673	702	93,000	0.08	7	0.22
iRFP713	690	713	98,000	0.06	6	0.18
iRFP720	702	720	96,000	0.06	6	0.17
Katushka	588	635	65,000	0.34	22	0.66
Katushka2S	588	633	67,000	0.44	29	0.88
Kriek (photostable mCherry)	593	618	100,000	0.08	8	0.24
LanFP6-G	499	517	36,800	0.01	2	0.01
LanFP10-A	492	504	59,000	0.08	5	0.14
LanFP10-G	492	502	57,000	0.03	2	0.05
lanRFP-ΔS83	521	592	71,000	0.10	7	0.21
LanYFP	513	524	150,000	0.95	143	4.24
LSS-mKate1	463	624	31,200	0.08	2	0.07
LSS-mKate2	460	605	26,000	0.17	4	0.13
LSSmOrange	437	572	52,000	0.45	23	0.70
mAG (monomeric Azami Green)	491	504	52,000	0.76	40	1.18
mAmetine	406	526	45,000	0.58	26	0.78
mApple	568	592	75,000	0.49	37	1.09
Mar (GFPmut3*T65W66)	425	450	NA	NA	NA	NA
mBeRFP	446	611	65,000	0.27	18	0.52
mBlueberry2	402	467	51,000	0.48	24	0.73
mCardinal	604	659	87,000	0.19	17	0.49

continued

Table 4.4.1 Fluorescent Proteins Photophysics Data[a], *continued*

Fluorescent protein	Abs or Ex max (nm)	Em max (nm)	Extinction coefficient	Quantum yield	Brightness index	Brightness relative to eGFP
mCerulean2	432	474	47,000	0.60	28	0.84
mCerulean2.N	440	484	49,000	0.48	24	0.70
mCerulean2.N(T65S)	439	481	40,000	0.87	35	1.04
mCerulean3	434	474	34,000	0.84	29	0.85
mCherry	587	610	72,000	0.22	16	0.47
mCherry (Cranfill et al., 2016)	586	610	85,000	0.30	26	0.76
mCherry cp196V1.2	587	610	49,500	0.21	10	0.31
mCherry (Nakahata, 2016)	585	611	78,000	0.17	13	0.40
mCherry (I202Y) "dark"	590	620	32,000	0.02	1	0.02
mCherry (I202T) "dark"	587	617	42,000	0.04	2	0.05
mCitrine	516	529	77,000	0.76	59	1.74
mClover3	506	518	109,000	0.78	85	2.53
meffRFP	560	576	99,600	0.56	56	1.66
meleRFP	573	579	45,600	0.85	39	1.15
mEmerald	487	509	57,000	0.68	39	1.15
mGarnet	598	670	95,000	0.09	9	0.25
mGarnet2	598	670	105,000	0.09	9	0.27
miniSOG	447	496	16,700	0.37	6	0.18
mKalama1	385	456	36,000	0.45	16	0.48
mKate2	588	633	62,500	0.40	25	0.74
mKeima	440	620	14,400	0.24	3	0.10
mKO (monomeric Kusabira-Orange)	548	559	51,600	0.60	31	0.92
mKOκ	551	563	105,000	0.61	64	1.91
mLumin	587	621	70,000	0.46	32	0.96
mMiCy (monomeric Midoriishi-Cyan)	470	496	22,150	0.70	16	0.46
mNeonGreen	506	517	116,000	0.80	93	2.76
mNeptune	600	650	59,000	0.20	12	0.35
mNeptune S28H	590	652	70,000	0.25	18	0.52
mNeptune2.5	599	643	95,000	0.28	27	0.79
modBFP	390	455	27,000	0.33	9	0.27
modBFP H148K	390	455	25,000	0.17	4	0.13
mOrange	548	562	71,000	0.69	49	1.46
mOrange2	549	585	58,000	0.60	35	1.04
Mostaza (eGFP*Y203)	425	450	NA	NA	NA	NA
mPapaya (Cranfill et al., 2016)	528	540	62,000	0.74	46	1.37

continued

Table 4.4.1 Fluorescent Proteins Photophysics Data[a], *continued*

Fluorescent protein	Abs or Ex max (nm)	Em max (nm)	Extinction coefficient	Quantum yield	Brightness index	Brightness relative to eGFP
mPapaya1	530	541	43,000	0.83	36	1.06
mPlum	590	649	41,000	0.10	4	0.12
mPlum (Cranfill et al., 2016)	589	645	80,000	0.33	26	0.79
mRaspberry	598	625	86,000	0.15	13	0.38
mRFP1 (Cranfill et al., 2016)	586	609	55,000	0.35	19	0.57
mRojoA	596	633	82,000	0.02	2	0.05
mRojoA-VHSV	592	622	117,000	0.04	5	0.14
mRojoA-VYGV	591	616	60,000	0.05	3	0.09
mRuby	558	605	112,000	0.35	39	1.17
mRuby2	559	600	113,000	0.38	43	1.28
mRuby3	558	592	128,000	0.45	58	1.71
mRuby-N143S-T158S	556	602		0.15		
mRuby-N143S-T158C	577	610		0.14		
mRuby625	582	625		0.06		
mRuby625-M41Q	571	601		0.04		
mRuby625-H197A	592	642		0.02		
mRuby625-H197L	589	634		0.02		
mScarlet	569	594	100,000	0.70	71	2.12
mScarlet-I	569	593	104,000	0.54	57	1.70
mScarlet-H	551	592	74,000	0.20	15	0.45
mStable (before activation)	603	644	13,000	0.07	1	0.03
mStable (after activation)	597	633	45,000	0.17	7	0.22
mStrawberry	574	596	90,000	0.29	26	0.78
mTagBFP	399	456	41,400	0.63	26	0.78
mTagBFP2	399	454	50,600	0.64	32	0.96
mTFP1	462	492	64,000	0.84	54	1.60
mTurquoise (Cranfill et al., 2016)	434	474	31,000	0.84	26	0.78
mTurquoise2 (Cranfill et al., 2016)	434	473	31,000	0.92	29	0.85
mTurquoise2	434	474	30,000	0.93	28	0.83
mUKG	483	499	60,000	0.72	43	1.29
mvCitrine-145(3) (Cl- low sensitivity)	516	529	66,000	0.73	48	1.43
mVenus	515	528	92,000	0.57	52	1.56
mWasabi	493	509	70,000	0.80	56	1.67
NirFP	605	670	15,700	0.06	1	0.03
NowGFP	492	502	57,000	0.76	43	1.29
NTnC GECI, zero Ca^{2+}	505	518	108,000	0.71	77	2.30

continued

Table 4.4.1 Fluorescent Proteins Photophysics Data[a], *continued*

Fluorescent protein	Abs or Ex max (nm)	Em max (nm)	Extinction coefficient	Quantum yield	Brightness index	Brightness relative to eGFP
NTnC GECI, saturated Ca^{2+}	505	518	52,000	0.65	34	1.01
NTnC-G166D/G202D	505	518	108,000	0.71	77	2.30
oxBFP	385	448	31,000	0.56	17	0.52
oxCerulean	435	477	56,000	0.41	23	0.68
oxGFP	486	510	87,000	0.58	50	1.50
oxmCerulean3 (moxCerulean3)	434	474	41,000	0.87	36	1.06
oxmNeonGreen (moxNeonGreen)	505	520	111,000	0.74	82	2.44
oxVenus	514	526	89,000	0.49	44	1.30
PhiYFP Ser161Ala	524	537	103,000	0.76	78	2.33
PhiYFPv	524	537	101,300	0.59	60	1.78
pmimGFP (copepod, tetrameric)	491	505	79,000	0.92	73	2.16
PpFbFP	450	495	12,500	0.17	2	0.06
psamCFP	404	492	30,800	0.96	30	0.88
RFP639	588	639	69,000	0.18	12	0.37
R-GECO GECI Ca^{2+}free	445	577	22,000	0.06	1	0.02
R-GECO GECI Ca^{2+}saturated	561	589	51,000	0.20	10	3.05
Sandercyanin BLA (bilivirdin IX alpha)	375 630	675	21,000 13,500	0.02	1 1	0.01 0.10
Sapphire	399	511	29,000	0.64	19	0.55
Sapphire-T (T- Sapphire)	399	511	44,000	0.60	26	0.79
sarcGFP	483	500	76,700	0.96	74	2.19
scubRFP	570	578	66,400	0.60	40	1.19
sfGFP (superfolder)	485	510	83,000	0.65	54	1.61
ShadowG (dark acceptor)	486	510	89,000	<0.01	None	None
sgBCP (S. gigantea)	608		122,500		None	None
sgBCP-Q62M	608		123,000		None	None
sgBCP-S157T	611		85,600		None	None
sgBCP-S157C	604		58,000		None	None
shBFP (*Stichodactyla haddoni*)	401	458	15,400	0.79	12	0.36
shBFP-N158K/L173I	375	458	19,500	0.78	15	0.45
shBFP-N158S/L173I	375	458	24,100	0.84	20	0.60
Sirius	355	424	15,000	0.24	4	0.11
smURFP + biliverdin (BV)	642	670	180,000	0.18	32	0.96
smURFP + BVMe2	642	670	65,000	0.12	8	0.23

continued

Table 4.4.1 Fluorescent Proteins Photophysics Data[a], *continued*

Fluorescent protein	Abs or Ex max (nm)	Em max (nm)	Extinction coefficient	Quantum yield	Brightness index	Brightness relative to eGFP
sREACh (dark acceptor)	517	531	115,000	0.07	8	0.24
SCFP1	434	477	29,000	0.24	7	0.21
SCFP2	434	474	29,000	0.41	12	0.35
SCFP3A	433	474	30,000	0.56	17	0.50
SCFP3A	434	474	30,000	0.50	15	0.45
SHardonnay (eYFP-Y203F)	511	524	89,000	0.75	67	2.00
SYFP2	515	527	101,000	0.68	69	2.04
TagCFP	458	480	37,000	0.57	21	0.63
TagGFP	482	505	58,000	0.59	34	1.02
TagGFP2	483	506	56,500	0.60	34	1.01
TagRFP	555	584	100,000	0.48	48	1.43
TagRFP657	611	657	34,000	0.10	3	0.10
TagRFP675	598	675	46,000	0.08	4	0.11
TagRFP675 N143S	578	633	45,000	0.38	17	0.51
TagRFP675 Q41M	595	643	46,600	0.18	8	0.25
TagYFP	508	524	64,000	0.62	40	1.18
TDsmURFP + biliverdin (BV)	642	670	170,000	0.18	31	0.91
tdTomato	554	581	92,000	0.55	51	1.51
TGP (thermal green protein)	493	507	64,000	0.66	42	1.26
Topaz	514	527	94,500	0.60	57	1.69
UnaG	498	527	77,300	0.51	39	1.17
VafLOV	450	495	12,500	0.23	3	0.09
Venus2 (V2)	515	528	184,000	0.57	105	3.12
Venus3 (V3)	515	528	276,000	0.57	157	4.68
Venus4 (V4)	515	528	368,000	0.57	210	6.24
Venus5 (V5)	515	528	460,000	0.57	262	7.80
Venus6 (V6)	515	528	552,000	0.57	315	9.36
Violeta (GFPmut3*W66)	350	425	NA	NA	NA	NA
vsfGFP-0 (dimer)	485	510	209,000	0.76	159	4.73
vsfGFP-0 (monomer)	485	510	104,500	0.70	73	2.18
WasCFP	492	505	51,000	0.85	43	1.29
WiPhy (Wi-Phy)	700	722	118,000	0.06	7	0.21
WiPhy2 (Wi-Phy2)	696	719	118,000	0.09	10	0.31
YPet	517	530	104,000	0.77	80	2.38

continued

Table 4.4.1 Fluorescent Proteins Photophysics Data[a], *continued*

Fluorescent protein	Abs or Ex max (nm)	Em max (nm)	Extinction coefficient	Quantum yield	Brightness index	Brightness relative to eGFP
zFP506 *Zoanthus* sp.	496	506	35,600	0.63	22	0.67
zFP538 *Zoanthus* sp.	528	538	20,200	0.42	8	0.25

[a]Table 4.4.1 ignores photostability (photoinstability), molecular weight, monomer versus dimer versus tetramer, oligomerization, aggregation proneness, pKa (pH sensitivity) and more. Jellyfish (EGFP), coral, Amphioxus (as examples) fluorescent proteins require one or two oxygen molecules to manufacture the chromophore bonds (a product is H_2O_2). LOV proteins require Flavin cofactor. Wi-Phy, iRFPs, UnaG, require biliverdin. This table also excludes photocontrollable fluorescent proteins: Photoactivatable, photoconvertible, photoswitchable. Cranfill et al. (2016) published an experimental direct comparison of several popular fluorescent proteins with literature comparisons. NTnC GECI (genetically engineered Ca^{2+} ion indicator) is used as an example of a small, state of the art, fluorescent protein biosensor; also shown is Ca^{2+} ion insensitive double mutant control (Barykina et al., 2016). NTnC is an inverse signal (No Ca^{2+} bright, Ca^{2+} saturated ~50% brightness) FP biosensor—the paper shows simultaneous use with R-GECO (red fluorescence, dark to bright) FP biosensor—these could be used together to enhance ratiometric response. Subcellular localization, e.g., to cytoplasmic side of plasma membrane, could be used to further improve signal-to-noise ratio and provide compartment specific data. The NTnC Ca^{2+} insensitive double mutant and mCherry (R-GECO's parent, Zhao et al., 2011) could be simultaneously localized and concentrated to the nucleolus, Golgi body or other "out of the way" compartment. PubMed (*https://www.ncbi.nlm.nih.gov/pubmed*), Google, ScienceDirect, Highwire Press, and other search engines and publishers can be used to find full text publications of all fluorophores and fluorescent proteins listed. Photochangeable fluorescent proteins are reviewed in Turkowyd et al. (2016) and summarized in Lambert and Thorn (2016). Sandercyanin:BLA is a lipocalin family member; non-fluorescent apo-protein is 18 kDa, fluorescent tetramer is 75 kDa; quantum yield in 70% D_2O is 1.66 times that in H_2O (0.0267 versus 0.016; Ghosh et al., 2016). GE Healthcare Life Sciences, 2017 Imaging Principles and Methods, is a good introduction to fluorescence imaging for both macroscopic (i.e., Western blots) and microscopy. Recommendation on reporting standards for fluorescent proteins can be found in Evanko (2012), along with request for improvements in reporting requirements (*http://blogs.nature.com/methagora/2012/12/our-reporting-standards-for-fluorescent-proteins-feedback-wanted.html*). Updates can be found at *www.GeoMcNamara.com*.

Table 4.4.2 Fluorophores Photophysics Data[a]

Fluorophore	Abs or Ex max (nm)	Em max (nm)	Extinction coefficient	Quantum yield	Brightness index
Acridine orange	271	520	27,000	0.20	5
Alexa Fluor 430	431	541	16,000	0.55	9
Alexa Fluor 488	495	519	71,000	0.94	67
Alexa Fluor 532	532	553	81,000	0.80	65
Alexa Fluor 546	556	573	104,000	0.96	100
Alexa Fluor 568	578	603	91,300	0.75	69
Alexa Fluor 594	590	617	73,000	0.64	47
Allophycocyanin (APC)	650	660	700,000	0.68	476
Atto 390	390	479	24,000	0.90	22
Atto 425	436	484	45,000	0.65	29
Atto 430LS	433	547	32,000	0.65	21
Atto 465	453	508	75,000	0.75	56
Atto 490LS	496	661	40,000	0.30	12
Atto 520	525	547	105,000	0.95	100
Atto 532	534	560	115,000	0.90	104
Atto 565	566	590	120,000	0.97	116
Atto 590	598	634	120,000	0.90	108
Atto 610	616	646	150,000	0.70	105
Atto 620	620	641	120,000	0.50	60
Atto 635	637	660	120,000	0.45	54
Atto 655	655	680	125,000	0.50	63
Atto 680	675	699	125,000	0.40	50
ATTO-Dino 1 (dsDNA)	490	531	179,000	0.70	125
ATTO-Dino 2 (dsDNA)	506	535	162,000	0.70	113
Bacteriochlorin (“BC”)	713	717	120,000	0.11	13
Bacteriochlorin BC-T2-T12	737	744	120,000	0.14	17
Bacteriochlorin BC-Ph3-Ph13	736	742	120,000	0.12	14
Bacteriochlorin BC-T2-OMe5-T12	732	739	120,000	0.18	22
Bacteriochlorin BC-V3-V13	750	756	120,000	0.10	12
Bacteriochlorin BC-PE3-PE13	763	768	120,000	0.15	18
Bacteriochlorin BC-A3-A13	768	774	120,000	0.09	11
Bacteriochlorin BC-F3-F13	771	777	120,000	0.07	8
BODIPY 507/545	513	549	82,800	0.73	60
BODIPY FL	504	510	70,000	0.90	63
BODIPY TR	588	616	68,000	0.84	57
B-phycoerythrin (B-PE)	545	575	2,410,000	0.98	2362
Calcein	494	516	81,000	0.78	63
Cascade Blue	378	423	26,000	0.54	14

continued

Table 4.4.2 Fluorophores Photophysics Data[a], *continued*

Fluorophore	Abs or Ex max (nm)	Em max (nm)	Extinction coefficient	Quantum yield	Brightness index
Chromeo 488	488	517	73,000	0.27	20
Chromeo 494	494	628	55,000	0.15	8
Chromeo 505	505	526	70,000	0.30	21
Chromeo 546	545	561	98,800	0.15	15
Chromeo 642	642	660	180,000	0.21	38
Chromeo P429 Py-Dye	429	536	75,000	0.10	8
Chromeo P503 Py-Dye	503	600	24,000	0.50	12
Chromeo P540 Py-Dye	533	627	50,000	0.20	10
Chromeo P543 Py-Dye	543	590	57,000	0.15	9
Coumarin 6	456	500	54,000	0.78	42
Cresyl violet perchlorate	603	622	83,000	0.54	45
Cy3	552	570	150,000	0.15	23
Cy3B	552	570	130,000	0.67	87
Cy5	649	670	250,000	0.28	70
Cy5.5	675	694	250,000	0.23	58
Cy7	755	778	250,000	0.28	70
DAPI (in DMSO)	353	465	27,000	0.58	16
DAPI (in H_2O)	344	487	27,000	0.04	1
DsRed	558	583	75,000	0.70	52
Eosin Y	525	543	112,000	0.67	75
EYFP	514	527	84,000	0.61	51
Fluorescein	490	514	90,000	0.92	83
Fluorescein FH3+ (pH <3)	437		53,000		
Fluorescein FH2 (pH 4)	434		11,000		
Fluorescein FH- (pH 5.3)	472	515	29,000	0.37	11
Fluorescein F2- (pH >8)	490	515	76,900	0.92	71
FM 1-43	479	598	40,000	0.30	12
Fura-2, Ca^{2+} free	363	512	28,000	0.23	6
Fura-2, Ca^{2+} saturated	335	505	34,000	0.49	17
Fura-2, Mn^{2+}saturated	335			0	0
Fura-2, Zn^{2+} saturated	345	505	34,000	0.69	24
Hoechst 33258 (in DMF)	354	486	46,000	0.35	16
Hoechst 33258 (in H_2O)	345	507	46,000	0.03	2
Indo-1, Ca^{2+} free	346	475	33,000	0.38	13
Indo-1, Ca^{2+} saturated	330	401	33,000	0.56	18
IRDye38	778	806	179,000	0.35	62
IRDye40	768	788	140,000	0.38	53
IRDye700	681	712	170,000	0.48	81
IRDye78	768	796	220,000	0.31	68

continued

Table 4.4.2 Fluorophores Photophysics Data[a], *continued*

Fluorophore	Abs or Ex max (nm)	Em max (nm)	Extinction coefficient	Quantum yield	Brightness index
IRDye80	767	791	250,000	0.21	53
IRDye800	787	812	275,000	0.15	41
Janelia Fluor 354 (JF354)	354	467	15,000	0.96	14
Janelia Fluor 387 (JF387)	387	470	24,000	0.84	20
Janelia Fluor 464 (JF464)	464	553	18,000	0.28	5
Janelia Fluor 492 (JF492; JF A.O.)	492	531	47,000	0.52	24
Janelia Fluor 505 (JF505)	505				
Janelia Fluor 519 (JF519)	519	546	59,000	0.85	50
Janelia Fluor 549 (JF549)	549	571	101,000	0.88	89
Janelia Fluor 608 (JF608)	608	631	99,000	0.67	66
Janelia Fluor 637 (JF637; SiRhQ)	637	654	77,000	0.38	29
Janelia Fluor 646 (JF646)	646	664	152,000	0.54	82
Janelia Fluor 647 (JF647)	647	661	99,000	0.24	24
JOE	520	548	73,000	0.60	44
Lucifer Yellow CH	230	542	24,200	0.21	5
Merocyanine 540	559	579	138,000	0.39	54
neo-Cy5 (DMSO)	656	675	195,000	0.25	49
NIR1	761	796	268,000	0.23	62
NIR2	662	684	250,000	0.34	85
NIR3	750	777	275,000	0.28	77
NIR4	650	671	260,000	0.43	1112
Oregon Green 488	496	516	76,000	0.90	68
Oregon Green 514	506	526	88,000	0.96	85
Oyster - 645 (ethanol)	651	669	250,000	0.40	100
Oyster - 656 (ethanol)	665	684	220,000	0.50	11
Pacific Blue	400	447	29,500	0.55	16
Perylene	253	435	38,500	0.94	36
Phenylalanine	222	279	195	0.02	<0.1
POPOP	256	407	47,000	0.93	44
Quinine sulfate (in 0.5 M H_2SO_4)	256	451	5700	0.55	3
Rhodamine 110	496	520	80,000	0.89	71
Rhodamine 6 G	530	552	116,000	0.95	110
Rhodamine B	543	565	106,000	0.70	74
Riboflavin	262	531	34,800	0.37	13
Rose bengal	559	571	90,400	0.11	10
R-Phycoerythrin (R-PE)	480	578	1,960,000	0.68	1333
SNIR1	666	695	218,000	0.24	52

continued

Table 4.4.2 Fluorophores Photophysics Data[a], *continued*

Fluorophore	Abs or Ex max (nm)	Em max (nm)	Extinction coefficient	Quantum yield	Brightness index
SNIR3	667	697	245,000	0.24	59
Star 440 SXP	436	515	22,700	0.68	15
Star 470 SXP	472	624	29,000	0.12	4
Star 488	503	524	64,500	0.89	57
Star 512	511	530	84,000	0.82	69
Star 520SXP	515	612	60,000	0.05	3
Star 580	587	607	72,000	0.90	65
Star 600	604	627	43,500	0.73	32
Star 635	639	654	63,000	0.51	32
Star 635P	635	651	125,000	0.92	115
Star Red	638	655	212,000	0.90	191
Sulforhodamine 101	576	591	139,000	0.90	125
Texas Red	586	605	108,000	0.77	83
Texas Red-X	583	603	116,000	0.90	104
TMR	540	565	95,000	0.68	65
Trp	287	348	6000	0.31	2
Tyr	275	303	1500	0.21	0.3
Polymers: Brilliant Violets, Brilliant Ultraviolets, Brilliant Blue; Super Bright					
Brilliant Violet BV421	405	421	2,500,000	0.65	1625
Brilliant Violet BV510	405	510	577,000	0.44	254
Brilliant Violet BV570	405	570	2,300,000	0.08	184
Brilliant Violet BV605	405	603	2,400,000	0.29	696
Brilliant Violet BV650	405	645	2,500,000	0.17	425
Brilliant Violet BV711	405	711	2,800,000	0.15	420
Brilliant Violet BV785	405	785	2,500,000	0.04	100
Brilliant Ultraviolet BUV395	348	395			
Brilliant Ultraviolet BUV496	348	496			
Brilliant Ultraviolet BUV563	348	563			
Brilliant Ultraviolet BUV661	348	661			
Brilliant Ultraviolet BUV737	348	737			
Brilliant Ultraviolet BUV805	348	805			
Brilliant Blue BB515	490	515			
Brilliant Blue BB480	436	478	1,450,000	0.69	1001
Super Bright 436 (SB436)	414	436			
Super Bright 600 (SB600)	414	600			
Fluorescent nanocrystal quantum dots					
Product	Em Peak	Em FWHM	Extinction coefficient	Quantum yield	Brightness index
QD525	525	≤32	320,000	0.60	192
QD565	565	≤34	1,100,000	0.40	440

continued

Table 4.4.2 Fluorophores Photophysics Data[a], *continued*

Product	Em Peak	Em FWHM	Extinction coefficient	Quantum yield	Brightness index
QD585	585	≤34	2,200,000	0.40	880
QD605	605	≤27	2,400,000	0.40	960
QD625	625		9,900,000		>2300
QD655	655	≤34	5,700,000	0.40	2280
QD705	705	Wide	8,300,000		
QD800	800		10,600,000		
QD585 Vivid	585		5,300,000		
QD605 Vivid	605		7,700,000		
QD625 Vivid	625		9,900,000		
QD655 Vivid	655		11,000,000		
QD705 Vivid	705		10,000,000		
QD800 Vivid	800		11,000,000		
eVolve 605	605				
eVolve 655	655				

[a]Brightness Index = Extinction coefficient × Quantum Yield / 1000. Table features fluorophores for which all four major photophysical parameters—absorption (excitation) maximum, fluorescence emission maximum extinction coefficient (M^{-1} cm^{-1}) and fluorescence quantum yield—are available. QD625 values details have not been published, but they are brighter than QD605 or QD655.

Antibody, streptavidin, tetramers/pentamers/dextramers, and other macromolecular labeling have "degree of labeling" (DoL) issues. As a simplistic rule of thumb, one fluorophore can be conjugated to the surface of a protein for every 25,000 dalton molecular weight. An IgG molecule is ~155,000 dalton, so ~6 fluorophores can be conjugated without too much quenching or causing the protein to crash out of solution. With random labeling of lysines, such as isothiocyanate chemistry (FITC, TRITC), there is a risk of the reactive dye making a covalent bond in an Fab binding site, which would occlude binding to the target antigen epitope. If both Fabs were occluded, this dye-IgG would not bind antigenic epitope at all, but could bind non-specifically, increasing background. If there are 50 reactive lysines on the surface of an IgG molecule, and degree of labeling is 6 (± some variability), the population of antibody molecules applied to a specimen is going to be very heterogeneous: A small reaction may not have any identical antibody molecules. DoL of different batches of antibodies are unlikely to be identical. Isotype controls, whether a mouse IgG1 monoclonal antibody (defined specificity different than your interest), or polyclonal affinity purified from sera, are at best imperfect controls. Immunoglobulins also vary in glycosylation, disulfide bonding, and single nucleotide polymorphisms—including some that result in amino acid substitutions that affect Fc Receptor binding affinity. A recent (2015) trend has been for vendors, e.g., Miltenyi Biotec REAfinity, to use the same "backbone" for their entire product line antibodies.

The fluorophore dyes section of the table is abridged from a 4700 plus entry data table Excel file the authors posted on the internet, *https://works.bepress.com/gmcnamara/9* with project title PubSpectra.

The Web site download also contains 400 plus entry fluorescent proteins data table Excel file. Spectra for many of these dyes, and commercial filters and light sources, are available through an interactive Web site at *http://www.spectra.arizona.edu/*.

QD### Vivid from Prost, Kishen, Kluth, and Bellamy, 2017; QD### data from Quantum Dot Corp (acquired by Molecular Probes/Invitrogen/Thermo Fisher Scientific). eVolve 605 and eVolve 655 are Cd containing quantum dots from Affymetrix/eBiosciences (acquired by Thermo Fisher Scientific). Bacteriochlorins (BCs) have small Stokes shifts (Emission maximum – Excitation maximum). They have almost as large extinction coefficients in the ultraviolet, 350-390 nm range, so for practical use have a huge, practical Stokes shifts on the order of 400 nm. They also have an additional excitation peak in the 480-550 nm range. Taniguchi et al. (2008) include a graph comparing the full width half maxima (FWHM) emission spectra of cyanine dyes (~50 nm), near-infrared quantum dots (66 nm QD705, 74 nm QD800), BCs (~20 nm), and "expanded" porphyrins (>120 nm). We suggest with the right excitation light sources (355 nm laser or ~360 and ~390 nm LEDs), and emission separation (filter wheel one camera, cascading filters to multiple cameras or PMTs), that four or more BCs could be 700-800 nm emission range. If a palette of five BCs could be closely conjugated to Brilliant Blue BB515, excitation peak 488 nm, extremely efficient energy transfer in the visible absorption peaks (~500-550 nm) could enable extreme multiplexing. Additional multiplexing may be gained by 355 nm excitation of BUV395 to five BCs. Our thanks to Bruce Pitner, NIRvana Sciences, for discussions on extinction coefficient estimates with respect to NIRvana dyes and Taniguchi et al. (2008) and Taniguchi and Lindsey (2017). Additional dye data from Sednev, Belov, and Hell (2015, BioLegend, 2016, Brilliant Violets, *http://www.biolegend.com/brilliantviolet*, and BB480 from Chroma Technology Corp, 2017.

An alternative online dataset can be retrieved at *http://www.fluorophores.tugraz.at/substance*.

You can look for updates at *www.GeoMcNamara.com*.

Table 4.4.3 Fluorescent Protein Biosensors (FPB)[a]

Analyte or activity	Biosensor(s)
2-oxoglutarate (alpha-ketoglutarate)	OGSor-GA, mOGsor, PROBS-2
ABL, BCR-ABL activity	Abl indicator, Picchu-Z/EGFR-Z, Prickle
activation of plasma membrane Ca^{2+} pump	BFP-PMCA-GFP
Akt (PKB)	Eevee-iAkt, Aktus, BKAR, AktAR, ReAktion, GFP–Akt–YFP, GFP-PKB-RFP
AMPK activity	AMPKAR, ABKAR, organelle specific ABKARs, T2AMPKAR (FLIM based)
Ammonium transport & concentration	AmTrac, MepTrac
Annexin A4 self-association	CYNEX4
Arabinose	FLIParaF.Ec-250n
Arginine	cpFLIPR, FPIPR-AhrC (CFP[-ahrC-YFP), FLIP-cpArgT194, FLIP-cpArtJ185, FRET arginine reporter
Autophagy	mTagRFP-LC3
ATM	ATOMIC
ATP	cyto-ATeam, GO-ATeam-2, ATeam3.10, AT1.03NL
ATP in mitochondria	mit-Ateam
ATP:ADP ratio	PercevalHR (high dynamic range), Perceval
Aurora B kinase	Aurora B sensor
BAI2 (a furanosyl borate diester)	CLPY
BDNF concentration (extracellular)	Becell (fusion protein TrkB ligand binding domain, EGFR kinase domain "BBD-Ecat," coexpressed with Ecaus biosensor; on cell of interest or on "sentinel" cell)
	In principle, generalizable to any RTK
Bile acid sensors	BAS
Ca^{2+}	"GECIs": NTnC, YC Cameleons, NanoCaMeleons, GCaMPs, RCaMPs, D3cpV, TN-XXL, Twitch-1CD, PeriCams, Case 12, Case 16, Camgaroos, FIP-CBSM, FIP-CA3, FIP-CA9, FIP-CBSMTN-XL, B-GECO, R-GECO, jRCaMP1a, jRCaMP1b, Ca^{2+} #2 (ECFP[]cp173Venus)
Ca^{2+} in endoplasmic reticulum (ER)	D1ER, D4ER (low affinity Ca^{2+} probes)
Ca^{2+} in lysosomes	LAMP-1-YCaM
Ca^{2+} in mitochondria	4mt-D3cpV
Ca^{2+} in vesicles	Ycam2
Calcineurin activity (phosphatase)	caNAR1
CaMKII	Camuiα4m, CamuiαamCYCaMIIα
Caspase-3 protease activity	SCAT3.1; CC3AI, RC3AI, VC3AI, mKate2-DEVD-iRFP, eqFP650-DEVD-iRFP

continued

Table 4.4.3 Fluorescent Protein Biosensors (FPB)[a], *continued*

Analyte or activity	Biosensor(s)
Caspase-3 protease activity, caspase-6 activity	CFP-c3-YFP-c6-mRFP
Caspase-6 protease activity	CA6-GFP
Caspase-7 protease activity	CA6-GFP
Caspase-8 protease activity (SCAT8.1	SCAT8.2
Cd^{2+}	Cd-FRET-2
Cdc42 activation	Raichu-cdc42, A-probe.2
CDK/cyclin	CDKsens, CDKact, CyclinB1-CDK1 sensor
Cell cycle progression	FUCCI, FUCCI2, PCNA-Chromobody, HypoxCR
Cyclic AMP (cAMP)	cADDis (cAMP Difference Detector in situ), Epac1-camps, Epac2-camps, RI-camps, ICUE, YR-ICUE, HCN2-camps, (T)Epac(VV); FP-PKARII/FP-PKAcat, PKA Riα #7
Cyclic GMP (cGMP)	Cygnet-1, Cygnet2, FlincG, CGYs, cGES, cGi, PKG #7 (cp173Venus-ECFP)
Citrate (citric acid)	FLIPcit affinity series, CIT
Cl^-	CloMeleon, LSSmClopHensor, Cl-sensor, EYFP (chloride and other halide ions)
CREB activation	ICAP
Cu^+	Ace1-FRET, Mac1-FRET, Amt1-FRET
CyclinB-Cdk1	CyclinB-Cdk1 sensor
Diacylglycerol (DAG)	Upward DAG2, Upward DAG mNeon 1G8, Upward DAG mNeon 2D1, Downward DAG3, Daglas, DAGR, DIGDA, Cys-1-GFP, DAGR; CKAR (PKC activity)
EGFR	FLAME, EGFR reporter, Ecaus, Bescell/BBD-Ecat, EGFR-ECFP/PTV-EYFP
EGFR homodimerization	EGFR-VC & EGFR-VN (Bimolecular Fluorescence Complementation, BiFC; note: early versions irreversible)
EGFR interaction with Gαi3 (GTPase alpha subunit)	EGFR-CFP & Gαi3-int YFP (internally tagged Galpha; also made "CT" C-terminal version)
EGFR–GIV–Gαi3 ternary complexes	EGFR-VC and VN-GIV-CT (bimolecular fluorescence complementation, BiFC) and Gαi3-int CFP (internally tagged; also made "CT" C-terminal version)
ERK (extracellular signal-regulated kinase)	EKAR, EKAR-EV, EKAR2G2, EAS, Erkus, Miu2, Erk KTR (kinase translocation reporter), FIRE (prototype biosensor kinase activity by substrate stabilization)
Estrogen receptor (ER)	CEY (ligand binding domain conformation)
FAK (focal adhesion kinase)	FAK biosensor

continued

Table 4.4.3 Fluorescent Protein Biosensors (FPB)[a], *continued*

Analyte or activity	Biosensor(s)
Fyn (specific Src family kinase)	"Fyn sensor" (Yingiao Wang, UC, San Diego; GM still waiting for "Lck this" sensor)
G protein activation	FP-Gα/FP-Gβ(γ)
Glucokinase	FRET-GCK Reporters (mCerulean-GCK-mVenus)
Glucose	FLIPglu affinity series, AcGFP1-GBPcys-mCherry, LoogerGlu
Glutamate	iGluSnFr, SuperGluSnFR, GluSnFR, FLIPE affinity series, FLIP-cpGLtI210
Glutamine	FLIPQTV3.0 (affinity series) (glnH-mTFP1-glnH-Venus), FLIP-cpGlnH183, FRET glutamine reporter, LoogerGln
Granzyme B	GrzB Reporter, GrzB-Breakaway (G. McNamara, A. Korngold, B. A. Rabinovich [personal communication] propose CD19-TM-linker-mClover3-human optimized cleavage site-linker-mouse optimized cleavage site-linker-mRuby3-NoLS-mRuby3)
Halide ions	CloMeleon, YFP-H148Q, YFP-H148QI152L, EYFP (quenched by chloride and other halide ions)
Hg^{2+}	eGFP205C, IFP/BV sensor
Histidine	FLIP-HisJ, FLIP-cpHisJ194
Histone H3 (K9) lysine methylation	K9 reporter
Histone H3 (K27) lysine methylation	K27 reporter
Histone H3 (S28) phosphorylation	H3 phosphorylation reporter
Histone H4 lysine acetylation	Histac-K5, Histac-K7, Histac-K12
Inositol trisphosphate (IP3)	LIBRA, FIRE1, FIRE-2, FIRE-3, IRIS-1
Insulin Receptor kinase activity	Phocus-2pp, phocus, sinphos
JNK activity	JuDAS, JNKAR; JNK KTR, controls: JNK KTR_AA (nuclear only), JNK KTR_EE (cytoplasm only)
Lactate	Laconic
Leucine	FLIPLeu, FLIP-Leu-Y, FLIP-LivJ, FLIP-cpLivJ261
Lysine	FLIPK (affinity series)
M(1) muscarinic receptor activation	M1R-YFP-CFP
Macromolecular crowding	Cerulean-(GSG)6 A(EAAAK)6 A(GSG)6 A(EAAAK)6 A(GSG)6-Citrine
Malonyl-CoA	FapR-D2eGFP
Maltose	FLIPmal affinity FRET series, Mal-### single FP series, EcMBP165-cpGFP. PPYF.T203V

continued

Table 4.4.3 Fluorescent Protein Biosensors (FPB)[a], *continued*

Analyte or activity	Biosensor(s)
MAPKAP K2	GMB
Mechanical strain	cpstFRET, stFRET, PriSSM, VinTS
Methionine	FLIPM
Mg^{2+}	Cerulean-HsCen3-Citrine
MK2	GFP-MK2-BFP
MT1-MMP activity	MT1-MMP biosensor
Neurotrophic factor	BBD-ECat/ECaus ("sentinel" cell-based)
Nitric oxide (NO)	Piccell, FRET-MT, geNOps (C-geNOp and M-geNOp excite at 430 nm, G-geNOp and Y-geNOp at 480 nm, O-geNOp at 515 nm; based on super enhanced cyan, mint green, EGFP, Venus yellow, mKOk)
O_2 (oxygen)	FluBO, HIF-GFP, 8×HRE promoter-FP, HypoxCR, dUnGOHR
O-GlcNAc transferase	O-GlcNAc sensor
Organic hydroperoxides	OHSer
p38 (MAPK)	p38 KTR
PARP1 localization (poly(ADP-ribose) polymerase 1)	PARP1 chromobody (nanobody-FP, recognizing ZnF2 domain, including aa 161, 188, 189)
Pb^{2+} (lead ions)	PbGFP (bright unbound, quenched by μM concentrations of Pb^{2+} ions)
Proliferating cell nuclear antigen (PCNA) localization	PARP1 chromobody (nanobody-FP)
PDK1 activation	GFP-PDK1-RFP, PARE
pH	Super-ecliptic pHluorin, pHluorins (ecliptic, ratiometric), AlpHi, pHRed, SypHer, cpYFP, LSSmClopHensor, E2GFP, deGFP1-4, GFpH, YFpH, CFP-YFP tandem, pHuji
Phosphatidic acid (PA)	Pii
Phosphatidylserine (PS)	GFP-Lact-C2
PO_4^{3-} (phosphate ion)	FLIPPi
Protease activity	Many: See Caspases, Granzyme B, for examplesiProtease, iTEV, iCasper (to 2015)
Protein kinase A (PKA)	Epacs, AKAR4, AKAR3, AKAR2, AKAR, AKAR1-34, ART, CRY-AKAR; PKA KTR
Protein kinase C (PKC)	CKAR, δCKAR (PKC δ isoform specific), KCP-1
Protein kinase D (PKD)	DKAR
Protein dynamics	Fast-FT (fast timer), Medium-FT (medium timer), Slow-FT (slow timer); DsRed-Timer, many photochangeable FPs

continued

Table 4.4.3 Fluorescent Protein Biosensors (FPB)[a], *continued*

Analyte or activity	Biosensor(s)
Protein-protein interactions	mSplit reporters, using bimolecular fluorescence complementation (BiFC; generalizable)
Phosphoinositide's dynamics	PIPlines
PtdIns(3,4)P2	Pippi-PI(3,4)P2; also binds PIP3: GFP-PHGRP1, GFP-PHPDK1, YFP-PHTAPP1, GFP-Svp1p, GFP-PHBtk, GFP-Ent3p, CAY
PtdIns(3,4,5)P3 (PIP3)	Fllip, GFP-PHGRP1, GFP-Cytohesin-1, GFP-PHPDK1, YFP-PH-TAPP1, GFP-PH-Svp1p, GFP-PHBtk, GFP-PH,FP-CRAC, GFP-Ent3p, CAY, Pippi-PI(3,4,5)P3: Lipid binding domain (LBD) Pleckstrin homology domain derived from Grp1
PtdIns(3,5)P2	GFP-PHGRP1, GFP-PHPDK1, GFP-PHTAPP1, GFP-Svp1p, GFP-PHBtk, GFP-PHBtk, GFP-PHEnt3p
PtdIns(4)P	FP-PHFAPP1, Pippi-PI(4)P, GFP-PHOSH2, PHOSBP, GFP-PHFAPP
PtdIns(4,5)P2	Pippi-PI(4,5)P2, PPHPLCd1-YFP, GFP-ARNO, GFP-Cytohesin-1, GFP-PHOSH2, PHOSBP, GFP-PHFAPP, CAY
PtdIns(4,5)P2, Ins(1,4,5)P3 dynamics	GFP-PHPLC, FP-Tubby, FP-PHPLCδ1(FRET)
PtdIns(4,5)P2 / PLC activity	CYPHER (PLC activity)
PtdIns(3)P	GFP-FYVEEEA1, GFP–p40phox iPX, InPAkt
Putrescine	FLIP-AF1
Pyruvate	Pyronic
Quinones	QsrY
Receptor tyrosine kinase activity (general)	Picchu
Redox and voltage	roGFP, rxYFP149_202, CY-RL5, CY-RL7, HSP-FRET, Redoxfluor, HyPer, HyPEr2, mt-cpYFP, cpYFP
Redox: H_2O_2	HyPer, HyPer3, roGFP2-Orp1
Redox: H_2O_2 (picomolar H_2O_2)	p130cas stabilized; PTEN oxidation blocks plasma membrane localization
Redox: glutathione	roGFP2-Grx1
Redox: superoxide	mt-cpYFP, pcYFP
Redox: peroxiredoxin	roGFP2-Prx
Redox; thioredoxin	Trx(CXXS)-cpYFP-Prx
Redox	HSP-FRET
Redox: NADH	Frex, T-Rex, rexYFP (rxYFP)

continued

Table 4.4.3 Fluorescent Protein Biosensors (FPB)[a], *continued*

Analyte or activity	Biosensor(s)
Redox: NADH/NAD^+ ratio	Peredox, SoNAR
Redox: NAD^+	"NAD^+ Sensor"
Redox: $NADP^+$	Apollo-$NADP^+$ (Cameron, 2016)
Redox	Redoxfluor
Redox: RL5	RL7 (CY-RL7)
Retinoic acid	GEPRA
Rho family GTPase activation: cdc42	Raichu-cdc42
Rho family GTPase activation: CRIB	Raichu-CRIB
Rho family GTPase activation: Rac1	Raichu-Rac1
Rho family GTPase activation: RalA	Raichu-Ral
Rho family GTPase activation: Rap1	Raichu-Rap
Rho family GTPase activation: Ras	Raichu-Ras
Rho family GTPase activation: RhoA	Raichu-RhoA, RhoA2G
Rho family GTPase activation: RhoC	RhoC FLARE
RhoGDI activity	Raichu-RBD
Ribose	FLIPrib affinity series
RTK–GIV–Gαi ternary complexes	EGFR-VC & VN-GIV-CT (bimolecular fluorescence complementation, BiFC) and Gαi3-int CFP (internally tagged; generalized)
Sarco/endoplasmic reticulum Ca^{2+}-ATPase (SERCA)	CFP-SERCA
Sphingosine-1-phosphate	S1PR1-eGFP to S1PR1NB-tRFP (former is cell surface unless bound to S1P)
Src	Srcus, BG-Src
Sucrose	FLIPsuc (affinity series)
synNOTCH	Synthetic Notch signaling chimeric antigen receptors (CARs), i.e., extracellular binding domain-[key Notch activation components]-Gal4-VP64 artificial transcription factor (replacement for Notch ICD)
Taspase1 (threonine aspartase 1)	TS-$Cl2^+$ (NLS-GFP-GST-[MLL 2713KISQLDGVDD2722]-myc tag-NES (multi-color translocation biosensor assays, when coexpressing Taspase1-BFP, cleavage results in NLS-GFP-GST localizing in nucleus; see Granzyme B Breakaway for an alternative)
T-cell receptor signaling	T-cell localization reporters (series of 30 translocation reporters)
Trehalose	Tre-C04 (Nadler, 2016)
Trehalose-6-phosphate	T6P-TRACK

continued

Table 4.4.3 Fluorescent Protein Biosensors (FPB)[a], *continued*

Analyte or activity	Biosensor(s)
Tryptophan	FLIPW-CTYT, FLIPW (affinity series)
Ubiquitin K63-linked sensor	TAB2 NZF
Voltage membrane potential	GEVI's: Arch3, eArch(D95N), Arclight, CaViar (Ca^{2+} and Vm), pHlaVor (pH and Vm), Mermaid, Butterfly VSP3.1, ASAP1, Ace2N-2AA-mNeon, MacQ-mCitrine; FlaSh, FlaSh-CFP/YFP, Flare, SPARC, VSFP-cpEGFP, VSFPs, PROPS
Wiskott-Aldrich syndrome protein (WASP) conformation	Cdc42-GEF sensors
Zn^{2+}	eCALWY-6, eCALWY4, eZinCh, ZapCY1, ZapCY2, ZifCY1, ZinCh, CLY9-2His, Cys2His2, GZnP1

[a]Many biosensors in this table use dim fluorescent proteins. EGFP is from 1996 and is less than one-third the brightness of mNeonGreen or mClover3. This limits signal-to-noise ratio and dynamic range. We recommend replacement with bright FPs, such as mNeonGreen or mClover3 (green), mRuby3 (orange-red). Longer wavelengths (green, not blue or cyan) will also shift the fluorescence from high autofluorescence (NADH, NADPH, flavins, flavoproteins) to lower autofluorescence. We also recommend localizing the FP(s) if possible, for example, to plasma membrane (Lck-biosensor), or even to the channel/transporter being measured (i.e., GLUT4-linker-FLIPglu). We also suggest multimerizing FPs or FP biosensors whenever possible, for example LacI-nls-FP onto LacO 256× operator array on the same DNA plasmid. This could be made more efficient now by replacing the original LacI-nls-EGFP with LacI-nls(mNeonGreen)3, which would be 10× brighter per protein molecule, enabling use of LacO 25× operator array. In the nucleus, one could localize to nucleolus (NoLS-mTFP1), PCNA replication factories (anti-PCNA nanobody-mNeonGreen), telomeres (Trf2-mRuby3), centromeres (CENP-mKate2), nuclear envelope (Nup-mCardinal2 × 2). See also Colorful Cell, whose MXS-Chaining kit enables efficient cloning for multi-part expression. (We do note that DNA plasmids enable two or more copies of similar or identical sequences, whereas manufacturing lentivirus or retroviruses typically results in deletions; this also has implications for expression of multiple shRNAs or microRNAs.)

Sentinel cells: You could introduce an FP biosensor onto or into another cell. For example, to sense either adenosine or prostaglandin E2, you could introduce A2AR or EP2 G-protein coupled receptors (GPCRs), respectively, into HEK293 cells, along with a cyclic AMP biosensor. The biosensor could even be fused to the cell surface receptor. You could also knockout (CRISPR/Cas9 nuclease/nuckase, TALENs) or knockdown (RNAi by siRNA, shRNA or microRNA) all other receptors that signal through cyclic AMP. Optionally also KO/KD phosphodiesterases, though this could limit dynamic range; conversely, you could enforce expression of PDEs (maybe away from plasma membrane) to optimize both dynamic range and temporal sensitivity.

You could multiplex the sentinel cells by having different cell surface receptors (A2AR or EP2), the same intracellular reporter (cAMP biosensor), and color code the Sentinel cells on either the receptor (mRuby3 vs mCardinalx2) or some out of the way location (i.e., nucleolus, with NoLS), or both (appropriate strength alternative splicing).

Translocation reporters, i.e., your favorite protein fused to a bright fluorescent protein ("fav"-mNeonGreen) are simple, powerful, tools. Singleton et al. (2009, 2011) did this for 30 proteins in the T-cell receptor signaling pathway. Regot et al. (2014) did this for four different kinase translocation reporters ("KTR"), including three simultaneously (JNK, p38 MAPK, Erk).

Histone marks can be reported on by FP fusion proteins to BET family members (BRDT, BRD2, and BRD4); histone acetyltransferases (TAFII250, PCAF, and GCN5), ATP-dependent chromatin remodeling factors; or by nanobody-FP fusions (llama, camel, shark, mouse, or human VHH antibody domains), single chain fragment variable (scFv)-FP fusions, or by protein transfection of Fab-fluorophores ("FabLEM").

Table 4.4.4 Useful Light Microscopy Web Sites

Name of resource	URL
Light microscopy (overview)	
Confocal Listserv (not just for confocal microscopes)	*https://lists.umn.edu/cgi-bin/wa?A0=confocalmicroscopy*
G. McNamara: Multi-Probe Microscopy (content last updated 2005, includes extensive glossary)	*https://works.bepress.com/gmcnamara/2/*
Molecular Expressions, National High Magnetic Field Laboratory (NHMFL), Florida State University	*http://micro.magnet.fsu.edu/*
Microscopedia: Resources: Guide To Light Microscopy	*http://www.microscopedia.com/Microscopy/Light*
Molecular Probes/Invitrogen/Thermo Fisher Scientific (many links to useful and informative sites)	*https://www.thermofisher.com/us/en/home/brands/molecular-probes.html*
Photonics buyer's guide (much more comprehensive than this list)	*http://www.photonics.com/BuyersGuide.aspx*
Science Exchange: Reproducibility Initiative (focus on commercial antibodies and uses)	*https://www.scienceexchange.com/applications/reproducibility*
University of Arizona (UA): Web resources, umbrella site for all UA microscopy core facilities, Spectra Database at UA	*http://swehsc.pharmacy.arizona.edu/micro* *http://microscopy.arizona.edu* *http://www.spectra.arizona.edu*
Wikipedia: Chromosomes	*https://en.wikipedia.org/wiki/Chromosome*
Wikipedia: Microscope	*http://en.wikipedia.org/wiki/Microscope*
Societies	
Association of Biomolecular Resource Facilities, Light Microscopy Research Group (ABRF, LMRG)	*https://abrf.org/research-group/light-microscopy-research-group-lmrg*
Euro-Bioimaging	*http://www.eurobioimaging.eu*
European Light Microscopy Initiative: Community of light microscopy labs	*http://www.embl.org/elmi/index.html*
European Microscopy Society (EMS)	*http://www.eurmicsoc.org*
German BioImaging.org	*http://www.germanbioimaging.org/wiki/index.php/Main_Page* *http://www.germanbioimaging.org/wiki/index.php/Workgroup6/SoftwarePackages*
International Society for Advancement of Cytometry (ISAC)	*http://isac-net.org/*
Microscopy Society of America (MSA)	*http://www.microscopy.org*
Royal Microscopical Society (RMS)	*http://www.rms.org.uk*
Major microscope companies	
Leica Microsystems	*http://www.leica-microsystems.com* *http://www.leica-microsystems.com/science-lab* *http://www.leica-microsystems.com/products/confocal-microscopes/details/product/leica-tcs-sp8-sted-3x/*
Nikon Instruments	*https://www.nikoninstruments.com* *https://www.microscopyu.com* *https://www.nikoninstruments.com/Products/Live-Cell-Screening-Systems/BioStation-CT*

continued

Table 4.4.4 Useful Light Microscopy Web Sites, *continued*

Name of resource	URL
Olympus America	*http://www.olympus-lifescience.com/en* *http://olympus.magnet.fsu.edu*
Zeiss (Carl Zeiss)	*http://www.zeiss.com* *http://www.zeiss.com/corporate/en_us/home.html* *http://zeiss-campus.magnet.fsu.edu/index.html* *http://www.zeiss.com/microscopy/en_de/products/microscope-cameras/axiocam-702-mono.html*
Karyotype systems and digital pathology	
Digital Pathology Blog: See educational sponsors for comprehensive list of digital pathology vendors	*http://tissuepathology.com/*
3DHistech: Digital pathology, Pannoramic scanners, Confocal, isacs staining; coverslipping/scanning unit in one device	*http://www.3dhistech.com* *http://www.3dhistech.com/pannoramic_confocal* *http://www.3dhistech.com/isacs*
Agilent Pathology Solutions/Dako: IHC and ISH reagents, autostainers	*http://www.dako.com/dk/index/knowledgecenter/omnis.htm* *http://www.dako.com/dk/ar42/productgroups.htm*
Applied Spectral Imaging: SKY Spectral karyotyping, GenASIs digital pathology, automated metaphase spread finding	*http://www.spectral-imaging.com* *http://www.spectral-imaging.com/applications/spectral-imaging* *http://www.spectral-imaging.com/applications/pathology* *http://www.spectral-imaging.com/applications/cytogenetics/karyotyping/metaphase-finder*
Bioview: Pathology and FISH cytogenetics automated scanners	*http://bioview.com* *http://bioview.com/products/duet-3*
Definiens (MedImmune/AstraZeneca): Digital pathology image analysis (with deep learning algorithms)	*http://www.definiens.com*
Huron Digital Pathology: Large area confocal scanning (entire human brain slices)	*http://www.hurondigitalpathology.com/*
Leica Biosystems: CytoVision Cytogenetics/FISH, Aperio digital pathology	*https://www.leicabiosystems.com/clinical-microscopy-surgery-radiology/cytogenetics* *https://www.leicabiosystems.com/digital-pathology*
MetaSystems International: Karyotyping, FISH, digital pathology, automated metaphase spread finding	*https://metasystems-international.com/en/products* *https://metasystems-international.com/us/products/metafer/*
Molecular Probes/Thermo Fisher Scientific: Evos FL Auto and Evos Floid cell imaging stations, high content screening (HCS; Cellomics)	*https://www.thermofisher.com/us/en/home/life-science/cell-analysis/cellular-imaging/cell-imaging-systems/evos-fl-auto.html* *https://www.thermofisher.com/us/en/home/life-science/cell-analysis/cellular-imaging/cell-imaging-systems/floid-cell-imaging-station.html* *https://www.thermofisher.com/us/en/home/life-science/cell-analysis/cellular-imaging/high-content-screening/high-content-screening-instruments.html*
Philips: Digital pathology	*http://www.usa.philips.com/healthcare/solutions/pathology*
Ventana/Roche Digital Pathology: Digital pathology, FISH	*http://www.ventana.com/digitalpathology*
Visiopharm: Digital pathology image analysis (with deep learning algorithms), stereology	*http://www.visiopharm.com/*

continued

Table 4.4.4 Useful Light Microscopy Web Sites, *continued*

Name of resource	URL
Filter and filter sets manufacturers	
Alluxa	*http://www.alluxa.com*
BMV Optical	*www.bmvoptical.com*
Chroma Technology	*http://www.chroma.com*
Edmund Optics: Filters, prisms	*http://www.edmundoptics.com/optics/optical-filters/bandpass-filters/fluorescence-filter-kits/3226* *http://www.edmundoptics.com/optics/prisms*
Iridian Spectral Technologies	*http://www.iridian-optical-filters.com/product-category/fluorescence-sets*
Newport (Spectra-Physics, Oriel, Bookham New Focus)	*https://www.newport.com/c/optical-filters*
Omega Optical	*http://www.omegafilters.com/*
Optolong (Kunming Yulong Optical & Electronics Technology)	*http://www.optolong.com/en/products/fluorescence-filters*
Schott Glass Technologies	*http://www.schott.com* *http://www.us.schott.com/advanced_optics/english/syn/advanced_optics/products/optical-components/optical-filters/interference-filters/index.html*
Semrock (IDEX, CVI, Melles Griot)	*http://semrock.com*
ThorLabs: Optical filters	*https://www.thorlabs.com/navigation.cfm?guide_id=21*
Major sCMOS camera companies (your next microscope cameras should likely be sCMOS, not CCD or EMCCD)	
Andor Technology (Oxford Instruments)	*http://www.andor.com/scientific-cameras/neo-and-zyla-scmos-cameras* *http://www.andor.com/42plus.aspx (Zyla 4.2 PLUS 3rd gen sCMOS)*
Hamamatsu	*https://www.hamamatsu.com/us/en/community/life_science_camera/sensor_technologies/scientific_cmos_scmos_image_sensor/index.html* *http://www.hamamatsu.com/us/en/community/life_science_camera/product/search/C11440-22CU/index.html* *https://www.hamamatsu.com/resources/pdf/sys/SCAS0120E_C13440-20CU.pdf (ORCA-FLASH4.0 v3, 3rd gen sCMOS)*
PCO	*https://us.pco-tech.com/scmos-cameras* *https://www.pco.de/scmos-cameras/pcopanda (PCO.panda 3rd gen sCMOS)* *https://lists.umn.edu/cgi-bin/wa?A2=CONFOCALMICROSCOPY;e90d20b.1702 (Gerhard Holst, 02/10/2017)*
Photometrics	*http://www.photometrics.com/products/scmos* *https://www.photometrics.com/news/pressrelease/Photometrics-Prime-95B-sCMOS-Camera (press release on Prime 95B using Gpixel GSENSE400BSI-TVISB sensor)* *https://www.photometrics.com/products/scmos/prime95B (back-illuminated sCMOS sensors)* *https://www.photometrics.com/products/datasheets/Prime95B-Datasheet.pdf (standard size sensor)* *https://www.photometrics.com/products/datasheets/Prime95B-25 mm-Datasheet.pdf (25 mm diagonal field of view)*

continued

Table 4.4.4 Useful Light Microscopy Web Sites, *continued*

Name of resource	URL
Princeton Instruments	*http://www.princetoninstruments.com/products/KURO-CMOS-cameras (same back-illuminated sCMOS as sister company Photometrics Prime 95B; typically PI to physics and spectroscopy markets)*
Raptor Photonics: FALCON III "next generation" EMCCD, CCD (200-1100 nm), SWIR Cameras (400-1750 nm), X-ray cameras (0.01-1200 nm)	*http://www.raptorphotonics.com/products/falcon-iii-emccd* *http://www.raptorphotonics.com/products/eagle-v-ccd* *http://www.raptorphotonics.com/product-type/swir* *http://www.raptorphotonics.com/products/eagle-xv*
sCMOS sensor manufacturers	
BAE Fairchild	*http://www.fairchildimaging.com/category/product-category/focal-plane-arrays/scmos*
Gpixel	*http://www.eureca.de/pdf/optoelectronic/gpixel/GSENSE400BSI_EN.pdf*
Teledyne e2v	*http://www.e2v.com/products/imaging/cmos-image-sensors* *http://www.e2v.com/products/imaging/cmos-image-sensors* *http://www.e2v.com/products/imaging/qe-curves* *http://www.teledyne.com/news/tdy_12122016.asp*
Fluorescent proteins, luciferases (DNA plasmids and/or other expression products)	
490BioTech: LuxABCDE	*http://490biotech.com/vectors-2/*
Abberior	*http://www.abberior.com/shop/Labels-by-Function/Fluorescent-Proteins:::7_14.html* *http://www.abberior.com/shop/Labels-by-Application:::1.html*
Addgene.org	*www.addgene.org* *https://www.addgene.org/fluorescent-proteins* *https://www.addgene.org/fluorescent-proteins/biosensors* *https://www.addgene.org/fluorescent-proteins/localization* *https://www.addgene.org/optogenetics/* *https://www.addgene.org/fluorescent-proteins/davidson/* *https://www.addgene.org/Roger_Tsien/*
Allele Biotechnology	*http://www.allelebiotech.com/Fluorescent-Proteins*
Bell Biosystems: Magnelle living MRI contrast agents (magnetotactic bacteria taken up by human cells in vitro) with fluorescent proteins; in vivo cell tracking	*http://www.bellbiosystems.com/Products-and-Services/Cell-Tracking-Solutions*
BioBricks Foundation	*http://biobricks.org*
BioPop (Intrexon): Dinoflagellates bioluminescence luciferase/luciferin	*https://biopop.com/products*
Chromotek: Chromobodies, Nano-Boosters (llama nanobodies attached to or detecting FP)	*http://www.chromotek.com/products/chromobodies* *http://www.chromotek.com/products/chromobodies/cell-cycle-chromobodyr* *http://www.chromotek.com/products/nano-boosters*
DNA 2.0 chromogenic and fluorescent protein paintbox (not really IP-Free)	*https://www.dna20.com/products/protein-paintbox*
Evrogen	*http://evrogen.com/products/basicFPs.shtml* *http://evrogen.com/products/Biosensors.shtml* *http://evrogen.com/products/Organelle-labeling.shtml*
iGEM/BioBricks: Reporter proteins, including fluorescent proteins	*http://parts.igem.org/Protein_coding_sequences/Reporters*

continued

Table 4.4.4 Useful Light Microscopy Web Sites, *continued*

Name of resource	URL
iGEM Registry of Standard Biological Parts	*http://parts.igem.org/Main_Page*
InvivoGen: GFP, Lucia luciferase reporters	*http://www.invivogen.com/dual-reporter*
MBL International: Fluorescent proteins	*https://www.mblintl.com/products/fluorescent-proteins* *http://ruo.mbl.co.jp/bio/e/product/flprotein/fucci.html*
Millipore-Sigma/Sigma-Aldrich: Firefly luciferase, D-luciferin	*http://www.sigmaaldrich.com/life-science/metabolomics/enzyme-explorer/analytical-enzymes/luciferase.html*
Molecular Probes,/Invitrogen/Thermo Fisher Scientific: Bacmam 2.0 fluorescent proteins, biosensors, FUCCI	*http://www.probes.com/* *http://www.thermofisher.com/us/en/home/brands/molecular-probes.html* *https://www.thermofisher.com/us/en/home/industrial/pharma-biopharma/drug-discovery-development/target-and-lead-identification-and-validation/pathway-biology/cellular-pathway-analysis/bacmam-system/bacmam-reagents.html*
Montana Molecular: Genetically encoded fluorescent biosensors and probes for cell-based assays and live cell imaging	*http://montanamolecular.com/products/products-overview*
NanoLight Technologies: Renilla GFP, luciferases	*http://www.nanolight.com/NanoFluors/GFP_Expression_Vectors.html* *https://www.biotoy.com/en/learn*
n3D Biosciences: Generate 3D cell spheroids, high throughput screening image changes using smartphone camera inside incubator	*http://www.n3dbio.com/products/magnetic-3d-bioprintinghttp://www.n3dbio.com/products/assays*
New England BioLabs (NEB): Cypridina, Gaussia luciferases	*https://www.neb.com/applications/cellular-analysis/reporter-systems*
Promega: Monster GFP, NanoLuc	*https://www.promega.com/products/reporter-assays-and-transfection/reporter-vectors-and-cell-lines/monster-green-fluorescent-protein-phmgfp-vector* *https://www.promega.com/products/reporter-assays-and-transfection/reporter-vectors-and-cell-lines/nanoluc-luciferase-reporters/nanoluc-genetic-reporter-vectors/*
Fluorescence products (reagents)	
AAT Bioquest	*http://www.aatbio.com* *https://www.aatbio.com/resources/catalog/IFLUOR.pdf*
Advanced Cell Diagnostics (Bio-Techne): Branched DNA probe sets for RNA FISH	*https://acdbio.com/products*
Affymetrix/eBioscience/Thermo Fisher Scientific: Branched DNA probe sets for RNA FISH, Super Bright polymer dyes (SB436, SB600, staining buffer)	*http://www.affymetrix.com/estore/promotions/viewrnaish/index.affx* *http://www.ebioscience.com/knowledge-center/product-line/super-bright.htm*
Anaspec: HiLyte Fluorophores, FRET probes	*https://www.anaspec.com/products/productcategory.asp?id=10*
Antibody Resource Page	*http://www.antibodyresource.com/*
Biocompare: Antibodies	*http://www.biocompare.com/Antibodies*
Cell Signaling Technology: Fluorescence antibodies	*https://www.cellsignal.com/browse/immunofluorescence-immunocytochemistry/if-paraffin/if-frozen*

continued

Table 4.4.4 Useful Light Microscopy Web Sites, *continued*

Name of resource	URL
Essen Biosciences: Bacmam 3.0 ready to use FP gene transfection reagents	*http://www.essenbioscience.com/en/products/reagents-consumables/incucyte-nuclight-red-bacmam-30-reagent-nuclear-labeling-cat-no-4621/*
GE Healthcare/Amersham Biosciences	*http://www.gelifesciences.com/webapp/wcs/stores/servlet/catalog/en/GELifeSciences-us/brands/cydye/*
Global Biological Standards Institute (GBSI): Antibody Validation Initiative	*http://www.gbsi.org/work/antibodies*
Goryo Chemical	*http://www.goryochemical.com*
Human Protein Atlas (academic), Atlas Antibodies (commercial arm), US distributor	*http://www.proteinatlas.org/* *https://atlasantibodies.com/* *http://www.sigmaaldrich.com/life-science/cell-biology/antibodies/prestige-antibodies.html*
Integrated DNA Technologies (IDT): Oligonucleotides, fluorescent dyes for oligonucleotides, locked nucleic acid probes (LNA), MGB Eclipse quenchers	*http://www.idtdna.com* *http://www.idtdna.com/site/Catalog/modifications/dyes* *http://www.idtdna.com/pages/products/modifications/fluorophores/freedom-dyes* *http://www.idtdna.com/site/Catalog/Modifications/Category/4* *http://www.idtdna.com/pages/products/modifications/fluorophores/freedom-dyes* *http://www.idtdna.com/pages/products/genotyping/lna-primetime-probes* *http://www.idtdna.com/pages/products/gmp-manufacturing/mgb-probes*
Jackson ImmunoResearch	*https://www.jacksonimmuno.com/*
KPL (formerly Kirkegaard & Perry Laboratories)/SeraCare	*http://www.kpl.com/*
LGC Biosearch Technologies: Dyes for oligonucleotides, single molecular RNA FISH image gallery	*https://www.biosearchtech.com/support/education/fluorophores-and-quenchers* *http://stellarisfish.smugmug.com* *http://singlemoleculefish.com* *https://www.biosearchtech.com/products/rna-fish (typically 48 × 20 base oligonucleotides)*
Marker Gene Technologies (MGT)	*http://www.markergene.com/fluorescent-reagent*
Miltenyi Biotec: REAfinity recombinant engineered antibodies (no Fc Receptor binding), FASER fluorescence amplification kits, NiraWave fluorophores (indocyanine green formulations)	*http://www.miltenyibiotec.com/en/products-and-services/macs-flow-cytometry/reagents/antibodies-and-dyes/recombinant-antibodies.aspx* *http://www.miltenyibiotec.com/en/products-and-services/macs-flow-cytometry/reagents/support-reagents/faser-kits.aspx* *http://www.miltenyibiotec.com/en/products-and-services/viscover-imaging/optical-imaging.aspx*
Molecular Probes/Invitrogen/Thermo Fisher Scientific: Largest vendor of fluorophores, Molecular Probes Handbook (Web resource), Tyramide Signal Amplification kits	*http://www.probes.com/* *https://www.thermofisher.com/us/en/home/references/molecular-probes-the-handbook.html* *https://www.thermofisher.com/us/en/home/references/molecular-probes-the-handbook/tables/tyramide-signal-amplification-tsa-kits.html*
NIRvana Sciences	*http://nirvanasciences.com* *http://nirvanasciences.com/?page_id=3088*
One World Lab: Antibody search	*http://oneworldlab.com/antibodies*
CytoCell/Oxford Gene Technologies: DNA FISH probes, human, mouse, pig, chicken	*http://www.cytocell-us.com*

continued

Table 4.4.4 Useful Light Microscopy Web Sites, *continued*

Name of resource	URL
Perkin Elmer: Nucleotides, labeling kits, Tyramide Signal Amplification Kits (TSA), Opal 7plex discovery panel kit based on sequential TSA	*http://www.perkinelmer.com/category/fluorescent-hapten-nucleotides* *http://www.perkinelmer.com/category/fluorescent-agents-labeling-kits-dyes* *http://www.perkinelmer.com/lab-solutions/resources/docs/BRO_TSAsignalamplification.pdf* *http://www.perkinelmer.com/product/opal-7-immunology-discovery-kit-op7ds1001kt*
Rockland	*http://www.rockland-inc.com/commerce/index.jsp*
TEFLabs: Fluorescent ion indicators (Ca^{2+}, Cl^-, K^+, Mg^{2+}, Na^+, pH, Zn^{2+}), ionophores, fluorophores	*http://www.teflabs.com/ion-indicators*
Vector Laboratories	*http://www.vectorlabs.com/*
Live cell imaging dishes and multi-well plates ("glass bottom dishes")[a]	
Leicester Imaging Technologies (LITE), University of Leicester: Table of dishes for live cell imaging	*http://www2.le.ac.uk/colleges/medbiopsych/facilities-and-services/cbs/lite/aif/tips-and-tricks-1/dishes-for-live-cell-imaging*
NIC Wiki: Plates and Dishes for Imaging	*http://nic.ucsf.edu/dokuwiki/doku.php?id=imaging_dishes*
BD Biosciences 2007 application note: Navigating the High-Content Imaging Process (the BD Pathway 855 and 435 imaging systems are defunct, the choice of arc lamps is defunct, many Web links are defunct, the early 21st century camera specifications are quaint, the high content principles are excellent)	*http://www.bdbiosciences.com/documents/AppNote_High-Content_Imaging.pdf*
Bellco Glass: Glass flat bottom plate	*http://www.bellcoglass.com/node/1046*
Bioptechs: Interchangeable coverslip dish ($0.36 per experiment)	*http://www.bioptechs.com/product/interchangeable-coverslip-dish*
Brooks Automation: Clear bottom optical imaging microplates	*http://www.brooks.com/products/life-science/consumables/matrical-microplates-microtubes-racks-lids/glass-bottom-optical-imaging-microplates*
Cell E&G: Glass bottom cell culture dishes, plates	*http://celleg.com/product.html*
Cellvis: Glass bottom dishes and plates	*http://www.cellvis.com/_35-mm-glass-bottom-dishes_/products_by_category.php?cat_id=3*
Corning: Glass bottom microplates	*http://catalog2.corning.com/LifeSciences/en-US/Shopping/Category.aspx?categoryname=Microplates%20-%202015(Lifesciences)|Assay%20Microplates%20-%202015(Lifesciences)* *http://catalog2.corning.com/LifeSciences/en-US/search/Search.aspx?searchfor=High%20content&rq=Well%2520Bottom:Flat* *http://csmedia2.corning.com/LifeSciences/media/pdf/CLS_AN_126_comparative_cellbase_analysis_1536surface.pdf*
CoyLab Products: PermPlates gas permeable plate, 6-, 24-, 96-well plates, 1- and 2-well slide plates; SensorDish reader and OxoDish (O_2) and HydroDish (pH) sensor plates	*http://www.coylab.com/documents/PermPlatesLit011312.pdf* *http://coylab.com/products/o2-ph-and-co2-sensors/#*

continued

Table 4.4.4 Useful Light Microscopy Web Sites, *continued*

Name of resource	URL
Design 1 Solutions: Custom microplates and fabrication services	*http://www.design1solutions.com/custom-microplates.html*
Eppendorf: Cell imaging dishes, imaging plates	*https://online-shop.eppendorf.com/OC-en/Cell-Culture-and-Imaging-Consumables-110320/Cell-Imaging-Consumables-120210/Eppendorf-Cell-Imaging-Dishes-PF-19457.html* *https://online-shop.eppendorf.com/OC-en/Cell-Culture-and-Imaging-Consumables-110320/Cell-Imaging-Consumables-120210/Eppendorf-Cell-Imaging-Plates-PF-19458.html*
Greiner Bio-One International: CellView glass bottom dishes, quadrant dishes	*https://shop.gbo.com/en/row/articles/catalogue/article/0110_0110_0040_0020/27513*
ibidi: u-Plates, glass bottom dishes, microfluidic slides	*http://ibidi.com/xtproducts/en/ibidi-Labware/m-Plateshttp://ibidi.com/xtproducts/en/ibidi-Labware*
Matsunami Glass	*http://www.matsunami-glass.co.jp/english/life/bio/data01.html*
Mattek: Glass bottom dishes and SBS plates	*https://www.mattek.com/store-category/cultureware/glass-bottom-dishes* *https://www.mattek.com/products/multi-well-plates*
NEST Biotechnology, Wuxi, Jiangsu, China	*http://www.nestscientificusa.com/products_detail/productId=31.html*
Pall (Danaher): Micro-24 MicroReactor System, SBS footprint plate, 3 to 7 ml working volume cell culture chambers, pH and dissolved oxygen (DO) sensors, transparent bottom enabling imaging	*http://www.pall.com/main/biopharmaceuticals/product.page?id=52961*
PerkinElmer: Glass bottom plates	*http://www.perkinelmer.com/SE/Catalog/Category/ID/Microplates*
Persomics: Reverse transfection cell microarrays; Beachfront validation plate 400 spots each of siRNA to RelA (NF-KappaA) and INCENP and nontargeting controls, Sargasso siRNA kinoma array (24 × 32 spots = 768 spots, including RelA, INCENP and nontargeting controls, Aegean 2080 spots miRNA mimics, Caspian 2080 spots miRNA inhibitors	*www.persomics.com* *http://www.persomics.com/products*
Porvair Sciences: Clear bottom assay plates, glass bottom assay plates (175 µm lass, 335 nm UV optical cutoff), UV clear bottom assay plates, 74 mm × 110 mm × 175 µm thickness glass sheets for SBS plate development (microscopes slides are 75 × 25 mm, so this is ~4 slides wide, SBS plate footprint)	*http://www.porvair-sciences.com/en/services-menu/life-sciences/clear-bottom-assay-plates* *http://www.porvair-sciences.com/en/services-menu/life-sciences/glass-bottom-assay-plates* *http://www.porvair-sciences.com/en/services-menu/life-sciences/uv-clear-bottom-assay-plates* *http://www.porvair-sciences.com/en/listings/view/P229217*
Sarstedt: Lumox ultra-thin, gas-permeable film base, glass bottom 35-mm and 50-mm imaging dishes, 24-, 96-, and 384-well plates.	*https://www.sarstedt.com/en/products/laboratory/cell-tissue-culture/lumox-technology*
Ted Pella: Glass bottom dishes, clear wall or black wall (manufactured by WillCo Wells)	*https://www.tedpella.com/section_html/706dish.htm*

continued

Table 4.4.4 Useful Light Microscopy Web Sites, *continued*

Name of resource	URL
Thermo Fisher Scientific: Thermo Scientific Nunc glass bottom dishes, Lab-Tek chambered coverglass	*https://www.thermofisher.com/order/catalog/product/150680* *https://www.thermofisher.com/order/catalog/product/155361PK* *https://tools.thermofisher.com/content/sfs/brochures/D21443.pdf*
Wafergen Biosystems: 5,184 or 4 × 841 = 3364 quadrant smartChip nanowell chips (pre-barcoded) for scRNAseq, single nucleus RNAseq (~2× as many cells can be NGS sequenced per Illumina HiSeq or miSeq lane, iCell8 single cell system includes MultiSample NanoDispener (MSND), The Imaging Station (upright fluorescence microscope with long working distance objective lens), CellSelect software	*http://www.wafergen.com/products/icell8-single-cell-system*
Warner Instruments (Harvard Apparatus): Culture dishes, perfusion systems	*https://www.warneronline.com/product_cat_info.cfm?id=1322*
Willco Wells: Glass bottom dishes	*www.willcowells.com*
World Precision Instruments: Fluorodish glass bottom dishes	*https://www.wpiinc.com/products/laboratory-supplies/fd35-100-fluorodish-cell-culture-dish-35 mm-23 mm-well-pkg-of-100*
Microscopes, microscopy accessories (accessorize!), reagents, resources, software	
3scan: Knife edge scanning microscope (images, slices, repeats, through specimen)	*http://www.3scan.com/data-2*
89North: X-Light confocal systems, illumination systems, emission systems, LDI Laser Diode Illuminator (for widefield microscopes and light sheet illuminators)	*http://www.89north.com* *http://www.89north.com/system-type/confocal-imaging-systems* *http://www.89north.com/system-type/illumination-systems* *http://www.89north.com/system-type/emission-systems*
Abberior	*http://www.abberior.com/shop/Labels-by-Function/Fluorescent-Proteins:::7_14.html* *http://www.abberior.com/shop/Labels-by-Application:::1.html*
Abberior Instruments: STED, RESOLFT precision localization super-resolution microscopes, STEDYCON convert any fluorescence microscope to STED	*http://abberior-instruments.com* *http://abberior-instruments.com/products/compact-line/abberior-stedycon* *http://www.abberior-instruments-america.com/home*
Active Motif: Chromeo dyes, Chromeo Py-Dyes (pyrylium dyes), fluorescent Click chemistry reagents	*http://www.activemotif.com* *http://www.activemotif.com/catalog/108/fluorescent-chromeo-dyes* *http://www.activemotif.com/catalog/545/fluorescent-chromeo-py-dyes* *http://www.activemotif.com/catalog/681/fluorescent-tools-for-click-chemistry*
Acquifer: Imaging machine (computer hardware) for high content screening, HIVE big data computing platform	*https://www.acquifer.de* *https://www.acquifer.de/screening* *https://www.acquifer.de/data-solutions*
Adobe Systems	*http://www.Adobe.com*

continued

Table 4.4.4 Useful Light Microscopy Web Sites, *continued*

Name of resource	URL
Affymetrix/eBioscience/Thermo Fisher Scientific: Microarrays	*http://www.affymetrix.com/estore/browse/level_one_category_template_one.jsp?parent=35796&category=35796* *http://www.affymetrix.com/estore/catalog/131547/AFFY/GeneChip%26%23174%3B+System+3000Dx+v.2%26%2342%3B#1_1*
Agilent Technologies: SureScan microarray scanner (array CGH, microRNA, SNPs, CNV)	*http://www.genomics.agilent.com/en/Microarray-Scanner-Processing-Hardware/SureScan-Microarray-Scanner/?cid=AG-PT-144*
Andor Technology (Oxford Instruments): sCMOS cameras, Dragonfly spinning disk confocal, Revolution DSD2 differential spinning disk confocal, photostimulation (fluorescence recovery after photobleaching, optogenetics), Mosaic3 DMD/DLP high speed light patterning (optogenetics, structured illumination), MicroPoint pulsed UV laser for ablation, DNA damage, photobleaching/activation, uncaging, accessories	*http://www.andor.com/scientific-cameras/neo-and-zyla-scmos-cameras* *http://www.andor.com/microscopy-systems/dragonfly* *http://www.andor.com/microscopy-systems/revolution-dsd* *http://www.andor.com/microscopy-systems/photostimulation* *http://www.andor.com/microscopy-systems/photostimulation/mosaic* *http://www.andor.com/microscopy-systems/photostimulation/micropoint* *http://www.andor.com/microscopy-systems/microscopy-components*
Apogee Instruments (Andor Technology): CCD cameras and filter wheels (mostly marketed for astronomy)	*http://www.ccd.com/andor.html*
Applied Scientific Instrumentation: Light sheet imager (iSPIM, diSPIM)	*www.asiimaging.com* *http://www.asiimaging.com/index.php/products/light-sheet-microscopy/selective-plane-illumination-microscopy-ispim-dispim/*
Applied NanoFluorescence: NS1 NanoSpectralyzer (Raman and UV-VIS, NIR), NS MiniTracer near-infrared spectrometer, NFM NanoFluorescence microscope, multi-laser light source; single wall carbon nanotubes (NIR II fluorophores)	*http://appliednano.com/products.html* *http://appliednano.com/products/ns1.html* *http://appliednano.com/products/product-list/77-ns-minitracer.html* *http://appliednano.com/products/nfm.html* *http://appliednano.com/products/ls-n.html* *http://www.nanowerk.com/news/newsid=24132.php*
Applied Spectral Imaging	*http://www.spectral-imaging.com*
Aratome: Array tomography proteomic imaging (high resolution fluorescence and correlative light-electron microscopy using ultrathin sections)	*http://www.aratome.com* *https://www.janelia.org/lab/spruston-lab/research/dendritic-integration/array-tomography*
ArgoLight: Fluorescence resolution test target slides	*http://argolight.com*
arivis: Vision4D, WebView, ImageCore: Image analysis, processing and visualization software for working with multi-channel 2D, 3D, and 4D images of almost unlimited size independent of available RAM	*https://www.arivis.com/en* *http://www.arivis.com/en/imaging-science/arivis-vision4d*
AttoCube: attoMICROSCOPY overview, attoCFM-Multichannel cryogenic (low temperature) confocal fluorescence microscopes, 0.8 NA objective lenses, 400-1000 nm spectral range	*http://www.attocube.com* *http://www.attocube.com/attomicroscopy/introduction/#tab-2* *http://www.attocube.com/attodownloads*
AutoQuant (Media Cybernetics) spatial deconvolution	*http://www.mediacy.com/autoquantx3*

continued

Table 4.4.4 Useful Light Microscopy Web Sites, *continued*

Name of resource	URL
Becker & Hickl	*http://www.becker-hickl.com/products.htm*
Berkeley Lights: Manueuver into nanowells, incubate, recover 4000 single cells per chip	*https://www.berkeleylights.com/technology*
Bioaxial: Codim imaging conical diffraction beam shaper for super-resolution (4 sub-images)	*http://www.bioaxial.com/codim-imaging*
Bioptechs: Live-Cell Micro-Observation Products	*http://www.bioptechs.com/*
Bionumbers: Database of useful biological numbers	*http://bionumbers.hms.harvard.edu/KeyNumbers.aspx*
Biostatus: DRAQ5, DRAQ7, ApopTRAK, CyTRAK Orange, CyGel, HypoxiTRAK	*http://www.biostatus.com/Products*
Bio-Tek: Cytation 3 Cell Imaging Multi-Mode Reader, Lionheart FX Automated Live Cell Imager	*http://www.biotek.com/products/imaging/cytation3_cell_imaging_multi_mode_reader.html* *http://www.biotek.com/products/imaging/lionheartfx_automated_live_cell_imager.html*
Biovision Technologies: Distributor for several imagers, including VT-iSIM instant super-resolution microscope	*http://biovision-technologies.com* *http://biovision-technologies.com/systems.html* *http://biovision-technologies.com/vtisim.html*
Bitplane (Andor/Oxford Instruments): Imaris imaging software	*http://www.bitplane.com*
BMV Optical: Custom lens assemblies and optical filters	*www.bmvoptical.com*
Bruker (previously Prairie Technologies, Vutara): Opterra confocal, Ultima Multiphoton, Vutara 352 single molecule localization microscopes	*https://www.bruker.com/products/fluorescence-microscopes/opterra-confocal-microscopy/overview.html* *https://www.bruker.com/products/fluorescence-microscopes/ultima-multiphoton-microscopy.html* *https://www.bruker.com/products/fluorescence-microscopes/vutara-super-resolution-microscopy/overview.html*
Cairn Research: Standard and custom accessories, e.g., Light Sheet Illuminator, MultiCam (4 cameras), custom design	*https://www.cairn-research.co.uk* *https://www.cairn-research.co.uk/product/l-spi-single-plane-illuminator (dual L-SPI for 4 illumination directions)* *https://www.cairn-research.co.uk/product/multicam* *https://www.cairn-research.co.uk/custom-design*
Cameca: NanoSIMS 50 liters (7plex stable isotope imaging)	*http://www.cameca.com/instruments-for-research/nanosims.aspx*
CellMic (formerly Holomic): Blood analysis or fluorescence imaging cytometer on a cell phone	*http://www.cellmic.com/content/advanced-technologies* *http://www.cellmic.com/content/fluorescent-imaging-cytometry-and-e-coli-detection-on-a-cell-phone*
CellOptic: Fresnel INcoherence correlation holography (FINCH)	*http://www.celloptic.com/index2.html*
CellProfiler: High content screening (HCS) image processing and analysis software	*http://cellprofiler.org*
ClearLight Diagnostics: CLARITY Optimized Light Sheet Microscopy (3D tissue optical clearing + light sheet imaging)	*http://www.clearlightdx.com/index.html*

continued

Table 4.4.4 Useful Light Microscopy Web Sites, *continued*

Name of resource	URL
Confocal.nl: Rescan confocal microscopy, to obtain 170-nm resolution with any pinhole diameter	*http://www.confocal.nl*
CoolLED: LED light sources	*http://www.coolled.com/product-detail/pe-4000*
Crest Optics SRL: X-Light confocal, X-Light v2 top performance (TP), X-Light V2 + VCS (VideoConfocal super-resolution)	*http://www.crestopt.com* *http://www.crestopt.com/html/x-light_v2_tp.html* *http://www.crestopt.com/html/x-light_v2_vcs.html*
CYTOO: Micropatterned coverglasses, SBS plates	*https://cytoo.com* *https://cytoo.com/products/chips* *https://cytoo.com/products/plates* *http://www.mehtrics.com/the-project* *https://youtu.be/SZkBJnFx5yY*
Cytoskeleton: Live cell imaging reagents, Spirochrome SiR bioimaging probes	*http://www.cytoskeleton.com/live-cell-reagents* *http://www.cytoskeleton.com/live-cell-reagents/spirochrome*
CytoViva: Darkfield imaging, hyperspectral imaging	*http://www.cytoviva.com/products/3 d-enhanced-darkfield-imaging/* *http://www.cytoviva.com/products/hyperspectral-imaging-2/hyperspectral-imaging*
Datacolor: Color calibration systems (match computer monitors and printers)	*http://www.datacolor.com*
Data Translation: Digitizer cards	*http://www.datx.com*
Delmic BV: Combined correlative scanning electron microscope with inverted fluorescence microscope	*http://www.delmic.com/delphi* *https://www.delphimicroscope.com* *http://www.delmic.com/secom-super-resolution*
Digital Light Innovations (DLi): CELscope C-mount LED Microscope using Texas Instruments DLP illuminator with a simple stand	*https://www.dlinnovations.com/dli-deep-dives-celscope-c-mount-led-microscope*
Double Helix: Single molecule localization microscope (Piestun)	*http://doublehelixoptics.com*
Echo Labs: Revolve microscope (flips upright and inverted), assemble your own microscope	*http://echo-labs.com/quote* *http://echo-labs.com/woodenscope*
Edinburgh Super-resolution Imaging Consortium (ESRIC)	*http://www.esric.org/*
Energetiq: Deep ultraviolet (DUV, high radiance 170-2100 nm) laser driven light source (LDLS)	*http://www.energetiq.com*
Epi Technology, CaliCube: Cube for fluorescence light path to inspect epi Illumination light source (lamp), fiber optic or liquid light guide	*http://www.epitechnology.com/epitechnology-1*
Essen Biosciences: Incucyte Zoom (imager inside incubator)	*http://www.essenbioscience.com/en/products/incucyte/*
Estigen Tissue Science: Manual and automated tissue arrayer (tissue microarray maker)	*http://www.estigen.com*

continued

Table 4.4.4 Useful Light Microscopy Web Sites, *continued*

Name of resource	URL
Excelitas Technologies (formerly Lumen Dynamics): X-Cite LEDs	*http://www.excelitas.com/Pages/Product/X-Cite-LED-Solutions.aspx*
Expansion Technologies (extbio): Expansion microscopy	*http://www.extbio.com/buycell*
FEI (formerly Till Photonics, now part of Thermo Fisher Scientific): Correlative LM-EM, single molecule Cryo-EM	*https://www.fei.com/life-sciences/cellular-biology* *https://www.fei.com/life-sciences/cellular-biology/correlative-microscopy* *https://www.fei.com/life-sciences/structural-biology*
Femtonics: Multi-photon microscopes, software, accessories, caged glutamate reagents, services	*http://femtonics.eu/products*
First Light Imaging: C-Red NIR imaging (800-2500 nm, NIR windows I, II, III, 650-950 nm, 1100-1350 nm, 1600-1870 nm; Shi et al., 2016), high speed visible EMCCD (400-1000 nm)	*http://www.first-light.fr/category/ranges/infrared*
Fluidigm: Helios imaging CyTOF mass cytometer (42plex), Callisto (32 independent chambers, dose with up to 16 independent factors, for 1-1000 cell populations, culture up to 3 week), Polaris functional genomics meets imaging (48 single cells, up to 24 hr, after single cell selection from a population)	*https://www.fluidigm.com/products/helios* *https://www.fluidigm.com/products/callisto* *https://www.fluidigm.com/products/polaris*
Fluoptics Imaging: Near-infrared fluorescence (NIRF) imaging for surgery, clinical and pre-clinical	*http://www.fluoptics.com/us/fluoptics_clinical.php* *http://www.fluoptics.com/us/fluoptics_preclinical.php*
GattaQuant: Nanorulers for high resolution microscopes and super-resolution microscopes performance testing, also gattabeads for small bright point sources	*http://www.gattaquant.com/Nanoruler* *http://www.gattaquant.com/products/localization-based.html* *http://www.gattaquant.com/products/gatta-beads.html*
GE Healthcare Life Sciences/Applied Precision: DeltaVision deconvolution, OMX, OMX SR	*http://www.gelifesciences.com/webapp/wcs/stores/servlet/productById/en/GELifeSciences-us/29065728* *http://www.gelifesciences.com/webapp/wcs/stores/servlet/catalog/en/GELifeSciences-us/products/AlternativeProductStructure_23807/29065721* *http://www.gelifesciences.com/webapp/wcs/stores/servlet/catalog/en/GELifeSciences-us/products/AlternativeProductStructure_23807/29115476*
GIGAmacro: Magnify2 gigapixel imagery of macroscopic and microscopic objects, Terapixel macro image	*http://www.gigamacro.com/gigapixel-macro-imaging-system* *http://www.gigamacro.com/worlds-first-terapixel-macro-image*
Glencoe Software: OMERO Plus enterprise data management for scientific images and any associated metadata (OME, Open Microscopy Environment), DataViewer, PathViewer	*https://glencoesoftware.com/omeroplus.html* *https://glencoesoftware.com/dataviewer.html* *https://glencoesoftware.com/pathviewer.html*
Gooch & Housego: Spectral imager	*https://goochandhousego.com/miniature-spectral-imaging-camera/* *http://www.ghinstruments.com/products/spectral-imaging-synthesis/hsi-440c-hyperspectral-imaging-system*

continued

Table 4.4.4 Useful Light Microscopy Web Sites, *continued*

Name of resource	URL
Hamilton Thorne: Stiletto and XYclone laser-objective to add cell and zona pellucida membrane ("egg shell" of mammalian oocytes) ablation add-ons	*http://www.hamiltonthorne.com/index.php/products/research-lasers/stiletto* *http://www.hamiltonthorne.com/index.php/research-lasers/xyrcos-xyclone/xyclone-components*
Hamrick-Vuescan Professional Edition: Best flatbed scanner software (supports most or all flatbed scanners, include raw scans)	*https://www.hamrick.com/reg.html*
Hindsight Imaging: Spectral imaging: HTVS high throughput virtual slit, VNIR visible to near-infrared	*http://hindsight-imaging.com*
Horiba Scientific: SWIFT ultra-fast Raman confocal imaging, Raman spectroscopy	*http://www.horiba.com/scientific/products/raman-spectroscopy/raman-imaging/swift* *http://www.horiba.com/scientific/products/raman-spectroscopy/raman-imaging* *http://www.horiba.com/scientific/products/raman-spectroscopy*
IATIA/Ultima Capital: QPm (quantitative phase microscopy)	*http://www.ultimacapital.net/iatiaimaging/Publications/Iatia%20Imaging/applicationNotes/qpmApplicationWithConfocalMicroscopes.pdf*
Ibidi: Heating and incubation systems, optical O_2 measurement systems, Nanolive 3D Cell Explorer, pump system, gas incubation system	*http://ibidi.com/xtproducts/en/Instruments-Accessories/Heating-Incubation-Systems* *http://ibidi.com/xtproducts/en/Instruments-Accessories/ibidi-OPAL-Optical-O2-Measurement-System* *http://ibidi.com/xtproducts/en/Instruments-Accessories/Nanolive-3D-Cell-Explorer* *http://ibidi.com/xtproducts/en/Instruments-Accessories/ibidi-Pump-System* *http://ibidi.com/xtproducts/en/Instruments-Accessories/Heating-Incubation-Systems/ibidi-Gas-Incubation-System*
iLAbSolutions (Agilent Technologies): Instrument management and scheduling software (cores and labs)	*http://www.ilabsolutions.com/instrument-access-control/*
ImageJ-Fiji ImageJ/NIH ImageJ/ImageJ: Fiji (Fiji is just ImageJ) is the main download site	*http://fiji.sc* *https://imagej.nih.gov/ij* *www.imagej.net* *http://research.stowers.org/imagejplugins/aboutjay.html* *Inscopix – nVista in vivo mouse brain imaging miniature microscope* *https://www.inscopix.com/products*
Intelligent Imaging Innovations (3i): Slidebook imaging software, Lattice light sheet (high speed, gentle to cells, high resolution imaging), Dual-view Inverted Selective Plane Illumination (diSPIM), VIVO 2-Photon (VIVO 2P) multiphoton microscopy, Everest intravital imaging, Marianas 3D real-time deconvolution timelapse spinning disk FRAP TIRF FLIM single molecule environmental control, Phasor-optogenetic photostimulation using digital holography, Yokogawa spinning disk confocal units	*www.intelligent-imaging.com* *https://www.intelligent-imaging.com/slidebook.php* *https://www.intelligent-imaging.com/systems.php#lattice* *https://www.intelligent-imaging.com/systems.php#dispim* *https://www.intelligent-imaging.com/systems.php#twophoton* *https://www.intelligent-imaging.com/systems.php#everest* *https://www.intelligent-imaging.com/systems.php#marianas* *https://www.intelligent-imaging.com/optogenetics.php* *https://www.intelligent-imaging.com/sdc.php*

continued

Table 4.4.4 Useful Light Microscopy Web Sites, *continued*

Name of resource	URL
IrfanView: Image viewer (shareware, comprehensive image file formats)	*http://www.irfanview.com*
ISS: Fluorescence lifetime imaging microscopy, fluorescence correlation spectroscopy (FCS), confocal imaging	*http://www.iss.com/microscopy/index.html*
JenLab, cyto-microscopy, multiphoton tomography	*http://www.jenlab.de/products.25.0.html* *http://www.jenlab.de/2PM-Cryo.133.0.html* *http://www.jenlab.de/Multiphoton-Tomography.68.0.html*
Jenoptik: Microscope cameras	*https://www.jenoptik.com/products/cameras-and-imaging-modules/microscope-cameras*
JPK Instruments: Integrated atomic force microscope (AFM), force sensing optical tweezers, optical trapping, single cell force spectroscopy (SCFS)	*http://www.jpk.com/index.2.en.html* *http://usa.jpk.com/optical-tweezers-optical-trapping.29.us.html* *http://usa.jpk.com/cellular-adhesion-cytomechanics.30.us.html*
Keyence: VK-X confocal (upright), BZ-X700 widefield (inverted), electronic light modulator (grid similar to OptiGrid and Apotome)	*http://www.keyence.com/ss/products/microscope/vkx/* *http://www.keyence.com/ss/products/microscope/bz-x700/index.jsp* *http://www.keyence.com/ss/products/microscope/bz-x700/product/sectioning/index.jsp*
KK Technology: CapiScope HVCS Handheld Video Capillaroscopy System (CytoScan)	*http://www.kktechnology.com/hvcs.html*
LaserSoft Imaging: SilverFast Ai Studio Scanner Software (see also Hamrick VueScan Professional), IT8 targets for color calibration	*http://www.silverfast.com/show/silverfast-ai-studio/en.html* *http://www.silverfast.com/show/it8-targets/en.html*
LaVision BioTec: TriMscope Multiphoton, TriM Scope II Adaptive Optics, UltraMicroscope II light sheet	*http://www.lavisionbiotec.de* *http://www.lavisionbiotec.de/trim-scope-overview.html* *http://www.lavisionbiotec.de/trim-scope-ii-adaptive-optics.html* *http://www.lavisionbiotec.de/ultramicroscope-ii-introduction.html*
Laxco: Upright and inverted microscopes	*http://www.laxcoinc.com/MICROSCOPES*
Lego: Lego Idea Microscopes	*https://ideas.lego.com/projects/44370* *http://www.nico71.fr/lego-working-microscope*
Li-Cor: Near-infrared fluorescent dyes and in vivo imaging agents, in vivo and Western blot imaging systems	*https://www.licor.com/bio/products/reagents* *https://www.licor.com/bio/products/reagents/irdye/brightsite_imaging_agents* *https://www.licor.com/bio/products/imaging_systems/odyssey_family.html* *https://www.licor.com/bio/products/imaging_systems/pearl* *https://www.licor.com/bio/products/imaging_systems/cdigit*
Life Imaging Services: "The Ludin chamber," "the cube & the box"	*http://www.lis.ch/thechamber.html* *http://www.lis.ch/thebox.html*
Lightform: PARISS imaging spectrometer	*http://lightforminc.com*
LMU Bioimaging	*http://www.bioimaging.bmc.med.uni-muenchen.de/links/websites/index.html* *http://www.bioimaging.bmc.med.uni-muenchen.de/learn/eduwebsites/index.html*
Ludl Electronic Products: Automated XY stages, focus motors, filter wheels	*http://www.ludl.com*

continued

Table 4.4.4 Useful Light Microscopy Web Sites, *continued*

Name of resource	URL
LumaCyte: Laser force cytology (laser trap meets microfluidics to suspend and manipulate single cells)	*http://www.lumacyte.com/about/technology*
Lumencor: LEDs fluorescence light sources	*http://lumencor.com/products*
Luxcel: Mitochondrial and cellular functions, O_2 sensor reagents	*http://luxcel.com/product+list*
Luxendo: Light sheet imager	*www.luxendo.eu*
Lyncee tec: Digital holography microscopy (DHM), high content screening by DHM	*http://www.lynceetec.com* *http://www.lynceetec.com/high-content-screening*
Mad City Labs: Nanopositioning	*www.madcitylabs.com*
Mauna Kea Technologies: CellVizio confocal laser endomicroscopy	*http://www.maunakeatech.com/en/healthcare-professionals/cellvizio-endomicroscopy-0*
MBF Bioscience: Stereology and neuron morphology quantitative imaging	*http://www.mbfbioscience.com*
McCrone Group	*www.mccrone.com/instrument-sales*
Media Cybernetics: Image Premier 3D, AutoQuant X3 deconvolution	*http://www.mediacy.com*
Meiji Techno America	*www.meijitechno.com*
MesoLens	*http://www.mesolens.com/product/technical-specifications* *http://www.mesolens.com/images* *https://www.biophotonics.strath.ac.uk/research_1.htm* *https://elifesciences.org/content/5/e18659 (*McConnell et al., 2016
Meyer Instruments: Pathscan Enabler, GigaMacro, digital pathology, telepathology	*http://meyerinst.com/* *http://meyerinst.com/pathscan-enabler-5* *http://meyerinst.com/gigamacro-gigapixel-macro-imaging* *http://meyerinst.com/home/scanners* *http://realtimetelepathology.com/*
Microarrays: Large-scale gene expression and microarray links and resources	*https://www.ebi.ac.uk/arrayexpress*
Micro-Manager, Device Support: Tabulates many microscope cameras and motorized accessories; every new camera and accessory should have a uManager driver to enable simple use with Fiji ImageJ	*https://micro-manager.org* *https://micro-manager.org/wiki/Device_Support* *https://open-imaging.com/*
Microvolution: (near) instant gratification spatial deconvolution using NVidia GPU card(s)	*http://microvolution.com*
Mightex Systems: Optogenetics DMD/DLP illuminator (digital micro-mirror device/ digital light processing)	*http://www.mightexsystems.com/index.php?cPath=245*
Millipore-Sigma/Merck KGaA (Amni, CellASIC, EMD Millipore): ImageStreamX and FlowSight imaging flow cytometers, ONIX2 Microperfusion System for microscopes	*https://www.emdmillipore.com* *https://www.emdmillipore.com/US/en/life-science-research/cell-analysis/amnis-imaging-flow-cytometers/Q6ub.qB.m3UAAAFLCKIp.ygJ,nav* *http://www.emdmillipore.com/US/en/life-science-research/cell-culture-systems/cellASIC-live-cell-analysis/d1Cb.qB.w58AAAE_0j13.MnA,nav*

continued

Table 4.4.4 Useful Light Microscopy Web Sites, *continued*

Name of resource	URL
Mitutoyo America	*www.mitutoyo.com* *http://ecatalog.mitutoyo.com/MF-U-Series-176-High-power-Multi-function-Measuring-Microscopes-C1413.aspx*
Molecular Devices Corporation/Universal Imaging Corporation (Danaher): MetaMorph, MetaFluor, high content systems (HCS)	*https://www.moleculardevices.com/systems/metamorph-research-imaging* *http://mdc.custhelp.com/app/answers/detail/a_id/19319* *https://www.moleculardevices.com/systems/high-content-imaging*
Molecular Machines & Industries: Laser microdissection and tweezer systems	*http://www.molecular-machines.com/home*
MUSE Microscopy: Deep UV illumination for shallow depth of field imaging	*http://www.musemicro.com*
Micro Video Instruments: DarkLite illuminator	*http://www.mvi-inc.com*
n3D Biosciences: Assembly 3D spheroids	*http://www.n3dbio.com/technical-resources/movie-tutorials*
NanoEnTek: JuLI Stage (imager inside incubator or on lab bench)	*http://www.julistage.com*
National Instruments: LabView software	*http://www.ni.com/en-us.html*
Navitar-Hoffman Modulation Contrast (HMC, alternative to differential interference contrast, phase contrast), custom lens design, UV/DUV, NUV imaging lenses	*https://navitar.com/markets/microscopy* *https://navitar.com/products/imaging-optics/custom-microscope-objectives/custom-microscope-objectives* *https://navitar.com/products/imaging-optics/uv-imaging*
National Center for X-ray Tomography (NCXT): Soft X-ray tomography (CT of hydrated cells), XM-2 dedicated biological SXT microscope, Carolyn Larabell, Director (see also SiriusXT)	*http://ncxt.lbl.gov* *http://ncxt.lbl.gov/sxt* *http://ncxt.lbl.gov/manual* *http://ncxt.lbl.gov/?q=carolyn*
Neogenomics (Clarient): MultiOmyx immunofluorescence or DNA FISH ("60plex")	*http://neogenomics.com/Pharma-Services/Lab-Services/MultiOmyx/Technology/MultiOmyx-IF-Assay-DNA-FISH-assay-NGS-from-ROI*
Nexcelom: Celigo imaging cytometer, Cellometer cell counters	*http://www.nexcelom.com/Celigo/index.php* *http://www.nexcelom.com/Products*
Nikon: Ti-LAPP modular illumination system (for Nikon Ti series microscopes): TIRF, Optogenetics	*https://www.nikoninstruments.com/Products/Photostimulation-and-TIRF/Ti-LAPP*
Nirmidas Biotech	*http://www.nirmidas.com/technology/nir* *http://www.nirmidas.com/products/niriidye*
NVidia: Pascal 10+ Gbps GPU cards for instant gratification deconvolution (software from Microvolution.com, SVI.nl)	*http://www.geforce.com/hardware/10series/geforce-gtx-1080* *http://www.geforce.com/hardware/10series/titan-x-pascal* *http://www.nvidia.com/object/quadro-graphics-with-pascal.html*
Ocean Optics: Spectrometers	*http://oceanoptics.com/product-category/modular-spectrometers*
Oko-Lab stage top incubator	*http://www.oko-lab.com/stage-top*
Open Microscopy Environment (OME): OMERO (see also Glencoe Software), Bio-Formats, LOCI	*https://www.openmicroscopy.org/site* *https://www.openmicroscopy.org/site/products/omero* *https://www.openmicroscopy.org/site/products/bio-formats* *https://www.openmicroscopy.org/site/support/bio-formats5.2/supported-formats.html* *https://www.openmicroscopy.org/site/about/development-teams/kevin*

continued

Table 4.4.4 Useful Light Microscopy Web Sites, *continued*

Name of resource	URL
OpenSPIM: Do-it-yourself selective plane illumination microscopy (light sheet imaging)	*http://openspim.org/Welcome_to_the_OpenSPIM_Wiki*
OpenSpinMicroscopy: Do-it-yourself SPIM/DSLM/OPT microscopes	*https://sites.google.com/site/openspinmicroscopy*
Ovizio: Differential digital holography (similar to quantitative phase imaging)	*http://www.ovizio.com/en/Home* *http://www.ovizio.com/en/Microscopes/QMod*
Oxford Gene Technologies: Microarrays; cytogenetics, molecule genetics, cancer research, pre-implantation genetic diagnosis	*http://www.ogt.com/clinical_genetics*
Oxford Nanoimaging: Single molecule(s) localization fluorescence resonance energy transfer (FRET; Kapanidis)	*www.oxfordni.com*
Pathology Devices: LiveCell stage top incubator and controller, tissue microarrayers (TMA makers)	*http://www.pathologydevices.com/LiveCell.htm* *http://www.pathologydevices.com/TMArrayer.htm*
PeCon: Microscope incubators	*http://www.pecon.biz*
Pembroke Instruments: Spectrometers, mini-lasers; short wavelength infrared cameras (SWIR), SWIR microscope	*http://pembrokeinstruments.com/qmini-spectrometer* *http://pembrokeinstruments.com/mini-lasers/* *http://pembrokeinstruments.com/swir-cameras* *http://pembrokeinstruments.com/swir-microscope*
PerkinElmer: In vivo imaging systems (IVIS, bioluminescence, NIR fluorescence), fluorescence molecular tomography (FMT), Solaris open air fluorescence imaging system (i.e., in vivo surgery), Vectra digital slide scanner, Operetta high content screening imagers	*http://www.perkinelmer.com/category/in-vivo-imaging-instruments* *http://www.perkinelmer.com/product/fmt-4-channel-fmt4000* *http://www.perkinelmer.com/product/solaris-cls139884* *http://www.perkinelmer.com/category/quantitative-pathology-imaging-instruments* *http://www.perkinelmer.com/category/high-content-screening-instruments-microscopes*
Phi Optics: CellVista SLIM Pro (quantitative phase microscopy)	*http://phioptics.com/*
Photometrics (Roper Scientific): DualView, QuadView	*http://www.photometrics.com* *http://www.photometrics.com/products/multichannel/*
Photon Technology International	*http://www.pti-nj.com/index.html*
PicoQuant: Fluorescence lifetime imaging microscopes (FLIM), STED, 3D-EasySTED	*https://www.picoquant.com/products/category/fluorescence-microscopes* *https://www.picoquant.com/applications/category/life-science/sted* *http://www.easysted.org*
Physik Instrumente (PI): Nanopositioning applications for microscopy, neuroscience and metrology	*https://www.physikinstrumente.com/en* *http://www.pi-usa.us/index.php*
PreSens Prescision Sensing: VisiSens measure and visualize oxygen, pH, or carbon dioxide distributions	*http://www.presens.de/products/brochures/category/imaging/brochure/imaging-solutions-biological-research.html* *http://www.presens.de/products/brochures/category/imaging/brochure/imaging-solutions-life-science-research.html*
Prior Scientific	*http://www.prior-us.com/*

continued

Table 4.4.4 Useful Light Microscopy Web Sites, *continued*

Name of resource	URL
Profusa: Lumee tissue-integrated biosensors scaffolds	*http://profusa.com/technology/*
RapidMiner: Data science platform	*https://rapidminer.com*
Reindeer Graphics: OptiPix, Fovea Pro: Plugins for Adobe Photoshop 6 and CS series	*http://www.reindeergraphics.com*
Renishaw: StreamLine fast chemical imaging, Raman spectroscopy	*http://www.renishaw.com/en/streamline-generate-chemical-images-rapidly–9449* *http://www.renishaw.com/en/raman-spectroscopy–6150*
Sanford Burnham Prebys: High content screening	*http://www.sbpdiscovery.org/technology/sr/Pages/LaJolla_HighContentScreening.aspx*
ScopeM: Scientific Center for Optical and Electron Microscopy, ETH Zürich	*http://www.scopem.ethz.ch*
SiriusXT: Soft X-ray tomography (SXT) microscope (CT scan hydrated cell)	*http://siriusxt.com*
SpectraGenetics: Fluorogen Activating Peptides (FAPs), new genetically encoded "binary" reporters	*http://spectragenetics.com/products/vectors-for-expressing-fluorogen-activating-proteins/fap-technology-overview*
Spirochrome: Silicon Rhodamine (SiR) and other fluorescent reagents probes for bioimaging	*http://spirochrome.com*
Stanford Photonics	*http://www.stanfordphotonics.com* *http://www.stanfordphotonics.com/Life%20Sciences/LifeSci.htm*
Stream Technologies: ColorFlow lens (multi-wavelength emission onto a camera)	*http://www.streamtechinc.com/#products*
Sutter Instrument Company	*http://www.sutter.com/* *http://www.sutter.com/MICROSCOPES/index.html* *http://www.sutter.com/IMAGING/index.html*
SVI Huygens: Professional (general image analysis), deconvolution, NVidia GPU deconvolution	*https://svi.nl/HuygensProfessional* *https://svi.nl/HuygensDeconvolution* *https://svi.nl/HuygensGPU*
Sysmex Partex: CyScope	*http://www.sysmex-partec.com/products/microscopy.html* *http://www.sysmex-partec.com/products/prdouct-detailview/cyscopeR-malaria-3238.html*
Tableau: Business analytics, data visualization	*http://www.tableau.com/h2*
Technical Instruments	*http://www.techinst.com/products.php*
TESCAN Brno: Tescan Q-PHASE multimodal holographic quantitative phase imaging system (QPi), optional fluorescence	*http://www.tescan.com/en/products/q-phase/q-phase* *http://q-phase.tescan.com* *http://q-phase.tescan.com/index.php/technology/specifications*
Ted Pella: Specialty light microscopy and electron microscopy supplies	*https://www.tedpella.com*
Texas Instruments: DLP 4100 development kit (digital light processing DMD digital micromirror device)	*http://www.ti.com/tool/dlpd4×00kit*

continued

Table 4.4.4 Useful Light Microscopy Web Sites, *continued*

Name of resource	URL
ThorLabs: iCyte imaging cytometer, multiphoton, confocal, EnVista digital slide scanning microscopes	*https://www.thorlabs.com/newgrouppage9.cfm?objectgroup_id=7473* *https://www.thorlabs.com/newgrouppage9.cfm?objectgroup_id=7494* *https://www.thorlabs.com/newgrouppage9.cfm?objectgroup_id=5696* *https://www.thorlabs.com/newgrouppage9.cfm?objectgroup_id=6570*
TIBCO, Spotfire: Data visualization and analytics software	*http://spotfire.tibco.com*
TIRF Labs, lightguide TIRF, prism TIRF, TIRF-electrochemistry (TIRF-EC), TIRF-dielectrophoresis (TIRF-DEP)	*http://www.tirf-labs.com* *http://www.tirf-labs.com/technologies.html*
TissueVision: Serial two photon tomography (image volume, ablate imaged volume with multiphoton laser, repeat)	*http://www.tissuevision.com/technology*
Tokai Hit: Stage top incubator	*http://www.tokaihit.com/english/product_guidance/option.html*
TopoNomos: Toponome Imaging Cycler, immunofluorescence (100plex)	*http://www.toposnomos.com/technology.html*
Ultivue, DNA-PAINT: Reagents, data processing service	*http://www.ultivue.com* *http://www.ultivue.com/products*
UMech Technologies: Cytovar HCS, up to 16 excitation wavelengths	*http://cloud.umech.com/products/* *http://cloud.umech.com/products/model/C16/*
Visitech: vt-iSIM instant super-resolution microscopy up to 1000 frames per second, confocal scanners and light engines	*http://www.visitech.co.uk/vt-isim.html* *http://www.visitech.co.uk/products.html*
Visitron Systems: High speed imaging systems	*http://www.visitron.de*
Visualsonics (Fujifilm): Photoacoustic imaging	*http://www.visualsonics.com/products/technology-overview*
Wicked Lasers	*http://www.wickedlasers.com* *http://www.wickedlasers.com/arctic*
WITec Wissenschaftliche Instrumente und Technologie: Imaging systems for FLIM, Raman, AFM, and SNOM analysis	*http://witec.de/products* *http://www.witec-instruments.com*
W.M. Keck Center for Adaptive Optical Microscopy (CfAOM) at UC, Santa Cruz	*https://cfaom.soe.ucsc.edu* *http://cfao.ucolick.org/pgallery*
Yokogawa: Spinning disk confocal scanner, live cell imager, high content screener, confocal quantitative cytometer	*http://www.yokogawa.com/solutions/products-platforms/life-science* *http://www.yokogawa.com/solutions/products-platforms/life-science/confocal-scanner-unit-csu/* *http://www.yokogawa.com/solutions/products-platforms/life-science/all-in-one-live-cell-imaging-solution/* *http://www.yokogawa.com/solutions/products-platforms/life-science/high-throughput-cytological-discovery-system/* *http://www.yokogawa.com/solutions/products-platforms/life-science/confocal-quantitative-image-cytometer/*
Zellkraftwerk (ChipCytometry): Immunofluorescence (80plex)	*http://www.zellkraftwerk.com/Products2.phtml* *http://www.zellkraftwerk.com/ZKWOne.phtml#Software* *http://www.chipcytometry.com/technology.phtml*
Fluorescence spectra data and graphing sites	
AAT Bioquest	*https://www.aatbio.com/spectrum*

continued

Table 4.4.4 Useful Light Microscopy Web Sites, *continued*

Name of resource	URL
BD Biosciences: Spectrum viewer, Brilliant fluorophores	*http://www.bdbiosciences.com/us/s/spectrumviewer* *http://www.bdbiosciences.com/us/applications/s/spectrumguidepage*
BioLegend: Spectra analyzer, Brilliant Violet fluorophores	*http://www.biolegend.com/spectraanalyzer* *http://www.biolegend.com/brilliantviolet*
Chroma Technology	*https://www.chroma.com/spectra-viewer*
eBioscience (Affymetrix, Thermo Fisher Scientific), fluorPlan: Multi-laser spectra viewer	*http://www.ebioscience.com/resources/fluorplan-spectra-viewer.htm* *Spectra Viewer (requires Java)*
Evrogen: Spectrum Viewer	*http://evrogen.com/spectra-viewer/flash/viewer.html*
Fluorophores.org: Fluorescent Substances	*http://www.fluorophores.tugraz.at/substance*
I Love GFP	*https://sites.google.com/site/ilovegfp/Home/fps*
Lambert and Thorn, UC, San Francisco, fluorescent protein properties	*http://nic.ucsf.edu/FPvisualization/*
Leica Microsystem: "FluoScout"	*http://www.leica-microsystems.com/fluoscout*
Molecular Probes/Invitrogen/Thermo Fisher Scientific: Fluorescence SpectraViewer	*http://www.thermofisher.com/us/en/home/life-science/cell-analysis/labeling-chemistry/fluorescence-spectraviewer.html* *https://itunes.apple.com/us/app/fluorescence-spectraviewer/id421031826 (iTunes App)*
Nightsea: Compendium of spectra web sites	*http://www.nightsea.com/sfa-sharing/fluorescence-spectra-viewers*
Omega Optical "Curvomatric"	*https://www.omegafilters.com/curvomatic/*
PhotoChemCAD 2.0 (Jonathan S. Lindsey) dye spectra database and chemistry calculator, NIRvana Sciences	*http://www.photochemcad.com* *http://nirvanasciences.com/?page_id=3088*
PubSpectra: Excel file data download	*https://works.bepress.com/gmcnamara/9*
UC, San Francisco (Lambert & Thorn, 2016): Fluorescent protein properties	*http://nic.ucsf.edu/FPvisualization*
University of Arizona: Fluorescent Spectra Database	*http://www.spectra.arizona.edu*
Semrock: Searchlight	*https://searchlight.semrock.com*
Spectroscopy Ninja: Links to spectral and fluorescence data, Spekwin32 spectroscopy software	*http://www.effemm2.de/info/info_specdata.html* *http://www.effemm2.de/index.html*
Zeiss: Interactive fluorescence dye and filter database, overview dyes, overview filter sets	*https://www.micro-shop.zeiss.com/?s=50479761ad21e5&l=en&p=us&f=f&a=i* *https://www.micro-shop.zeiss.com/?s=55721483f91174&l=en&p=us&f=f&a=d* *https://www.micro-shop.zeiss.com/?s=55721483f91174&l=en&p=us&f=f&a=f*
Researcher labs	
Alberto (Alby) Diaspro, Istituto Italiano di Tecnologia (IIT)	*http://www.lambs.it/index.php?page=People*
Alan Waggoner, Carnegie Mellon University (CMU)	*https://www.cmu.edu/bio/people/faculty/waggoner.html*
Alice Ting, Massachusetts Institute of Technology (MIT)	*http://www.tinglab.org/research/*

continued

Table 4.4.4 Useful Light Microscopy Web Sites, *continued*

Name of resource	URL
Allen Institute for Brain Science	*http://www.alleninstitute.org/what-we-do/brain-science*
Allen Institute for Cell Science	*http://www.alleninstitute.org/what-we-do/cell-science*
Amina Qutub, Rice University: How are human cells designed lab	*https://qutublab.org/qutub-lab*
Amy Herr, UC, Berkeley: Single-cell Western blots	*http://herrlab.berkeley.edu/*
Amy Palmer, University of Colorado Boulder	*https://palmerlab.colorado.edu/*
Andrew York, Calico Life Sciences	*https://www.calicolabs.com/team-member/andrew-york/*
Anne Carpenter, Broad Institute, CellProfiler	*https://personal.broadinstitute.org/anne*
Arjun Raj, University of Pennsylvania (UPenn): Single molecule RNA FISH quantitative understanding cellular functions	*http://rajlab.seas.upenn.edu/index.html http://www.popsci.com/science/article/2013-09/arjun-raj*
Atsuko Miyawaki, Laboratory for Cell Function Dynamics (CFDS): Fucci2 fluorescent proteins cell cycle indicator	*http://www.brain.riken.jp/en/faculty/details/30 http://cfds.brain.riken.jp http://cfds.brain.riken.jp/Fucci.html*
Aydogan Ozcan, UC, Los Angeles: New imaging and sensing architectures	*http://innovate.ee.ucla.edu/welcome.html http://www.hhmi.org/scientists/aydogan-ozcan*
Badri Roysam, University of Houston: FARSIGHT Toolkit	*http://www.ee.uh.edu/faculty/roysam http://www.farsight-toolkit.org/wiki/Main_Page*
Brian J. Ford: Microscopist and popularizer	*https://uk.linkedin.com/in/profbrianjford*
Carolyn Larabell, National Center for X-ray Tomography (LBNL), UC, San Francisco	*http://ncxt.lbl.gov/?q=carolyn http://profiles.ucsf.edu/carolyn.larabell*
Clare Waterman, National Heart, Lung, and Blood Institute (NHLBI), National Institutes of Health (NIH)	*https://www.nhlbi.nih.gov/research/intramural/researchers/pi/waterman-clare*
Dana Pe'er, Columbia University: Computational systems biology, viSNE and more software	*http://www.c2b2.columbia.edu/danapeerlab/html http://www.c2b2.columbia.edu/danapeerlab/html/cyt.html*
David Mayerich, University of Houston: STIM Laboratory, Scalable tissue imaging and modeling	*http://www.ee.uh.edu/faculty/mayerich http://stim.ee.uh.edu/*
David Piston, Washington University in St. Louis (WUSTL)	*http://www.cellbiology.wustl.edu/faculty/tenured/david-w.-piston-ph.d*
Diane Lidke and Keith Lidke, University of New Mexico	*http://pathology.unm.edu/research/faculty-laboratories/the-lidke-laboratory/index.html http://panda3.phys.unm.edu/~klidke*
Donna Arndt-Jovin and Thomas Jovin, Max Planck Institute for Biophysical Chemistry, Laboratory of Cellular Dynamics	*http://www3.mpibpc.mpg.de/groups/jovin/index.php/ResearchGroups/DonnaArdndt-JovinResearchAreasAndProjects http://www3.mpibpc.mpg.de/groups/jovin/index.php/ResearchGroups/ChairmanThomasJovinResearchAreasAndProjects*
Ed Boyden, Massachusetts Institute of Technology (MIT) Media Lab: Expansion microscopy (ExM), optogenetics	*http://syntheticneurobiology.org http://syntheticneurobiology.org/protocols http://syntheticneurobiology.org/publications http://www.ted.com/talks/ed_boyden_baby_diapers_inspired_this_new_way_to_study_the_brain http://www.extbio.com/buycell*

continued

Table 4.4.4 Useful Light Microscopy Web Sites, *continued*

Name of resource	URL
Elizabeth Blackburn, Salk Institute: Telomeres	*https://www.salk.edu/scientist/elizabeth-blackburn* *https://en.wikipedia.org/wiki/Elizabeth_Blackburn* *https://www.nobelprize.org/nobel_prizes/medicine/laureates/2009/blackburn-facts.html*
Elizabeth Hillman, Columbia University: Swept, confocally aligned planar excitation (SCAPE) high speed 3D microscopy, dynamic contrast enhancement to image and segment small animal organs live (DyCE), neuroimaging and neurovascular coupling	*http://orion.bme.columbia.edu/~hillman/Instrumentation.html* *http://orion.bme.columbia.edu/~hillman/SCAPE.html* *http://orion.bme.columbia.edu/~hillman/Molecular.html* *http://orion.bme.columbia.edu/~hillman/Brain_Imaging.html*
Eric Betzig, UC, San Francisco (moving from Howard Hughes Medical Institute Janelia Research Campus in 2016)	*https://www.nobelprize.org/nobel_prizes/chemistry/laureates/2014/betzig-facts.html*
Eva Sevick-Muraca, UT Health Science Center at Houston: Molecular imaging, clinical NIR fluorescence imaging	*https://www.uth.edu/imm/profile.htm?id=1005459* *https://www.uth.edu/imm/centers/molecular-imaging.htm*
Evelin Schrock, Technische Universität Dresden: Spectral karyotyping, cytogenetics	*https://www.researchgate.net/profile/Evelin_Schrock*
Garry Nolan, Stanford University: Mass cytometry, MIBI-ToF high throughput imaging mass cytometry (42plex)	*http://web.stanford.edu/group/nolan/resources.html* *http://web.stanford.edu/group/nolan/technologies.html*
George McNamara: Cell Morphometry (41), Figure 4.4.1 right top two panels (55), The Chase (2016, temporal area maps, "dynamic morphology"; 76), newsletter series on "The Chase" (73), direct Vimeo movie of "The Chase," Tiki_Goddess, LinkedIn, 10+plex blog, GeoMcNamara Web site.	*https://works.bepress.com/gmcnamara/41* *https://works.bepress.com/gmcnamara/55* *https://works.bepress.com/gmcnamara/76* *https://works.bepress.com/gmcnamara/73* *https://vimeo.com/175151196* *http://home.earthlink.net/~tiki_goddess* *https://www.linkedin.com/in/georgemcnamara* *https://www.linkedin.com/pulse/bd-biosciences-listed-tandems-horizon-brilliant-violets-mcnamara* *www.GeoMcNamara.com*
Gillian Griffiths, University of Cambridge: T-cell immunological synapse	*http://www.cimr.cam.ac.uk/research/principal-investigators/principal-investigators-a-h/griffiths*
Hari Shroff, National Institute of Biomedical Imaging and Bioengineering (NIBIB), National Institutes of Health (NIH)	*https://www.nibib.nih.gov/labs-at-nibib/section-high-resolution-optical-imaging-hroi*
Howard Hughes Medical Institute (HHMI) Janelia Research Campus (JFRC), Advanced Imaging Center, Open Science	*https://www.janelia.org/open-science/advanced-imaging-center-aic* *https://www.janelia.org/open-science*
Jay Unruh, Stowers Institute for Medical Research: Stowers ImageJ Plugins	*http://research.stowers.org/imagejplugins/aboutjay.html*
Jeanne Lawrence, University of Massachussetts Medical School	*http://www.umassmed.edu/cellbio/labs/lawrence/personnel/principal-investigator/*
Jennifer Lippincott-Schwartz, Howard Hughes Medical Institute (HHMI) Janelia Research Campus	*https://www.janelia.org/people/jennifer-lippincott-schwartz*
Jin Zhang, UC, San Diego	*http://profiles.ucsd.edu/jin.zhang*

continued

Table 4.4.4 Useful Light Microscopy Web Sites, *continued*

Name of resource	URL
Joe DeRisi, UC, San Francisco: 3D printable lab stuff	*http://derisilab.ucsf.edu/index.php?page=3D*
John Russ, Chris Russ, Fovea Pro: plugins for Adobe Photoshop	*http://www.drjohnruss.com/index.html* *http://www.drjohnruss.com/books.html* *http://www.reindeergraphics.com/foveaprotutorial.html*
Jonathan Lindsay, NC State University: PhotoChemCAS 2.1	*http://www4.ncsu.edu/~jslindse/* *http://www.photochemcad.com/pages/chemcad/chem-home.html*
Julie Theriot, Stanford University	*http://cmgm.stanford.edu/theriot/*
Karl Deisseroth, Stanford University: CLARITY optical tissue clearing, Optogenetics	*http://clarityresourcecenter.org/* *http://web.stanford.edu/group/dlab/optogenetics/index.html*
Karsten König (Koenig), Saarland University and JenLab: Biophotonics	*http://www.blt.uni-saarland.de/index_e.htm* *http://www.jenlab.de* *http://www.thelastescape-film.com*
Karsten Rodenacker: Image measurements	*http://karo03.bplaced.net/karo/Me/Misc_WWW/pdf/MicrosoftWord-EQUAPAT.pdf*
Kevin Eliceiri, University of Wisconsin-Madison: Open Source Photonics and Software, Laboratory for Optical and Computational Instrumentation (LOCI)	*www.loci.wisc.edu*
Klaus Kemp, Microlife Services: Diatoms and other prepared microscope slides	*http://www.diatoms.co.uk*
Kurt Thorn, UC, San Francisco	*http://thornlab.ucsf.edu* *https://nic.ucsf.edu/blog* *http://nic.ucsf.edu/FPvisualization* *http://gigapan.com/gigapans/163370*
Lihong Wang, Washington University in St. Louis (WUSTL): Optical Imaging Laboratory, photoacoustic tomography	*http://oilab.seas.wustl.edu/* *http://oilab.seas.wustl.edu/research_0.html*
Loren Looger, Howard Hughes Medical Institute (HHMI) Janelia Research Campus: iGluSnFr fluorescent protein biosensor	*https://www.janelia.org/lab/looger-lab*
Luke Lavis, Howard Hughes Medical Institute (HHMI) Janelia Research Campus: Janelia Fluor (JF) dyes	*https://www.janelia.org/lab/lavis-lab* *https://www.janelia.org/open-science/janelia-fluor-dyes* *http://blog.addgene.org/better-dyeing-through-chemistry-small-molecule-fluorophores*
Marcel Bruchez, Carnegie Mellon University (CMU)	*http://www.cmu.edu/bio/people/faculty/bruchez.html*
Mary-Lou Pardue, Massachusetts Institute of Technology (MIT): first ever in situ hybridization, with J. Gall	*https://biology.mit.edu/people/mary_lou_pardue* *https://en.wikipedia.org/wiki/Mary-Lou_Pardue*
Nancy Allbritton, UNC: Chemical cytometry, microraft arrays, organ-on-a-chip	*https://www.bme.ncsu.edu/index.php/component/comprofiler/userprofile/nlallbri* *http://www.bme.unc.edu/labs/allbritton/*
Navin Varadarajan, University of Houston (UH): single-cell lab	*http://www.chee.uh.edu/faculty/varadarajan* *http://singlecell.chee.uh.edu/contact.html*
Nicholas Shaner, Scintillon Institute: mNeonGreen	*http://www.scintillon.org/shaner_lab*

continued

Table 4.4.4 Useful Light Microscopy Web Sites, *continued*

Name of resource	URL
Rebecca Richards-Kortum, Rice University	*http://bioengineering.rice.edu/faculty/rebecca_richards-kortum.aspx*
Richard Neher: Blind spectral unmixing	*http://www.ukmn.gwdg.de/methods_unmix.html* *http://neherlab.github.io/PoissonNMF/Documentation/NMF/index.html* *https://neherlab.wordpress.com/* *https://neherlab.wordpress.com/image-analysis/*
Robert Campbell, University of Alberta: Fluorescent proteins, optogenetic proteins	*http://campbellweb.chem.ualberta.ca* *http://campbellweb.chem.ualberta.ca/projects-2*
Robert Murphy, Carnegie Mellon University: Cell measurements web services	*http://murphylab.web.cmu.edu/services*
Sabine Mai, University of Manitoba: Genomic Centre for Cancer Research and Diagnosis (GCCRD)	*https://www.umanitoba.ca/institutes/manitoba_institute_cell_biology/MICB/Platforms/GCCRD.html* *https://www.umanitoba.ca/institutes/manitoba_institute_cell_biology/MICB/Scientists/Mai/Awards.html*
Sally Ward and Raimund Ober, Texas A&M University	*http://www.wardoberlab.com*
Scott Prahl, OMLC: Optical Properties Spectra, PhotoChemCAD spectra online, Scattering calculator (Mie scattering)	*http://omlc.org/spectra* *http://omlc.org/spectra/PhotochemCAD/index.html* *http://omlc.org/calc*
Simon Watkins, University of Pittsburgh, Center for Biologic Imaging	*http://www.cbp.pitt.edu/faculty/watkins.html* *http://www.cbp.pitt.edu/faculty/lab/watkins.html* *http://www.cbi.pitt.edu*
Stefan Hell, Max Planck Institute for Biophysical Chemistry, Department Hell: NanoBiopohotonics	*http://www.mpibpc.mpg.de/hell* *https://en.wikipedia.org/wiki/Stefan_Hell* *https://www.nobelprize.org/nobel_prizes/chemistry/laureates/2014/hell-facts.html*
Sunney Xie, Harvard	*https://bernstein.harvard.edu*
Susan Cox: 3B microscopy	*http://www.coxphysics.com/index.html* *http://www.coxphysics.com/3b/*
Radim Chmelík, Center for Innovative Microscopy, Experimental biophotonics group	*https://www.ceitec.eu/ceitec-but/experimental-biophotonics/rg3* *http://www.biophot.cz/home*
Taekjip Ha, Johns Hopkins University: Single molecules	*http://ha.med.jhmi.edu*
Thomas Ried, National Cancer Institute (NCI), National Institutes of Health (NIH): SKY/M-FISH and CGH Database	*https://ccr.cancer.gov/Genetics-Branch/thomas-ried* *https://ccr.cancer.gov/Genetics-Branch/thomas-ried?qt-staff_profile_tabs=9#qt-staff_profile_tabs* *ftp://ftp.ncbi.nlm.nih.gov/sky-cgh/DATA/* *https://www.ncbi.nlm.nih.gov/dbvar*
Viviana Gradinaru, California Institute of Technology (CalTech): CLARITY/PACT, Optogenetics	*http://www.bbe.caltech.edu/content/viviana-gradinaru* *http://glab.caltech.edu*
Vladislav Verkhusha, Albert Einstein College of Medicine: Near-infrared fluorescent proteins	*http://www.einstein.yu.edu/labs/vlad-verkhusha/default.aspx* *http://www.einstein.yu.edu/research/facilities/fluorescent*
William E. Moerner, Stanford University	*http://web.stanford.edu/group/moerner*
Willard Wiggans: Micro gallery	*http://www.willard-wigan.com/gallery*

continued

Table 4.4.4 Useful Light Microscopy Web Sites, *continued*

Name of resource	URL
Wolf Frommer: Molecular sensors (fluorescent protein biosensors table)	*http://biosensor.dpb.carnegiescience.edu*
Xiaowei Zhuang, Harvard University	*http://zhuang.harvard.edu*
Yuval Garini, Bar-Ilan University: Nano-Bio-Photonics laboratory	*http://garinilab.biu.ac.il*
Microscopy magazines	
Imaging & Microscopy	*http://www.imaging-git.com/magazine*
Laser Focus World	*http://www.laserfocusworld.com/index.html*
Microscopy & Analysis	*http://www.microscopy-analysis.com/*
Microscopy Today	*http://www.microscopy-today.com/*
Microscopy-UK	*http://www.microscopy-uk.org.uk*
Photonics Spectra, Biophotonics	*http://www.photonics.com/Publications.aspx*
The Microscope Journal	*http://mcri.org/v/72/the-microscope-journal*
RMS Infocus Magazine	*http://www.rms.org.uk/study-read/infocus-magazine.html*
Nobel Prizes in light microscopy and related fields	
Chemistry, 1925, colloids (light sheet), Zsigmondy (Siedentopf & Zsigmondy, 1902)	*https://www.nobelprize.org/nobel_prizes/chemistry/laureates/1925*
Chemistry, 2000, conductive polymers, Heeger, MacDiarmid, Shirakawa (Brilliant Violets, Ultraviolets, Blues)	*http://www.nobelprize.org/nobel_prizes/chemistry/laureates/2000*
Chemistry, 2008, green fluorescent protein (GFP), Shimomura, Chalfie, Tsien	*http://www.nobelprize.org/nobel_prizes/chemistry/laureates/2008*
Chemistry, 2014, super-resolved fluorescence microscopy, Betzig, Hell, Moerner	*https://www.nobelprize.org/nobel_prizes/chemistry/laureates/2014*
Physics, 1953, Phase Contrast, Zernike	*https://www.nobelprize.org/nobel_prizes/physics/laureates/1953*
Physics, 2009, invention of an imaging semiconductor circuit—the CCD sensor, Kao, Boyle, Smith	*http://www.nobelprize.org/nobel_prizes/physics/laureates/2009*
Physics, 2014, efficient blue light emitting diodes, Akasaki, Amano, Nakamura	*http://www.nobelprize.org/nobel_prizes/physics/laureates/2014*
Physiology or Medicine, 2006, RNA interference—gene silencing by double stranded RNA, Fire and Mello	*http://www.nobelprize.org/nobel_prizes/medicine/laureates/2006*
Physiology or Medicine, 2006, specific gene modifications in mice by the use of embryonic stem cells, Capecchi, Evans, Smithies	*http://www.nobelprize.org/nobel_prizes/medicine/laureates/2007*
Physiology or Medicine, 2009, how chromosomes are protected by telomeres and telomerase, Blackburn, Greider, Szostak	*http://www.nobelprize.org/nobel_prizes/medicine/laureates/2009*
Physiology or Medicine, 2012, matured cells can be reprogrammed to become pluripotent, Gurdon, Yamamanka	*http://www.nobelprize.org/nobel_prizes/medicine/laureates/2012*

[a]We recommend these for simplified handing and processing versus either thick plastic dishes/plates or having to handle loose coverslips with your valuable cells.

Table 4.4.5 Light Sheet Manufacturers[a]

Manufacturer	Product or source
Commercial manufacturers	
3i	Marianas
3i	Lattice Lightsheet
ASI	diSPIM
ASI	oSPIM
Cairn Research	L-SPI Illuminator (two can be used together for four direction illumination)
LaVision	Ultramicroscope
Leica	SP8 DLS
Leica	SCAPE
Luxendo	MuVi-SPIM
Luxendo	InVi-SPIM
M2 Lasers (M-Squared Lasers)	Airy Light Sheet
Phaseview	Alpha3
Zeiss	Lightsheet Z1
Zeiss	Lattice lightsheet
Open source projects	
OpenSPIM	*http://openspim.org/Welcome_to_the_OpenSPIM_Wikihttp://www.hfsp.org/frontier-science/hfsp-success-stories/openspim-open-access-light-sheet-microscopy-platform*
OpenSpinMicroscopy	*https://sites.google.com/site/openspinmicroscopy/*
Overview of both OpenSPIM and OpenSpinMicroscopy	*http://labrigger.com/blog/2013/06/27/openspim-and-openspinmicroscopy-for-light-sheet-microscopy/*
Light sheet fluorescence microscopy	*https://en.wikipedia.org/wiki/Light_sheet_fluorescence_microscopy*

[a]This list is from the Confocal Listserv, Feb 2017, by Michael Weber and Jim Mansfield.

Table 4.4.6 Radiation Wavelength Ranges[a]

Name	Abbreviation	Wavelength	Photon energy (eV)	Notes/alternative names
Ultraviolet				
Ultraviolet A	UVA	315-400 nm	3.10-3.94	Long-wave, black light, not absorbed by the ozone layer
Ultraviolet B	UVB	280-315 nm	3.94-4.43	Medium-wave, mostly absorbed by the ozone layer
Ultraviolet C	UVC	100-280 nm	4.43-12.4	Short-wave, germicidal, completely absorbed by the ozone layer and atmosphere
Near ultraviolet	NUV	300-400 nm	3.10-4.13	Visible to birds, insects, and fish
Middle ultraviolet	MUV	200-300 nm	4.13-6.20	
Far ultraviolet	FUV	122-200 nm	6.20-12.4	
Hydrogen Lyman-alpha	H Lyman-α	121-122 nm	10.16-10.25	Spectral line at 121.6 nm, 10.20 eV. Ionizing radiation at shorter wavelengths
Vacuum ultraviolet	VUV	10-200 nm	6.20-124	Strongly absorbed by atmospheric oxygen, though 150-200 nm wavelengths can propagate through nitrogen
Extreme ultraviolet	EUV	10-121 nm	12.4-124	Entirely ionizing radiation by some definitions; completely absorbed by the atmosphere
Near-Infrared[b]				
Near-infrared	NIR	780-3000 nm (0.78-3 μm)		
	IR-A	700 nm-1400 nm (0.7 μm-1.4 μm)		
	IR-B	1400 nm-3000 nm (1.4 μm-3 μm)		
	IR-C	3000 nm-1 mm (3.0 μm-1000 μm)		
	NIR I	650-950 nm		Shi et al. (2016)
	NIR II	1100-1350 nm		Shi et al. (2016)
	NIR III	1600-1870 nm		Shi et al. (2016)
	NIR IV	2100-2300 nm		Shi et al. (2016)

[a]The electromagnetic spectrum of ultraviolet radiation (UVR), defined most broadly as 10-400 nanometers, can be subdivided into a number of ranges recommended by the ISO standard ISO-21348 (*https://en.wikipedia.org/wiki/Ultraviolet*).
[b]Near-infrared ranges: Wikipedia (*https://en.wikipedia.org/wiki/Infrared*) tabulates several different division schemes, we chose one that looked useful, and added the NIR I, II, III, Windows from Shi et al., 2016, discussed in the text.